Centre for Drug Research
Division of Pharmaceutical Chemistry
Faculty of Pharmacy
University of Helsinki
Finland

Micropillar Array Based Microchips for Electrospray Ionization Mass Spectrometry, Microreactors, and Liquid Chromatographic Separation

Teemu Nissilä

ACADEMIC DISSERTATION
To be presented, with the permission of the Faculty of Pharmacy of the University of Helsinki, for public examination in Auditorium 1041, Viikki Biocentrum 2, on 27 May 2011, at 12 noon.
Helsinki 2011

Supervisors:
Adjunct Professor Raimo A. Ketola
Centre for Drug Research
Faculty of Pharmacy
University of Helsinki
Finland

Professor Risto Kostiainen
Division of Pharmaceutical Chemistry
Faculty of Pharmacy
University of Helsinki
Finland

Reviewers:
Professor Hubert Girault
Laboratory of Physical and Analytical Electrochemistry
École polytechnique fédérale de Lausanne
Switzerland

Adjunct Professor Ilkka Ojanperä
Hjelt Institute
Department of Forensic Medicine
University of Helsinki
Finland

Opponent:
Professor Janne Jänis
Department of Chemistry
Faculty of Science and Forestry
University of Eastern Finland
Finland

ISBN 978-952-10-6963-5 (paperback)
ISSN 1795-7079
ISBN 978-952-10-6964-2 (PDF)
http://ethesis.helsinki.fi

Helsinki University Print
Helsinki 2011

Abstract

This dissertation deals with the design, fabrication, and applications of microscale electrospray ionization chips for mass spectrometry. The microchip consists of micro-channels, which are divided to the sampling spot and the channel, which leads to a sharp electrospray tip. Microchannels contain micropillars that facilitate a powerful capillary action in the channels. The capillary action delivers the liquid sample to the electrospray tip, which sprays the liquid sample to gas phase ions that can be analyzed with mass spectrometry. The microchip uses a high voltage, which can be utilized as a valve between the microchip and mass spectrometry.

The microchips can be used in various applications, such as for analyses of drugs, proteins, peptides, or metabolites. The microchip works without pumps for liquid transfer, is usable for rapid analyses, and is sensitive. The characteristics of performance of the single microchips are studied and a rotating multitip version of the microchips are designed and fabricated. It is possible to use the microchip also as a microreactor and reaction products can be detected online with mass spectrometry. This property can be utilized for protein identification for example. Proteins can be digested enzymatically on-chip and reaction products, which are in this case peptides, can be detected with mass spectrometry. Because reactions occur faster in a microscale due to shorter diffusion lengths, the amount of protein can be very low, which is a benefit of the method. The microchip is well suited to surface activated reactions because of a high surface-to-volume ratio due to a dense micropillar array. For example, titanium dioxide nanolayer on the micropillar array combined with UV radiation produces photocatalytic reactions which can be used for mimicking drug metabolism biotransformation reactions. Rapid mimicking with the microchip eases the detection of possibly toxic compounds in preclinical research and therefore could speed up the research of new drugs.

A micropillar array chip can also be utilized in the fabrication of liquid chromatographic columns. Precisely ordered micropillar arrays offer a very homogenous column, where separation of compounds has been demonstrated by using both laser induced fluorescence and mass spectrometry. Because of small dimensions on the microchip, the integrated microchip based liquid chromatography electrospray microchip is especially well suited to low sample concentrations. Overall, this work demonstrates that the designed and fabricated silicon/glass three dimensionally sharp electrospray tip is unique and facilitates stable ion spray for mass spectrometry.

Acknowledgements

This study was carried out in the Centre for Drug Research of the University of Helsinki, Finland. Most of the work was done in facilities of the Division of Pharmaceutical Chemistry during the years 2006 - 2011. I acknowledge The Academy of Finland (projects no. 111991 and 129633), TEKES (project MISIMA 440006) and Centre for Drug Research for financial support of this work and the Division of Pharmaceutical Chemistry for the study facilities. Thanks are also due for all the additional support that I received from Helsinki University Research funds and the graduate school of Chemical Sensors and Microanalytical Systems (CHEMSEM).

There are many people I wish to acknowledge for their contributions to this work:

First of all I want to thank Adjunct Professor Raimo Ketola and Professor Risto Kostiainen for the opportunity to work under their inspirational supervision and also for introducing me to the world of science; Especially the enthusiasm of Ketola, his encouragement and invaluable advise for both me, and the work, made this study possible.

I am grateful to all of the co-authors for their valuable work. In particular, I would thank Professors Sami Franssila, Tapio Kotiaho, and Dr. Lauri Sainiemi. I want to especially express my appreciation to Lauri who has spent countless hours in the cleanroom fabricating the microchips that were used in these studies.

Very special thanks are due to my former and present colleagues of the Division of Pharmaceutical Chemistry for making the work fun and even enjoyable; So in particular thanks are due to Anu, Inkku, Kati H., Laura L., Laura H., Linda, Markus, Mikko, Niina, Nina N., Nina S., Päivi U., Raisa, Sirkku, Tiina K., Tiina S. and Timo.

Warm thanks to my parents Pirkko and Pentti for always nurturing me and teaching me the most important things in the world. Thanks also to my sisters and brothers for making my life happy, challenging and worth living when I was a child.

I reserve my deepest and warmest thanks for my love and wife, Taija-Tuulikki, who always waited for me to return home from work, and gave me the best possible support at home. Without your encouragement and love, this work would not have been able to be finished. I also want to thank my children Vesa, Eero, Leo and Iida for their ability to make life eventful and giving me an excellent counterbalance to work.

Contents

List of original publications

This thesis is based on the following publications:

I Teemu Nissilä, Lauri Sainiemi, Tiina Sikanen, Tapio Kotiaho, Sami Franssila, Risto Kostiainen, Raimo A. Ketola: **Silicon micropillar array electrospray chip for drug and biomolecule analysis**, Rapid Communications in Mass Spectrometry, 22, 3677-3682, 2007.

II Lauri Sainiemi, Teemu Nissilä, Ville Jokinen, Tiina Sikanen, Tapio Kotiaho, Risto Kostiainen, Raimo A. Ketola and Sami Franssila: **Fabrication and Fluidic Characterization of Silicon Micropillar Array Electrospray Ionization Chip**, Sensors and Actuators B, 132, 380-387, 2008.

III Teemu Nissilä, Lauri Sainiemi, Sami Franssila and Raimo A. Ketola: **Fully polymeric integrated microreactor/electrospray ionization chip for on-chip digestion and mass spectrometric analysis**, Sensors and Actuators B, 143, 414–420, 2009.

IV Teemu Nissilä, Lauri Sainiemi, Mika-Matti Karikko, Marianna Kemell, Mikko Ritala, Sami Franssila, Risto Kostiainen and Raimo A. Ketola: **Integrated photocatalytic micropillar nanoreactor electrospray ionization microchip for mimicking phase I metabolic reactions**, Lab on a Chip, 11, 1470-1476, 2011.

V Teemu Nissilä, Lauri Sainiemi, Nina Backman, Marjo Kolmonen, Antti Leinonen, Alexandros Kiriazis, Jari Yli-Kauhaluoma, Risto Kostiainen, Sami Franssila, Raimo A. Ketola: **Rotating multitip micropillar array electrospray ion source for rapid analysis and high throughput screening with mass spectrometry,** Manuscript

VI Teemu Nissilä, Lauri Sainiemi, Risto Kostiainen, Raimo A. Ketola, Sami Franssila: **Monolithically integrated micropillar liquid chromatography-electrospray ionization microchip for mass spectrometric detection,** Manuscript

The publications are referred to in the text by their roman numerals. The publications, and all figures and tables in the introduction chapter are reproduced with permissions from Elsevier, The Royal Society of Chemistry, IEEE, John Wiley & Sons Ltd., Wiley-VCH Verlag GmbH & Co. KGaA., and American Chemical Society.

Abbreviations

µPESI	micropillar array electrospray ionization
µTAS	miniaturized total chemical analysis systems / micro total analysis systems
Al_2O_3	aluminum oxide, alumina
ALD	atomic layer deposition
APCI	atmospheric pressure chemical ionization
APPI	atmospheric pressure photoionization
BSA	bovine serum albumin
C10	decylsilane
C18	octadecylsilane
CI	chemical ionization
COC	cyclo olefin copolymer
CYP450	cytochrome P450 enzyme
DNA	deoxyribonucleic acid
DRIE	deep reactive ion etching
EI	electron ionization
ESI	electrospray ionization
ESR	electron spin resonance
GC	gas chromatography
HF	hydrofluoric acid
HLM	human liver microsome
HPLC	high-performance liquid chromatography
HV	high voltage
ID	inner diameter
LC	liquid chromatography
LIF	laser induced fluorescence
MALDI	matrix assisted laser desorption/ionization
MEMS	microelectromechanical systems
MS	mass spectrometry/mass spectrometer
MS/MS	tandem mass spectrometry
MW	molecular weight
m/z	mass to charge ratio
NMR	nuclear magnetic resonance
PDDA	poly(diallyldimethylammonium chloride)
PDMS	poly(dimethylsiloxane)
PI	photoionization
PMMA	poly(methyl methacrylate)
PTFE	polytetrafluoroethylene, Teflon^{TM}
RIE	reactive ion etching
RSD	relative standard deviation
SEM	scanning electron microscopy

SiO_2	silicon dioxide, silica
SRM	selected reaction monitoring
SU-8	trade mark of epoxy based polymer
TiO_2	titanium dioxide
TOF	time-of-flight
UV	ultraviolet

1 Introduction

The focus of this work, and thus this literature review, is on electrospray ionization. Miniaturized electrospray ion sources offer many advantages over conventional ion sources used for mass spectrometry, in addition to integrated microreactors for electrospray mass spectrometry and micropillar arrays in various analytical applications.

1.1 Miniaturized electrospray ionization microchips combined with mass spectrometry (MS)

Mass spectrometry (MS) is a common technique for the analysis of ionized chemical compounds according to their mass to charge ratio (*m/z*). Analytes are ionized in an ion source using different kinds of ionization methods prior to mass analysis. Ionization methods are divided into two categories. Ionization methods developed early worked in a vacuum, such as electron ionization (EI), photoionization (PI), and chemical ionization (CI), while alternative ambient techniques, working at atmospheric pressure, such as electrospray ionization (ESI), atmospheric pressure photoionization (APPI), and atmospheric pressure chemical ionization (APCI) exhibit a rising profile. Furthermore, some of the ionization techniques, such as matrix assisted laser desorption/ionization (MALDI), can be performed both within a vacuum and also at ambient pressure. In this chapter, the discussion is focused on atmospheric pressure ionization methods, especially on electrospray and miniaturized electrospray ion sources.

1.1.1 Electrospray ionization

Ionization techniques play a crucial role in MS because if compounds are not able to be ionized, they cannot be analyzed or detected with MS. The electrospray phenomenon was first explored in the 18th century.[1] Electrospray ionization is a widely used method where small polar compounds are ionized well, and it is also widely used for the analysis of larger compounds such as proteins and peptides.[2,3] In ESI, a solvent containing analytes is injected through a small injection port using a device, such as capillary, needle, or microchannel, which is connected to a high voltage. The development of ESI started with the use of a 100-µm inner diameter (ID) stainless steel capillary.[4,5] A high electric field, produced by high voltage between the needle and the first lens of mass spectrometer, forms a Taylor cone[6] from the solvent which emits small droplets to a gas phase. Droplets have a net charge (either positive or negative depending on the ionization mode), and therefore the energy and velocity of the droplets are increased in an electric field. At the same time, droplets becomes smaller due to evaporation.[7,8] When the same number of charges are in the droplet that has a smaller diameter, electrostatic, Coulombic, repulsive forces inside the droplet overcome the force of surface tension causing a rupture of the droplet.[9] In a pure ion evaporate model, ions are emitted from the surface of the droplet,[7]

whereas in a charge residue model a droplet is divided so many times that only ions are left when the solvent is evaporated.[10] In ionization techniques, especially in ESI, one disadvantage is ion suppression which can diminish or completely abolish signals of the analytes.[7,11,12] One theory for ion suppression is that the ions share their places in the droplet due to their chemical properties and because the ions that lie on the surface of droplets are only emitted from the droplet and detected but the ions which are in the center of droplet can form clusters with counter ions causing the loss of net charge and are therefore not detected. ESI suits polar and ionic compounds well, offering relatively high sensitivity for those compounds. Other atmospheric pressure ionization methods, such as APCI and APPI, better ionize non-polar compounds. In APCI and APPI, a heater nebulizer is used to evaporate the sample solution and a corona discharge needle or VUV-light (10 eV) is used to form ions in the gas phase. Instead of separate nebulizing and ionizing, ESI forms gas phase ions directly without heating. There are also many variations and modifications of ESI such as ionspray and turboionspray. Due to ion suppression effects, ESI does not tolerate salts and other matrix compounds well, therefore sample pretreatment is normally needed prior to analysis. ESI emitters can also be utilized for various purposes such as sample preparation, reactions in solution, electrochemistry, and droplet extraction.[13] The structure of an ESI ion source is fairly basic, thus it is relatively easy to miniaturize.

1.1.2 Miniaturized electrospray ion sources

Miniaturized ion sources for mass spectrometry have been recently reviewed.[14,15,16] In ESI the size of the inner diameter of the needle is an important parameter. One of the first miniaturized ESI methods was nanoelectrospray ionization (nanoESI). The method was based on a small diameter pulled glass electrospray tip which was typically 1 to 2 µm wide.[17,18] Benefits of the nanoESI method are a lower flow rate, typically 20 nL/min, and high sensitivity, which decreases the amount of the sample needed. A lower electrospray voltage is also needed and therefore the nanoESI tip can be positioned closer to the MS orifice while the transmission of ions into the MS is therefore increased. Due to the smaller ESI needle diameter and lower flow rate of nanoESI, the droplets formed in the Taylor cone are smaller and therefore ion suppression effects are less with nanoESI ion sources than with normal ESI sources. In the nanoESI technique there are more charges available for one analyte molecule increasing the probability that the analyte will be ionized. Because of the low flow rate, low ion suppression, high ion transmission, and efficient charge separation, nanoESI can be used for trace analysis at low zeptomole levels.[19] One drawback of the nanoESI needles is the fabrication, where after pulling a narrow glass needle, the needle has to be cut manually which is not very reproducible, thus affecting the flow rate of the liquid as well as sensitivity and repeatability of the measurement.

Microfabrication technology, which is well known in electronic integrated circuit fabrication, can also be used for fabrication of microelectromechanical systems (MEMS)

and therefore microfluidic chips with integrated functionalities. Different materials are used for fabrication of microchips, such as silicon, glass, and a variety of polymers. Silicon is mechanically strong and has high electrical and thermal conductivity. Fabrication accuracy of silicon is in most cases superior compared to that of glass and especially of polymers. Glass (borosilicate, quartz, or fused silica) is thermally and electrically an insulator and therefore usable for electro-osmotic flow applications. Aspect ratios of 100:1 can be achieved using etching of glass with deep reactive ion etching (DRIE), but in practice 10:1 to 20:1 ratios are normally obtainable. This wide variety of polymers provides a considerable benefit to users as a certain type of polymer can be selected for each application. Important polymer material properties to consider are melting/degradation temperature, solvent compatibility, hydrophobicity or hydrophilicity, contact angle, transparency, porosity, and permeability. Polymer fabrication techniques, such as injection molding and hot embossing, make the fabrication of polymeric microchips suitable for mass production. The major drawback of polymer fabrication is that the precision of polymeric microchips is not as good as that of silicon or glass microchips.

Glass and silicon microchips for ESI

Ramsey and Ramsey reported the first glass MEMS microfabricated planar-edge devices for ESI (Fig. 1.1).[20] Injection channels were integrated on the chip and a direct mass spectrometric analysis of fluorescence compound, rhodamine, using an electro-osmotic flow was also demonstrated.

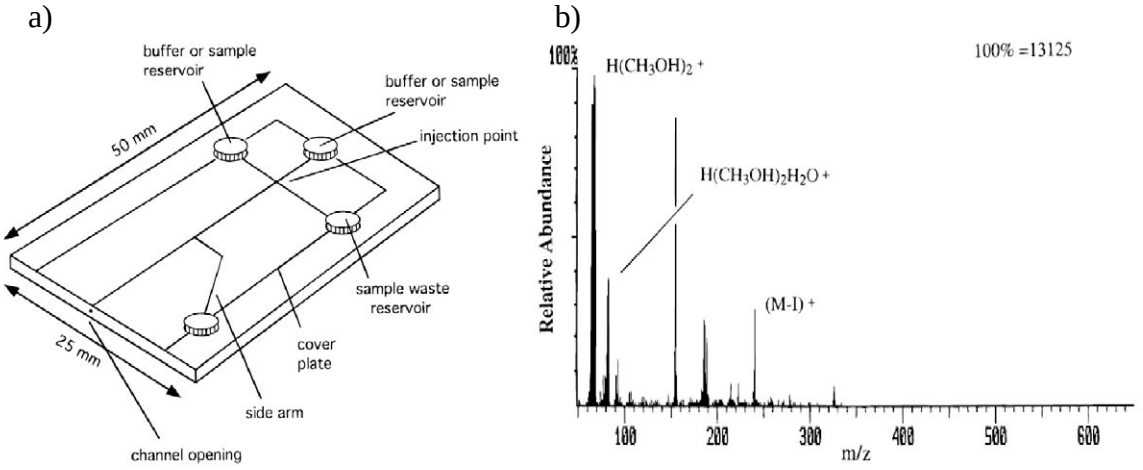

Figure 1.1. a) A MEMS fabricated glass ESI chip. **b)** An ESI mass spectrum of 10 µM tetrabutylammonium iodide from a 60% water / 40% MeOH solution measured with a microchip that uses electroosmotic flow for sample transportation.[20]

The first silicon ESI emitter, with a tip size of about 2 µm, was fabricated in 1997 by Lee *et al*.[21] The microchip also contained a particle filter to avoid clogging of the tip (Fig. 1.2a). A capillary was connected with epoxy glue to the backside of the microchip to enable continuous infusion and ionization, and a flow rate of 50 nL/min was used for

ionization of 4 µM gramicidin S (Fig. 1.2b). Additional background peaks were seen in the ESI mass spectrum and they supposedly originated from epoxy glue residues.

a) b)

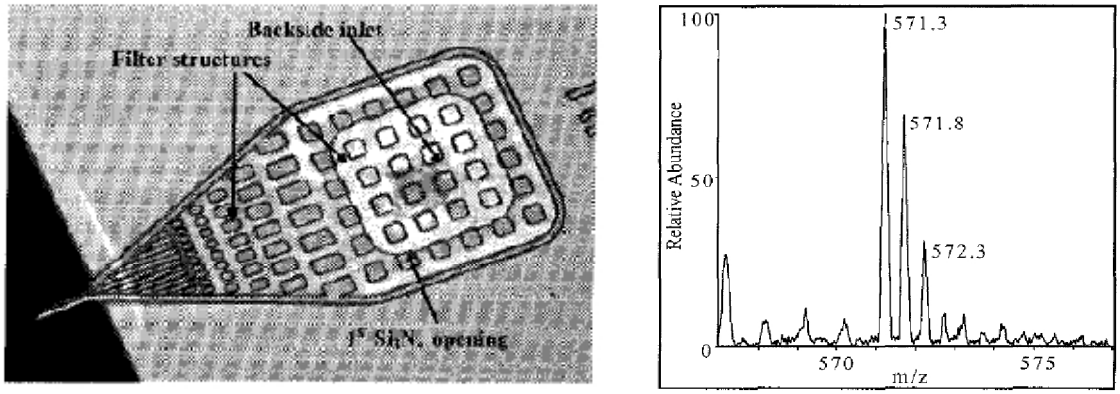

Figure 1.2. a) A top view of a miniaturized electrospray tip containing a particle filter. **b)** An ESI mass spectrum of 4 µM gramicidin S in a 50% water / 50% MeOH solution measured with the MEMS tip.[21]

A silicon multinozzle ESI array was developed by Kim *et al.* for proteomic micro total analysis systems (Fig. 1.3).[22] Their microchip worked at high potential from 4.5 to 4.8 kV and the best sensitivity for one nozzle was shown to be obtained at a flow rate of 120 nL/min. By changing the number of the electrospray nozzles on the chip it was possible to find the best sensitivity for each flow rate used. The multinozzle microchip is not as sensitive to clogging as microchips with only one nozzle because of multiple pathways for liquid at the tip.

a) b)

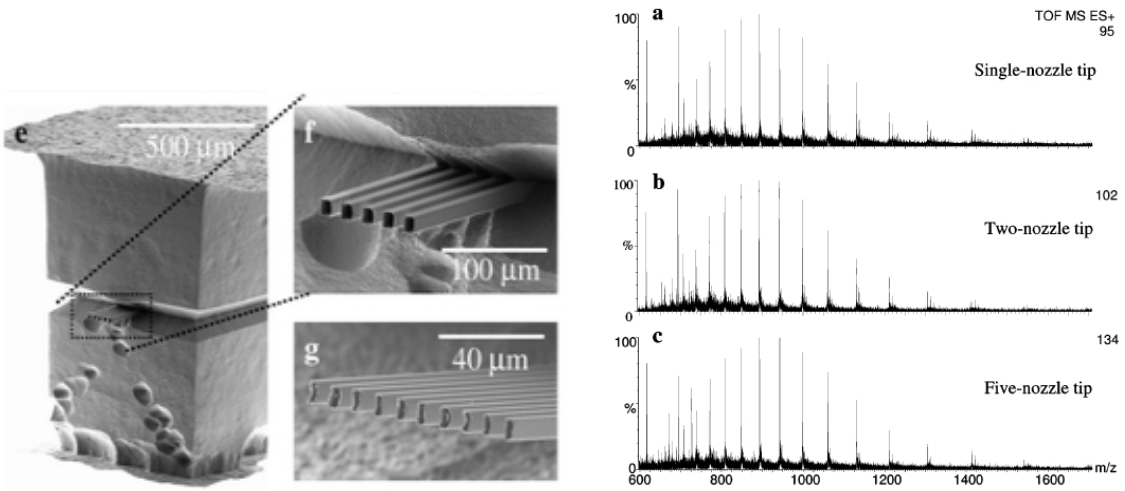

Figure 1.3.a) A multinozzle ESI tip with four and nine nozzles. **b)** Mass spectra of 1 µM myoglobin obtained with (top, a) a single-nozzle emitter, (middle, b) a two-nozzle emitter, and (below, c) a five-nozzle emitter. [22]

A polysilicon cantilever ESI nib tip (Fig. 1.4a) was shown to work with voltages as low as 0.7 kV and the microchip was able to spray water concentrations as high as 90%.[23,24,25] The microchip slot worked as a capillary, thus promoting a spontaneous filling of the slot by liquid when proper conditions and parameters were chosen.[26] The key properties for capillary filling of the slot were the contact angle of the material, surface area of the slot, and the slot width, which all had to be optimized for production of stable ES plume (Fig. 1.4b).

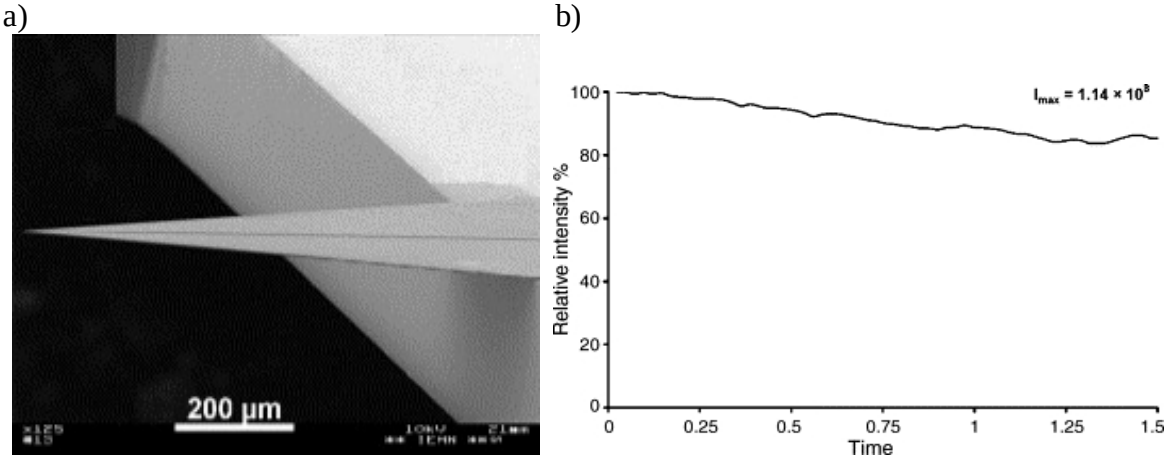

Figure 1.4. a) A polysilicon cantilever ESI tip. b) A total ion current signal over a 1.5 min period using a polysilicon-based ESI source, having capillary slot dimensions of 2.5 µm × 5 µm, from a 1 µM Glu-Fibrinopeptide B sample prepared in a 90:10 H_2O:MeOH, 0.1% formic acid solution.[23]

A silicon out-of-plane fabricated ESI microchip was introduced in 2000 by Schultz *et al.* (Fig. 1.5).[27] Their 15 µm wide ESI tip was able to spray everything from 100% organic to 100% aqueous solutions. Reproducibility of ionization between 10 different nozzles was 12% (relative standard deviation, RSD) and with a single nozzle 4% (RSD) whereas the signal stability was 2 – 4% with continuous infusion. The signal-to-noise ratio for 10 nM cytochrome c solution in 100% water with a flow rate of 100 nL/min was 450:1. Sensitivity was 1.5 to 3 times better when compared to that of pulled nanoESI capillaries. Most of the microfabricated ESI chips have been shown to work for qualitative analysis, but a quantitative bioanalysis was also shown to be possible with an automated sampling combined with the out-of-plane fabricated silicon ESI tip (Fig. 1.5b)[28], where the automated pipette was used to inject a sample through the ESI emitter.

a) b)

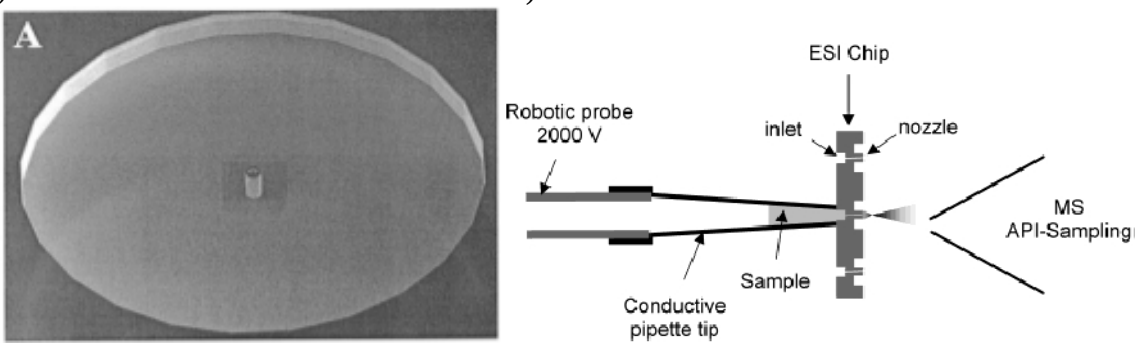

Figure 1.5. a) A silicon out-of-plane fabricated ESI nozzle. **b)** An interface of an automated pipette tip sample delivery system and the ESI chip.[27]

Polymeric microchips for ESI

Polymeric ESI tips have been fabricated, for example, from SU-8, poly(dimethylsiloxane) (PDMS), and parylene.[14] SU-8 polymer is used in microfabrication technology mostly as a photoresist for lithography. SU-8 is transparent in the UV range and it is thermally stable up to 300 °C. The polymer is strong and it tolerates many solvents, such as methanol and acetonitrile. PDMS is a viscoelastic polymer with a hydrophobic surface. Using plasma treatment, the surface can be changed to hydrophilic. PDMS is easy to fabricate with replica molding, and it is optically transparent down to 280 nm. PDMS tolerates water and some alcohols well, but most organic solvents are not usable with PDMS as they dissolve it.[29] With mass spectrometry, PDMS normally gives a higher background than SU-8 as there can be lot of unreacted monomers left on a surface. Parylene C is the most common of parylene (poly(p-xylylene)) polymers. Parylene C is insoluble with common solvents and microchips made from parylenes are fabricated using photo lithography and etching in oxygen plasma. PMMA (poly(methyl methacrylate)) is a hard, transparent polymer which is widely used, but due to its low solvent compatibility it is seldom used in microfluidic applications. PMMA is not suitable for continuous use with strong acids or alcohols, such as methanol, ethanol, or acetonitrile, but tolerates water and diluted or weak acids well. Injection molding, compression molding, and extrusion can be used for fabrication from PMMA as well as traditional drilling and sawing methods. In the following section, examples of different polymeric ESI tips and their performance characteristics are presented.

A similar self standing ESI nib tip, as presented in Figure 1.4a, has also been fabricated from the SU-8 polymer.[30,31,32,33,34,35] This SU-8 ESI nib tip (Fig. 1.6a) shows a stable ESI for two minutes of 5 µM gramicidin S (Fig. 1.6b) with calculated RSD of 6.9%. The microchip can be used with low spray voltages from 0.8 to 1.5 kV, depending on the distance to the MS orifice.

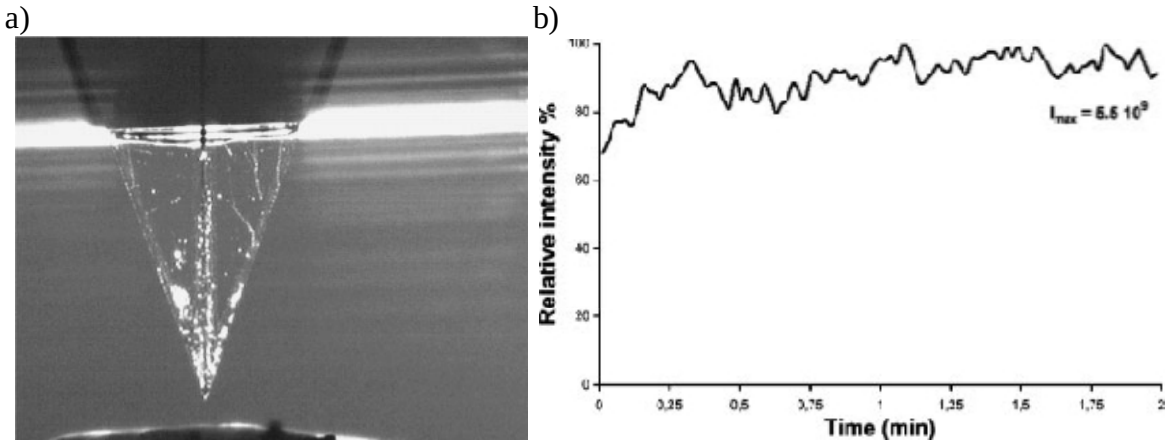

Figure 1.6. a) A miniaturized SU-8 ESI nib tip with a 16-µm wide spraying channel. **b)** Stability of spraying of 5 µM gramicidin S with 0.8 kV ESI voltage using a SU-8 ESI nib tip with an 8-µm wide spraying channel.[30]

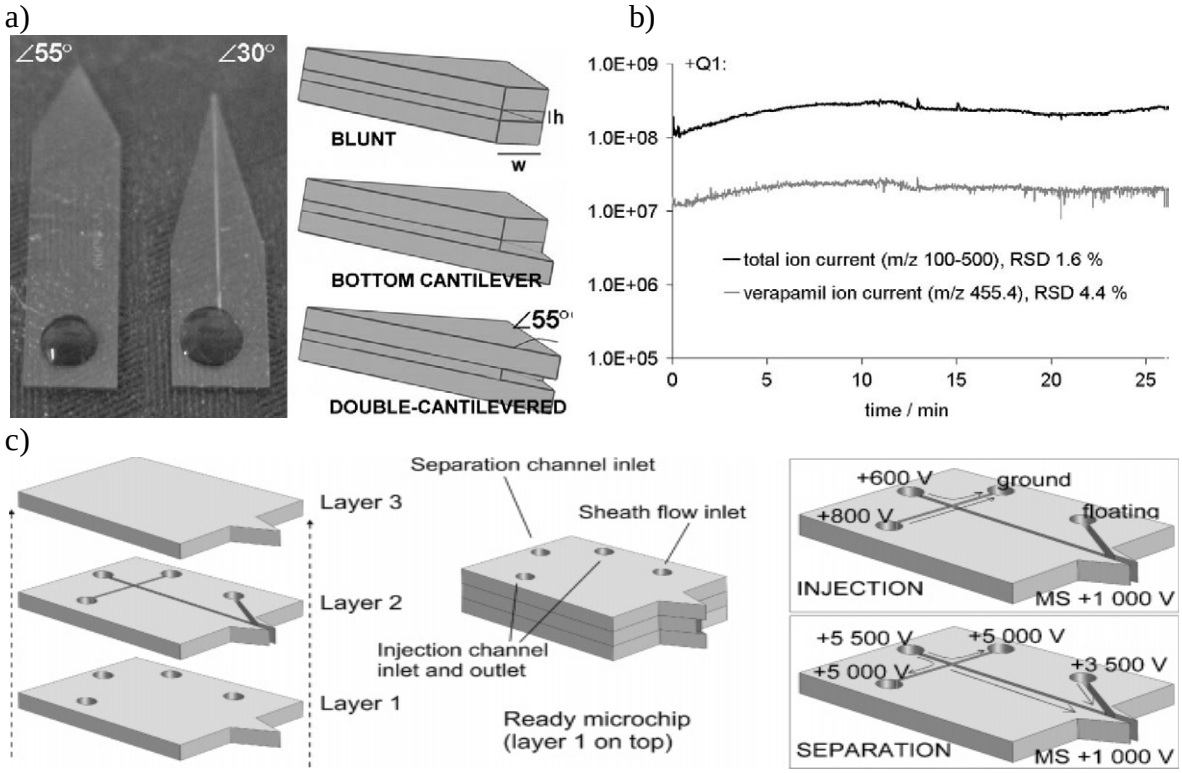

Figure 1.7. a) SU-8 electrospray microchips for mass spectrometry. **b)** Total ion current stability measured with the optimized emitter design under free flow conditions (5 µM verapamil). c) Schematic picture of design of SU-8-CE-ESI chip.[36,37]

The SU-8 polymer has also been utilized also in the fabrication of another type of ESI emitter (Fig. 1.7a).[36] The microchip was made from three separate layers of SU-8 polymer, resulting in a closed channel for spraying. Various nozzle designs were compared and the best chip design produced a stable ion emission with RSD 1.6 % for total ion current and 4.4 % for an ion current of verapamil (*m/z* 455) (Fig. 1.7b). SU-8 material properties were also studied, and it was shown to work well with acetonitrile and methanol, whereas

dichloromethane and dimethylformamide were not usable solvents due to their ability to dissolve SU-8. A high voltage of 2.5 kV was needed for stable ionization. The ESI emitter was also monolithically integrated with a capillary electrophoresis (CE) channel (Fig. 1.7c). [37]

Huikko *et al.* (2003) fabricated PDMS electrospray tips using SU-8 masters.[38] The inner dimensions of the spray channel were 10 – 25 µm x 10 µm. A high voltage of 3 – 4 kV was used and a detection limit of 20 pmol was obtained for buprenorphine in full-scan mode using a triple-quadrupole instrument. They concluded that with a long curing time in the fabrication process, high background from PDMS can be lowered to a negligible level.

Various ESI nozzle designs have been fabricated out of parylene polymer (Fig. 1.8).[39] Tapered tips of 5 µm x 10 µm produced an electrospray for 50% acetonitrile with 1% acetic acid and clear ESI mass spectra with negligible background observed for Gramicidin S with concentration of 9 µM when high voltage of 1 kV – 2 kV and a flow rate of about 50 nL/min were used.

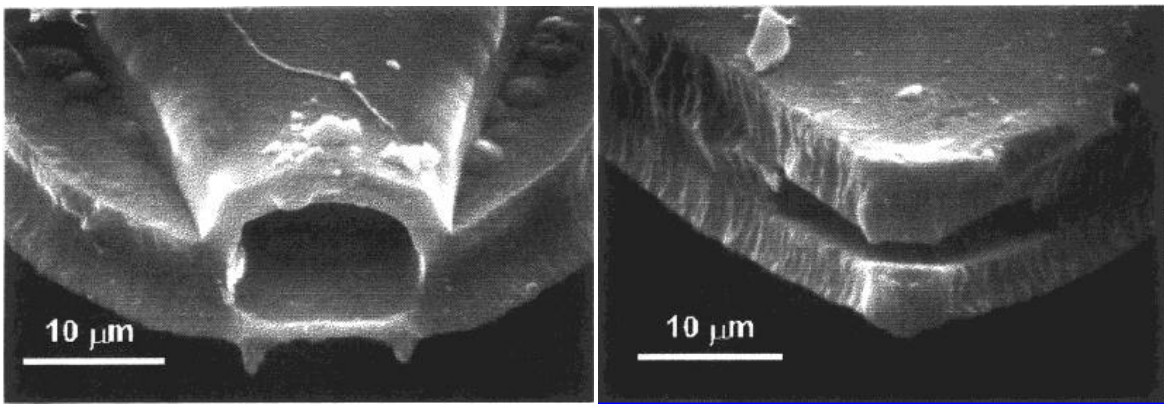

Figure 1.8. Parylene electrospray emitters with different nozzle designs.[39]

A PMMA (poly(methyl methacrylate)) disposable polymeric chip with eight electrospray nozzles for mass spectrometry was presented by Yuan and Shiea (2001).[40] This octagonal multinozzle chip contained eight open microchannels (375 µm wide, 300 µm deep, and 1.25 cm long) ending in eight separate electrospray nozzles, and it was constructed by sawing, polishing with an abrasive sheet, drilling, and cutting with a knife. These fabrication methods are available for everyone and they are cheap, although this kind of fabrication approach is not comparable to lithography or other microfabrication techniques in terms of reproducibility and mass production. A high voltage of 3.8 kV is used to form an electrospray from a solution containing 70% methanol in water. The idea of operating parallel nozzles on the same microchip can expand the usability of the chip to sequential or high throughput analysis.

In summary, various microchip designs for ESI are fabricated from glass, silicon, and different polymers such as PMMA, SU-8, PDMS, and parylene. However, these materials set limits for chip designs. Glass microfabrication techniques are cumbersome compared

to silicon micromachining and through-wafer processing is inaccurate. Polymer microfabrication is generally easy and fast, but at the moment it does not match silicon for fabrication of robust high aspect ratio structures and complex three-dimensional features which are advantageous, especially when sharp electrospray tips are fabricated. It is critical to choose the appropriate ionization solvent to match the polymer being used. If a solvent is able to dissolve a polymer it will be seen with a high background spectrum. Therefore with polymer chips the solvent to be used must be chosen carefully. The high voltage that is needed to operate the microchip defines the sharpness of electric potential around the ESI tip and also the proximity to the mass spectrometer that the microchip can be located. With a longer distance the ion gain to mass spectrometer is reduced hence the signal intensity is lower. Most of the chips were closed and had a cover. Sample application is not so easy with covered chips, because when the chip utilizes capillary action there is a clogging problem when air bubbles are formed inside the channel. If the chip doesn't use capillary action, it requires an external pump and junctions, or voltage source and electrodes, for liquid transfer. However, all of these microchips show potential for qualitative analyses with mass spectrometry, even though only one type of microchip has been shown to be suitable also for quantitative analyses with automated sampling.

1.2 Miniaturized and on-chip integrated liquid chromatography electrospray ionization microchips

Liquid chromatography (LC or high-performance liquid chromatography, HPLC) is the most common chromatographic method used in bioanalysis. HPLC is used to separate analytes due to their chemical properties mostly in particle packed or monolithic columns. Normal particle packed analytical columns have an inner diameter (ID) of 1.0 to 4.6 mm. When particle packed columns are miniaturized the packing process becomes more vulnerable as it can produce unfavorable small voids which deteriorate chromatographic separation. Therefore the need for perfect and homogenous packing is emphasized. The same challenge comes up with monolithically packed columns, where especially the batch-to-batch, repeatability is not necessarily high. Furthermore, all voids and dead volumes after the HPLC column reduce the column separation efficiency. A weak point for separate electrospray tips and HPLC columns comes from the interface between them, as the junction can give large dead volumes relative to the low flow rates. Therefore HPLC columns, which are integrated to the same microchip with an ESI emitter, provide better performance in principle.

Efforts to miniaturize HPLC columns focus on reduction of the inner diameter and extra-column dispersion sources of particle or monolithically packed columns in order to decrease flow rates, increase separation efficiency and lower detection limits.[41,42] Kutter *et al.* (2000) reviewed the possibilities and challenges of capillary electrophoresis in miniaturization, which was the first trend in miniaturization of separation channels.[43] CE is the most common technique applied to microchip separations, because it is easy to miniaturize as it needs only a narrow channel for the separation, and the electrodes needed

are easily fabricated on the microchip. For microchip HPLC columns there is a need for high pressure and to date there are not many genuinely working microchips made which are combined with MS. Tomer *et al* (1994), characterized the effect of miniaturization in HPLC where decreasing the inner diameter of the column by 100-fold increased the relative concentration at a detector over 8000-fold (Table 1.1).[44] The larger the column the higher stability and loading capacity of the column is obtained, whereas better sensitivity is achieved with the decrease of the column ID. Therefore, the choice of column dimensions is always a compromise between capacity and sensitivity.

Table 1.1. Characteristics of HPLC columns, adapted from Tomer *et al*.[44]

Column ID*	**Volume**	**Flow rate**	**Injection volume**	**Relative concentration at detector**	**Relative loading capacity**
4.6 mm	4.1 mL	1 mL/min	100 μL	1	8469
2.0 mm	783 μL	0.2 mL/min	19 μL	5.3	1598
1.0 mm	196 μL	47 μL/min	4.7 μL	21.2	400
320 μm	20 μL	4.9 μL/min	485 nL	206	41
50 μm	490 nL	120 nL/min	12 nL	8459	1

* all columns are 25 cm long.

The first article on particle packed 0.5 – 1.0 mm ID stainless steel capillaries was published in 1967,[45] and they can be considered the first miniaturized particle packed columns when compared to conventional analytical HPLC columns with 3.0 – 4.6 mm ID. Later, at the beginning of the 1980s, development of capillary LC columns was intensified.[46,47,48] Varga *et al.* published a review about miniaturization for proteomics research in 2003.[49] A year later, peptide separations with monolithically filled capillaries and a microcolumn with an integrated ESI nib were published.[50] The microchip was fabricated from SU-8 polymer and a monolithic stationary phase with C_{12} functionality was used for reversed-phase separations, however no chromatogram of microchip separations was presented. One of the first miniaturized HPLC columns combined with an integrated nanoESI source and an enrichment column with good performance was published in 2005 (Fig. 1.9).[51] The microchip was fabricated of laminated polyimide layers where channels were patterned using laser ablation technology. The drawback of using laser ablation is that each microchip has to be fabricated separately, increasing fabrication time and costs. The microchip consisted of an integrated injector, a sample enrichment column, a separation column, and a nanoESI tip. A typical flow rate on the microchip was 100 – 400 nL/min and the high voltage needed ESI was 2.4 kV. This microfluidic integration of nanoLC components allowed subfemtomole detection of tryptic digestion products. This microchip is also commercialized by Agilent Technologies (HPLC-Chip).

In 2005, Xie *et al.* published an integrated reversed-phase column with frits for bead packing, an ES nozzle, electrolysis based gradient pumps, and a low volume mixer (Fig.

1.10).[52] The microchip was fabricated on a silicon wafer using parylene and SU-8 polymers. The separation column was 12 mm long and packed with C_{18} coated particles. A flow rate of 80 nL/min was used for separations. The microchip was applied to an LC/MS analysis of a mixture of peptides from trypsin digestion. The microchip showed similar gradient separation when compared to commercial nanoflow LC separations. The flow control with integrated gradient pumps was challenging and therefore separations were difficult to get repeatable.

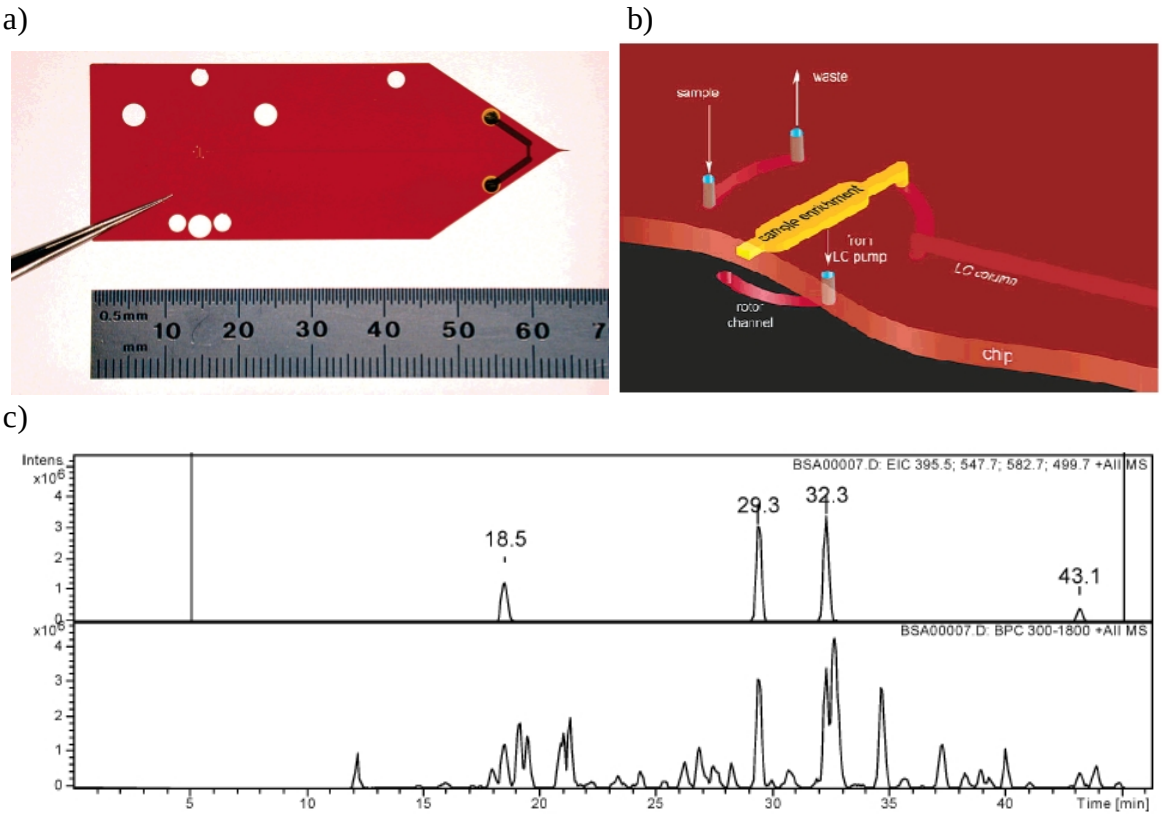

Figure 1.9. a) A polyimide microLC-ESI microchip. The dark pattern on the right end of the chip is the electrodeposited metal for contact to the fluid flow channel near the ES tip. **b)** Schematic of the chip−rotor interface shown in the LC run mode. The chip (brown) has ports (light blue) leading to the sample enrichment column (yellow) and to the LC separation column (brown). The rotor (black) has channels (red) that rotate with respect to the chip. **c)** (top) Extracted ion chromatograms of four ions (*m/z* 395.5, 547.7, 582.7, and 499.7) and (bottom) base peak chromatogram of 20 fmol BSA digest at 100 nL/min.[51]

In conclusion, only a few publications of integrated ES tips together with miniaturized HPLC columns have been published. The main challenge of the integrated microLC columns comes from the high pressure needed, thus making the production of tight fluidic connections and microchips that can tolerate high pressures critical. Furthermore, in order to obtain functional LC columns the packing procedure should be homogenous and reproducible with minimal dead volumes.

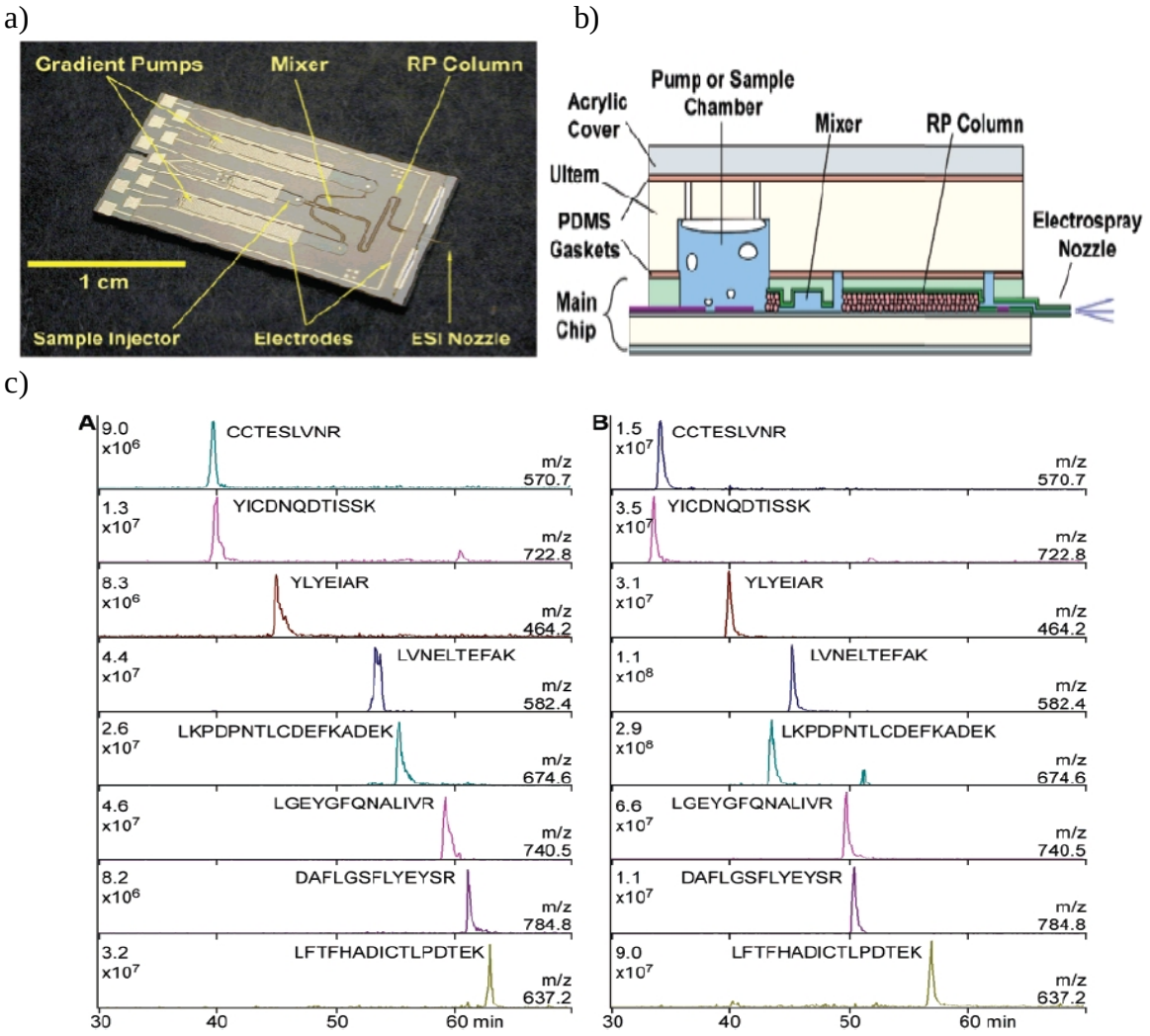

Figure 1.10. a) A photograph of a microfluidic LC-ESI microchip. **b)** A diagram of the LC-ESI microchip showing the placement of the solvent reservoir and cover plate on top of the main chip. **c)** Comparison of the extracted ion chromatograms for eight tryptic peptides from BSA separated using the microchip LC (left panel), and an Agilent 1100 series HPLC system (right panel). For the Agilent run, gradient formation started at 2 minutes. For the chip LC run, gradient formation started at time 28 minutes.[52]

1.3 Microreactors combined with mass spectrometry

One goal of microfluidics has been the integration of several functions, such as microreactors, sample pretreatment, separation, and analysis, on a single microchip.[53] Such integration would reduce the number of laborious manual steps currently used in analytical procedures. One major advantage of miniaturized fluidic chips is the reduced size because diffusion-limited reactions occur faster in microscale. Furthermore, when distances on the microchip are reduced down to micro-nanometer scales, liquid transfer is

more effective. The sample volumes required are also much smaller, which is advantageous, especially when dealing with difficult-to-obtain or otherwise expensive samples. In microscale, reactor's surface-to-volume ratios are orders of magnitude higher when compared to conventional round-bottom-flasks. Heat transfer is also improved, therefore higher reaction temperatures are reachable leading to higher product concentrations. When product concentrations are higher, the reactor volumes and amounts of catalysts can be reduced.[54] Thus, such microfluidic chips would make the reactions and analyses of samples faster and more cost-effective.

For the time being, there are only a few microchips that are capable of performing multiple functions.[55] Microreactors have been made of silicon, glass, and polymers, for various chemical and biological reactions, as previously reviewed.[56,57,58] Microscale reactors can contain packed microparticle beds, membranes, micropillars, and various kinds of fiber structures to increase surface-to-volume ratios for surface activated reactions. Liquid microreactors can contain a microscale Y-channel, where two different solutions are imported through the channels which are combined together. The reaction happens in the combined channel section. In this case, laminar flow, which exists in a microscale, is limiting the reaction rate and therefore a static micromixer is developed to increase both mixing and reaction efficiency of the microreactor. Brivio *et al.* (2005) demonstrated a microfluidic nanoreactor chip with an integrated mixer zone and a nanoESI interface for MS (Fig. 1.11).[59]

There are also other microreactors that are combined with MS. One common application area of microreactors has been enzyme based reactors which have been used for trypsin digestion of proteins where immobilized enzymes spotted on the walls of the reactorsor along the reaction channel have been utilized (Fig. 1.12a).[60] Peterson *et al.* (2002) demonstrated how to produce porous polymer monoliths with immobilized trypsin for peptide mapping and also proposed the possibility to connect ESI/MS or MALDI/MS for on-line studies of protein digests.[61] Krenkova *et al.* (2005) connected a monolithic porous mathacrylate based polymer inside a silica capillary grafted with immobilized trypsin to MS with a liquid junction microES interface (Fig. 1.12b).[62] An off-line nanoESI connection was used with trypsin immobilized in nanozeolite (Fig. 1.12c).[63] An on-line nanoESI connection to a 50 µm ID silica capillary with immobilized trypsin on capillary walls achieved 90% sequence coverage for 1 µM cytochrome c.[64] Pepsin has also been immobilized to capillary walls for LC/MS and protein identification.[65] An off-line MALDI-TOF interface,[66,67,68] an on-line HPLC, a DIOS interface[69] and a CE interface[70,71] have been used to connect trypsin reactors to MS. On-line digestion in a confluence of two liquid flows has been performed and the digestion products have been analyzed with a CE/ESI microchip.[72] In some studies porous silicon has been utilized as a carrier matrix for immobilization of enzymes.[73,74,75]

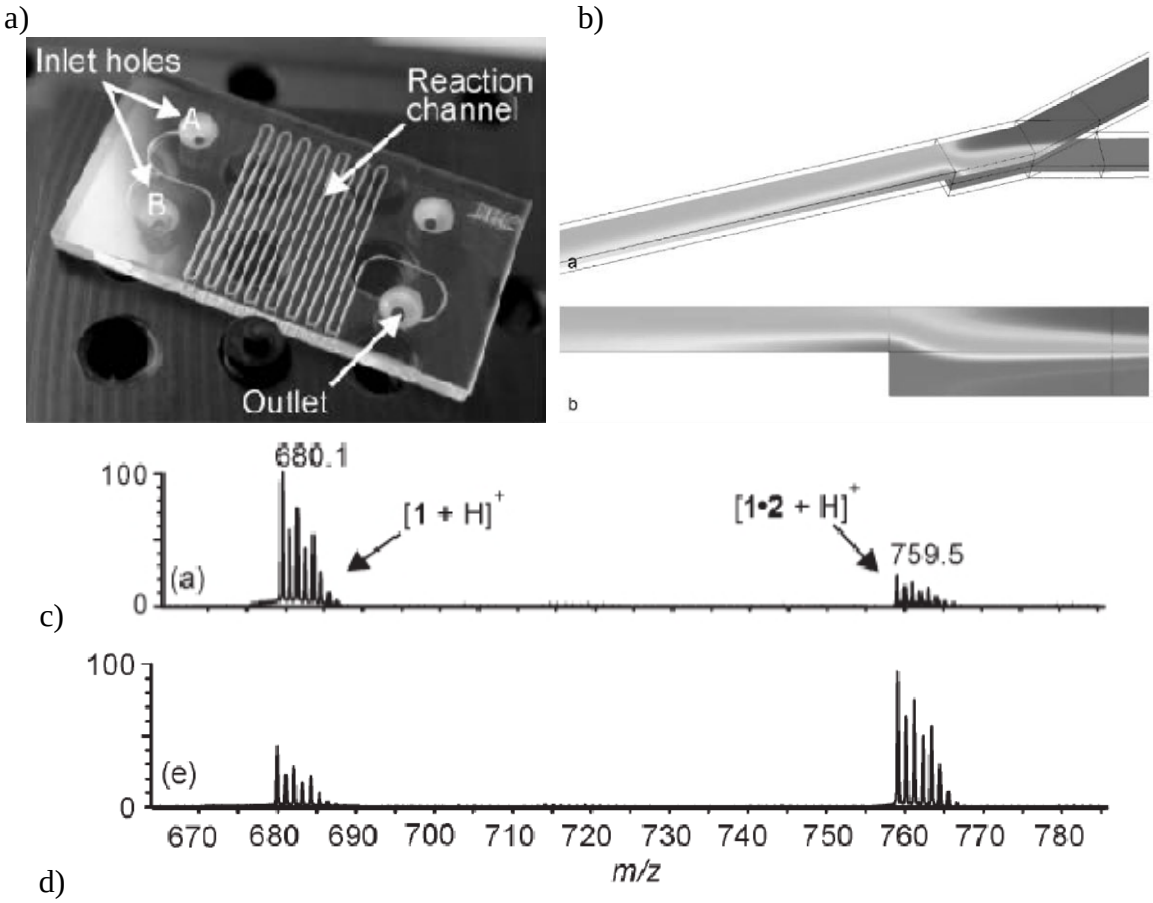

Figure 1.11. a) A glass microreactor chip with a Y-channel and a mixer. **b)** Design and simulation of a static micromixer. On-chip ESI-MS titration of Zn-porphyrin (1) with pyridine (2) performed with varying reagent injection speed ratios: (c) 9:1, (d) 1:9.[59]

Another field to which microreactors are applied is electrochemistry. Odijk *et al.* (2009) worked with a miniaturized electrochemistry cell for the study of electrochemical conversions of compounds to mimic drug metabolism reactions (Fig. 1.13).[76] The microchip contained a miniaturized electrochemical cell which had palladium and platinum electrodes and a volume of 9.6 nL. An on-line conversion efficiency of 97 % was obtained with amodiaquine, with a flow rate of 1 µL/min. They combined the microreactor chip with a liquid junction to LC/MS for sensitive analysis of the reaction products (Fig. 1.14).

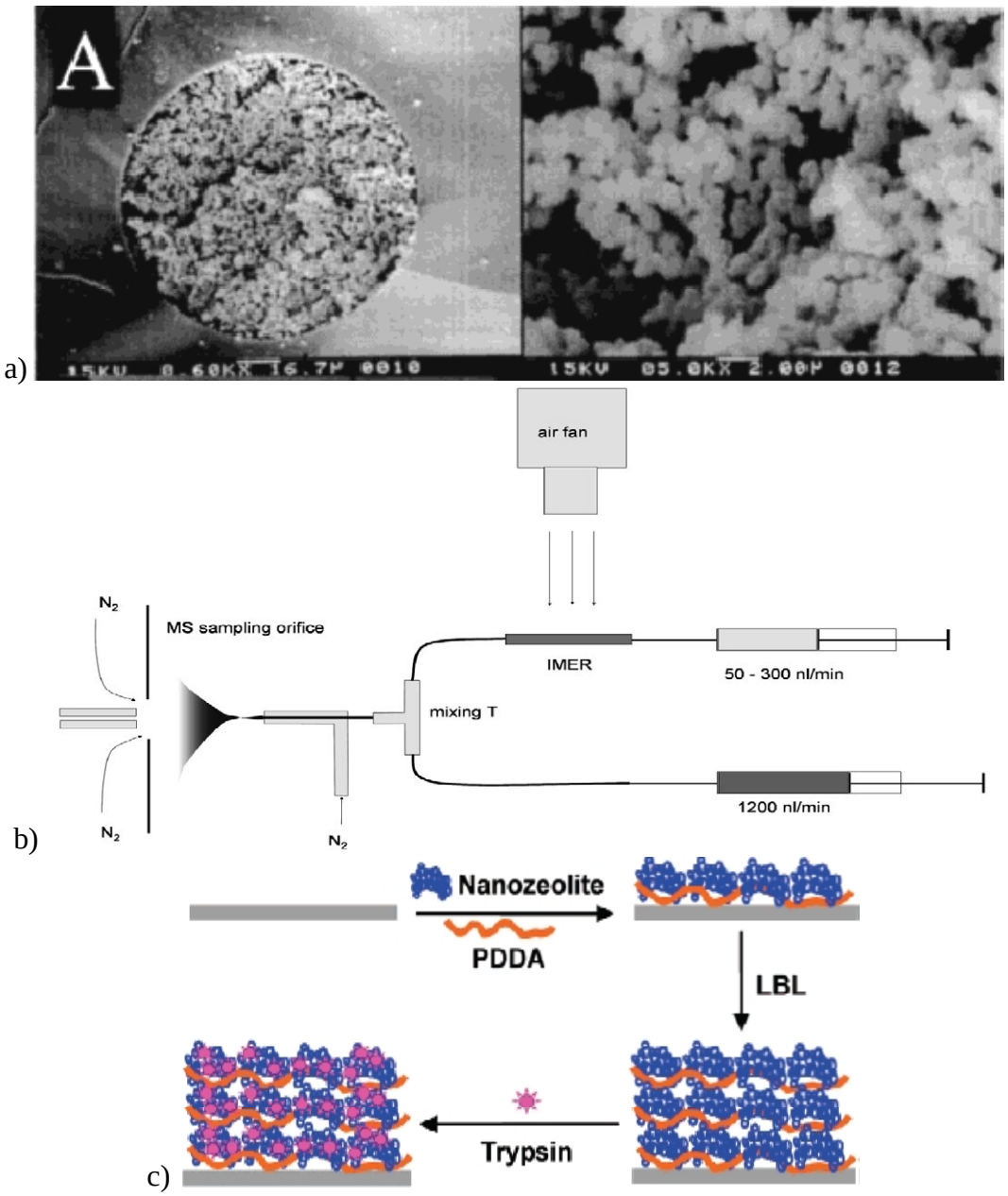

Figure 1.12. a) A SEM micrograph of porous monoliths.[61] **b)** An immobilized enzyme reactor (IMER) combined with MS with a liquid junction.[62] **c)** A microfluidic chip coating protocol based on the alternate deposition of poly(diallyldimethylammonium chloride) (PDDA) and zeolite nanocrystals.[63]

a) b)

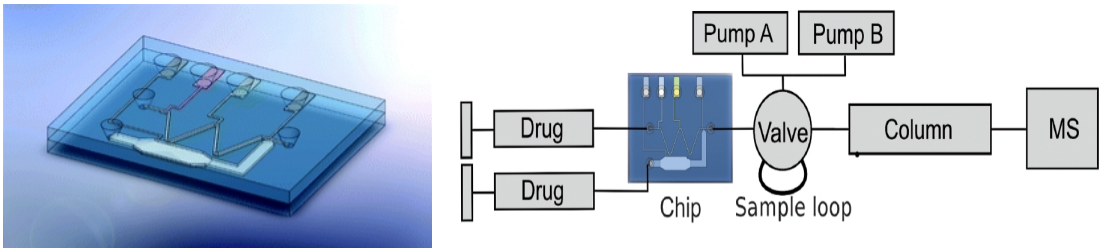

Figure 1.13. a) A miniaturized electrochemistry cell on a microchip. **b)** Combination of EC-chip to LC/MS.[76]

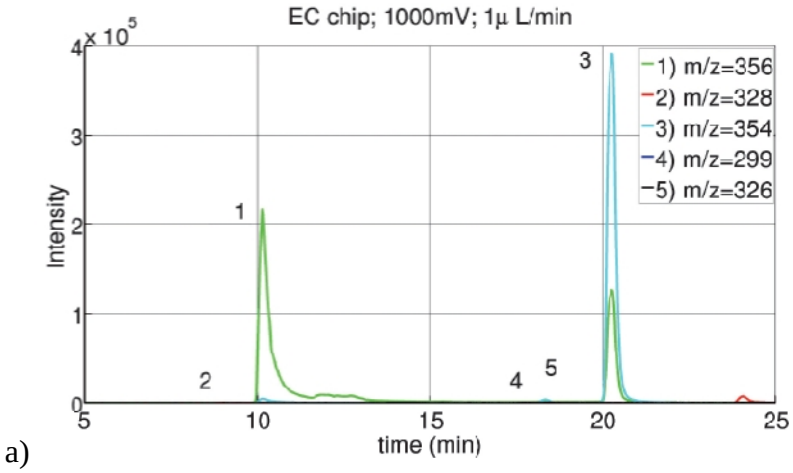

a)

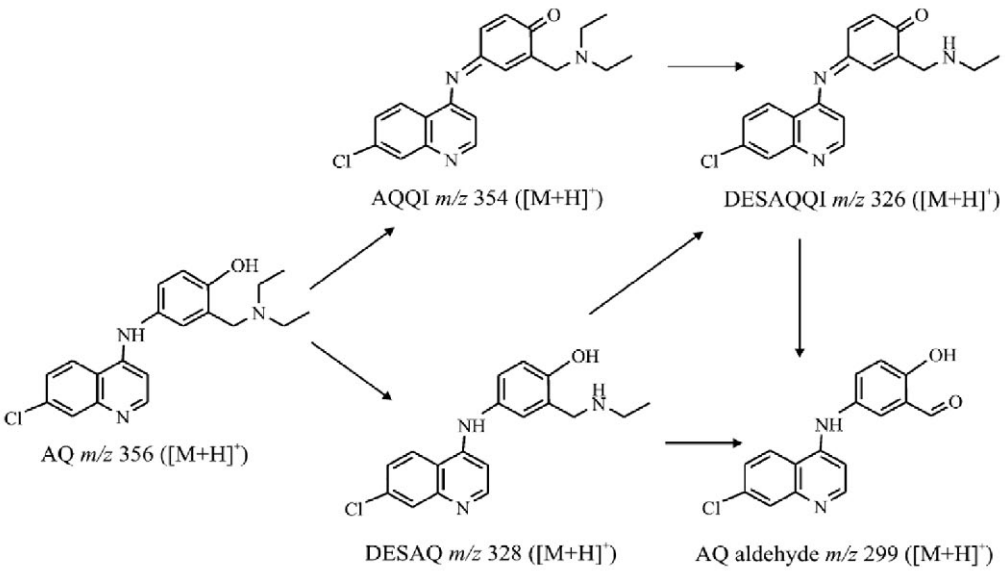

b)

Figure 1.14. a) Extracted ion chromatograms of amodiaquine reactions products produced by on-chip electrochemical conversion. **b)** Suggested amodiaquine EC conversion pathways which mimic drug metabolism pathways.[76]

1.4 Micropillar arrays in analytical applications

The focus of this chapter is on micropillar arrays, their properties, designs, materials, and analytical applications. Micropillar arrays are used to increase surface-to-volume ratios of microchannels. This property enhances surface activated reactions and all other surface based phenomena such as capillary filling. Capillary filling is based on free energy located on surfaces. The capillary is filled if the total surface energy is decreased when the liquid fills the capillary or microchannel. The contact angle of liquid to the surface is linked to surface energies. The higher the free surface energy, the lower is the contact angle. When the contact angle is low enough, liquid will spread to a surface due to higher energy of Laplace pressure from surface tension, and hydrostatic pressure. A micropillar array increases the surface area in a microchannel and thus also the free surface energy. Therefore capillary filling occurs more intensively in a pillar arrayed channel. With porous pillars, the surface area can be increased even more.

Another benefit of using micropillar arrays is that, due to lithography and deep reactive ion etching fabrication techniques, they can be ordered precisely with high aspect ratios. This is an important property when miniaturized HPLC columns are fabricated, because it has been proven experimentally that increased flow path homogeneity leads to a lower dispersion of sample in the mobile phase.[77] In order to get as homogenous a flow path for the column as possible, the micropillar arrays are superior to packed particle beds and monoliths. Liquid flows in micropillar arrays are simulated in order to optimize pillar array structure for optimal flat flow profile. The side wall effect is emphasized in miniaturized columns where the flow rate close to the side wall is reduced, producing parabolic flow profile. Therefore the side wall effects of columns should be minimized. It has been shown by simulations that the lowest band broadening in the pillar array column can be obtained using a “magic distance” between the side wall and the first pillar row.[78] The “magic distance” is determined to be 0.15 times the pillar diameter and it is valid for all practical flow rates, channel widths, and pillar diameters. The side wall effects for different kinds of pillars have also been studied, and it was noted that cylindrical and hexagonal pillars produce smaller side wall effects than others, such as diamond like quadrangle pillars.[79] In addition to non-porous pillars, porous pillars can also be fabricated with electrochemical anodization.[80] Porous pillars have higher retention capacity and mass loadability, and therefore the effect of top and bottom surfaces of the channel on the flow profile is nearly negligible.[81] Different kinds of flow distributors (i.e. distributes the flow from e.g. a 100 µm wide channel to a 1 mm wide column channel, Fig 1.15) are also studied in order to get a flow profile as flat as possible.[82] The flattest flow profile was obtained with a radially interconnected distributor with an array of diamond like quadrangular pillars (Fig 1.15 middle).

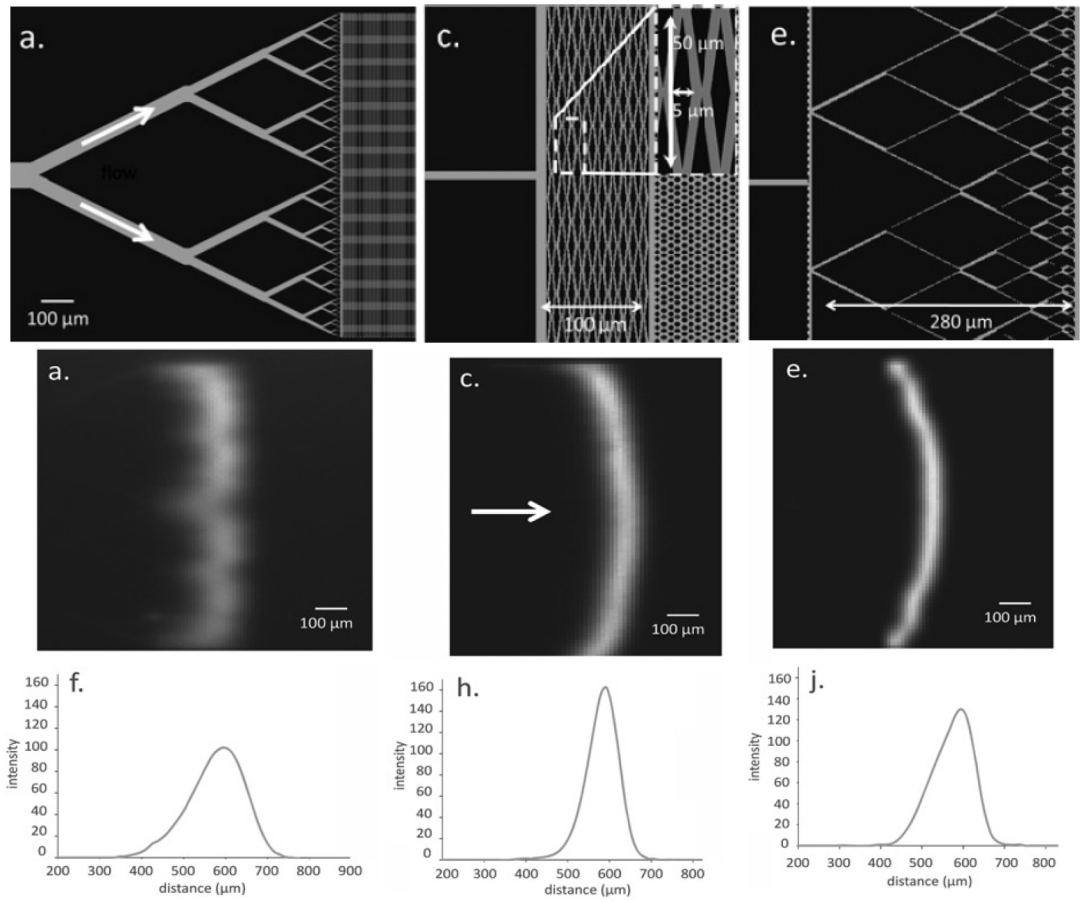

Figure 1.15. Bifurcating flow distributor (left), radially interconnected distributor (middle), and combined bifurcated and radially interconnected flow distributor (right) are shown in top row, and their flow profiles are shown in middle and bottom rows respectively.[82]

It was shown that perfectly ordered non-porous pillars, such as HPLC columns, have better performance for LC in terms of plate height *h* (Fig. 1.16) when compared with the best particle packed column and monolithically packed column.[83] However, with non-porous pillars the column capacity is lower and therefore the usability of the column is lower. Porous pillar arrays have a higher plate height but larger loading capacity. The separations in a two-dimensional (2D) micropillar array were simulated more thoroughly, leading to the conclusion that the better separation ability is achieved with more uniform the packing of the column.[84] Perfectly ordered pillar arrays, in particular, normally demonstrate better homogeneity and therefore separation efficiency than particle packed beds. The plate heights of silica monolithic columns were also predicted with computational methods[85] and the results obtained show that the plate height of monolithic columns is between those of packed and non-porous pillar columns.

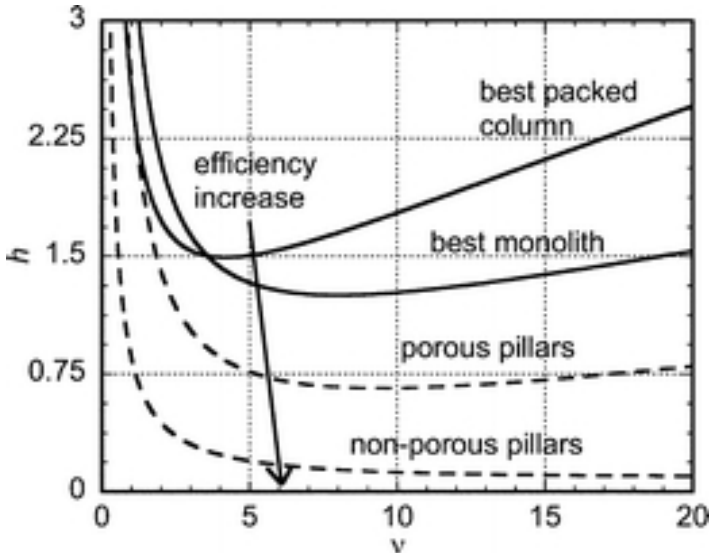

Figure 1.16. The reduced plate height *h* versus the reduced mobile phase flow velocity ν.[83] Measured curves (drawn lines) are for the best particle packed column[84] and the best monolith with a porosity of 0.8,[85] calculated curves (dotted lines) are for a porous pillar array with a porosity of 0.8 and for an array of non-porous pillars with a porosity of 0.4.[85]

Various micropillar chips have been microfabricated for chromatography since He *et al.* (2002) published inspirational articles about nanocolumns and collocated monolithic support structures (different kinds of micropillars) on separation performance for HPLC.[86,87] The micropillar arrays can also be used for size exclusion chromatography as exemplified with an analysis of blood cells (Fig. 1.17).[88] The pillar array was used for the separation of white and red blood cells and the main benefit of this kind of design was a rapid continuous separation of cells with low volumes. A quartz nanopillar array can be used as a sieving matrix for DNA fragments in an electroosmotic flow (Fig. 1.18a).[89] DNA fragments of 48.5 kilo base pairs (kbps) and 166 kbps were separated in 8 seconds where they moved a distance of 300 µm. Smaller DNA fragments could also be separated down to 1 kbps and 10 kbps (Fig. 1.18b).

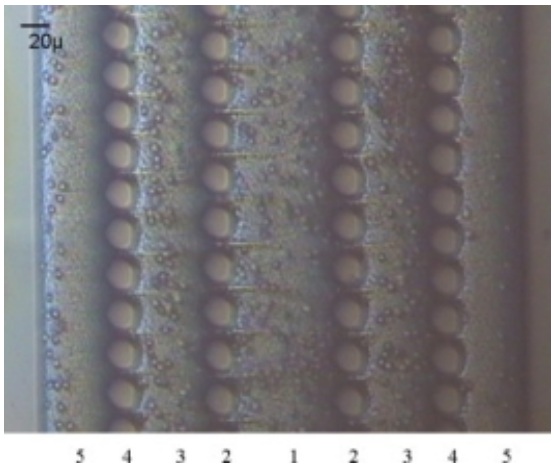

Figure 1.17. A photograph of filtration microchip for blood cell separation. The initial channel was divided into five channels of micropillars. (1) A feed stream channel for white blood cells; (2) micropillars with a gap of 6 µm, (3) channels for red blood cells, (4) micropillars with a gap of 2.5 µm, (5) channels for blood plasma.[88]

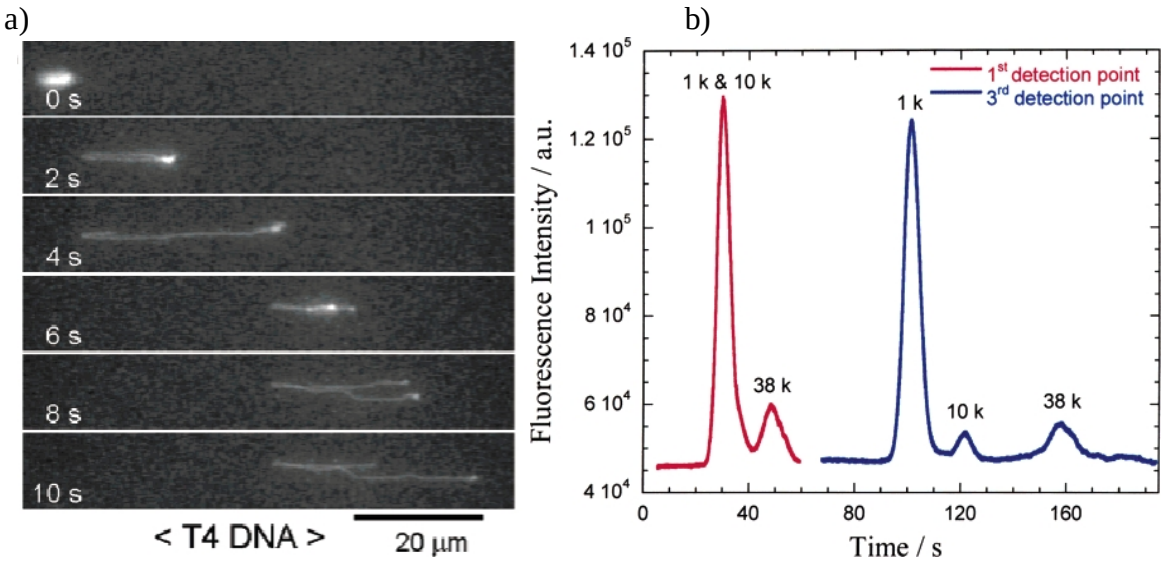

Figure 1.18. a) A T4 DNA migrating in a nanopillar region at 7 V/cm. **b)** Electropherograms for 1k, 10k, and 38 k base pair DNAs detected at 380 µm (red solid line) and 1450 µm (blue solid line) from the entrance of nanopillar channel.[89]

In the year 2007, Malsche *et al.* published micropillar array separation microchips for LC of coumarins combined with laser induced fluorescence (LIF) detection (Fig. 1.19).[90] The microchip was coated with C_8 reversed-phase material. Experimental plate heights of 2 µm and plate numbers N of 4000 – 5000 over the 10-mm long channel were achieved when the pH of the eluent was adjusted to 3. Within the micropillar array separation column it is possible to control the flow by placing micropillars wisely, therefore enabling reduction of band widening through the column at the both sidewalls of the column.[78] Another study by Mery *et al.* (2008), reported peptide separations with a micropillar array column combined with a polysilicon ESI nib.[91] Both liquid phase C_{18} and vapor phase C_{10}-perfluorated silane were tested as coating methods and materials. They were able to

separate five peptides (30 fmol) from cytochrome c trypsin digestion in 50 minutes and detect them with ESI/MS when using a C_{18} coated micropillar column (Fig. 1.20). High-aspect-ratio micropillars (1 µm diameter, 20 µm height, and 2 µm gap between pillars) covered by a silicon dioxide layer of 2 – 3 µm thickness were used as an HPLC column using fluorescence detection.[92] The microchip was covered with glass by using a polyethylene glycol-methyl ether methacrylate seal. Surprisingly, this normal-phase column indicated a hydrophobic separation mechanism. The reduced plate heights obtained were 1.1 and 1.8 µm for fluorescein and sulforhodamine B, respectively.

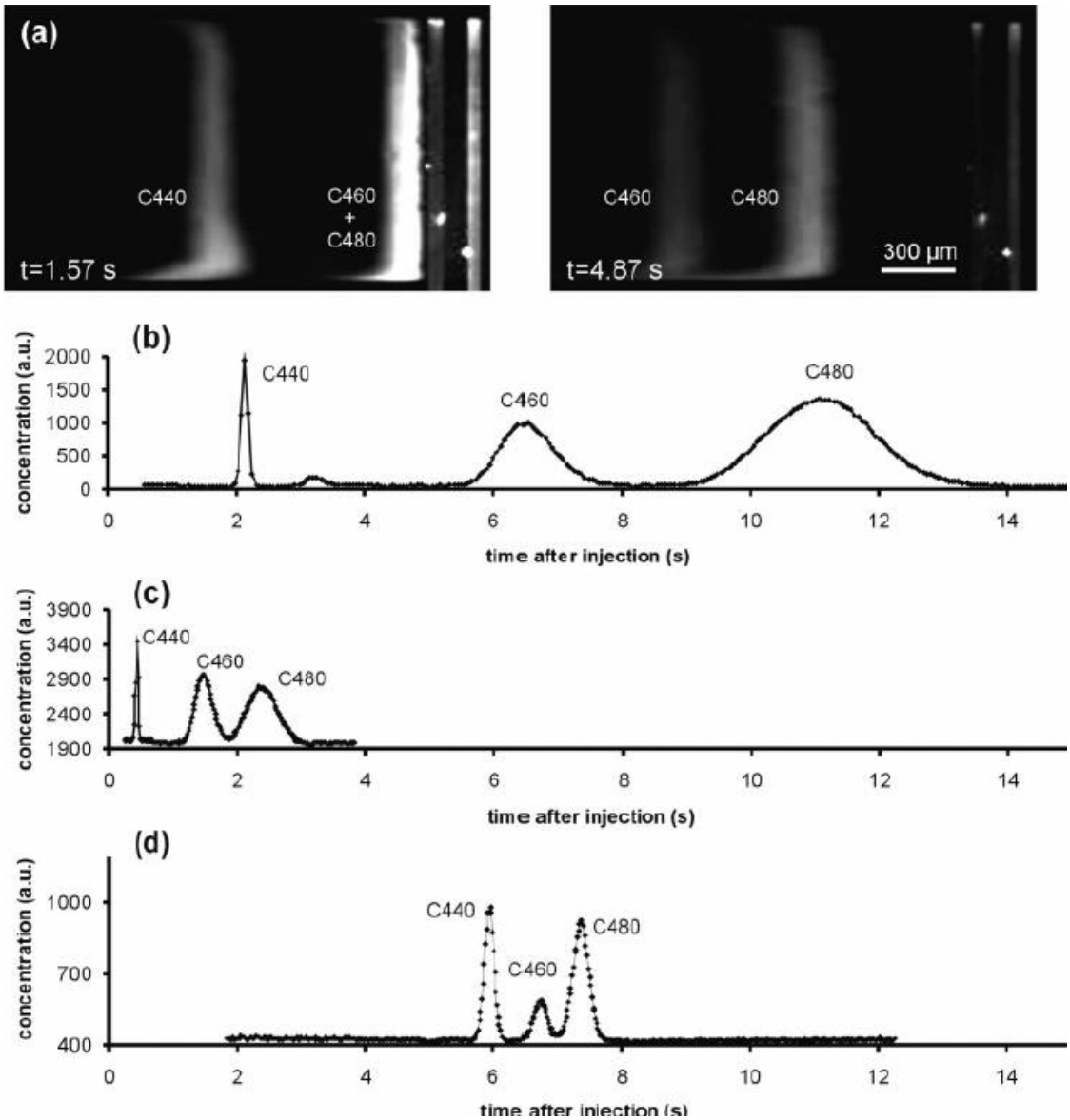

Figure 1.19. Separation of coumarins with a non-porous micropillar array using integrated injection and LIF detection.[90]

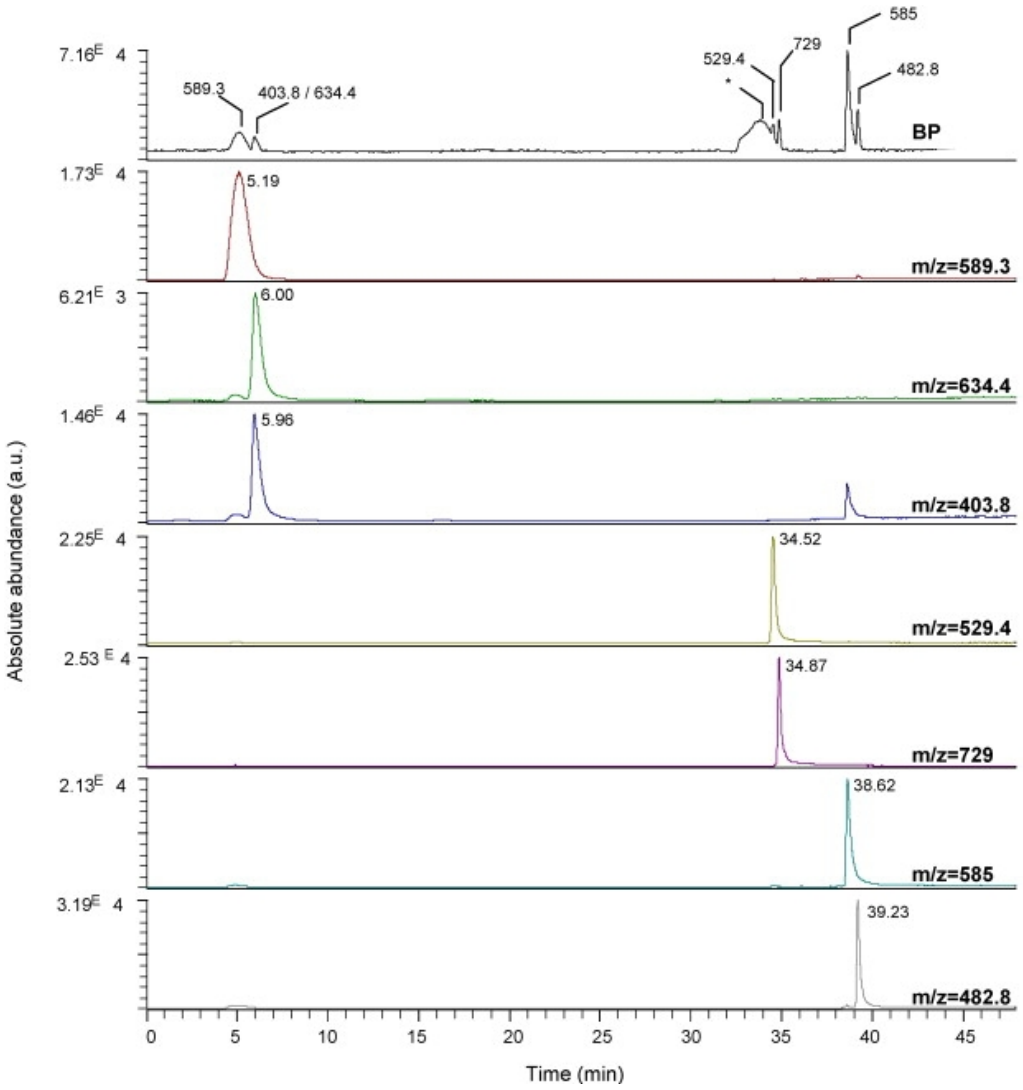

Figure 1.20. Tryptic digestion of cytochrome c analyzed with a C_{18}-grafted micropillar array LC column combined with MS. [91]

Liquid chromatographic separations were also made in a pillar array column which was fabricated from COC (cyclo olefin copolymer) (Fig. 1.21).[93] The pillar diameter was designed to be 16 µm with a distance to side wall of 2.4 µm, thus filling the requirement of the "magic distance" for minimum band broadening. The pillar array channel fabricated was 5 cm long, 4.3 µm deep, and the diameter of pillars was 15.3 µm. Due to inaccuracy of the injection molding technique the dimensions obtained were not exactly as designed. The flow path width between the pillars was 4.1 µm and the one between the side wall and the nearest pillar was 3.1 µm. External porosity was 43 % which was slightly above the value of 40 % that was originally designed for the column. The chip had an integrated 88 µm wide injection channel crossing the pillar column. Separation experiments were carried out using a solution of phosphate buffer (pH 7.0) and methanol (70/30 v/v). The chip tolerated 15 bar pressure well, which was used for separations. Absolute plate heights of 5 µm were observed for coumarin compounds.

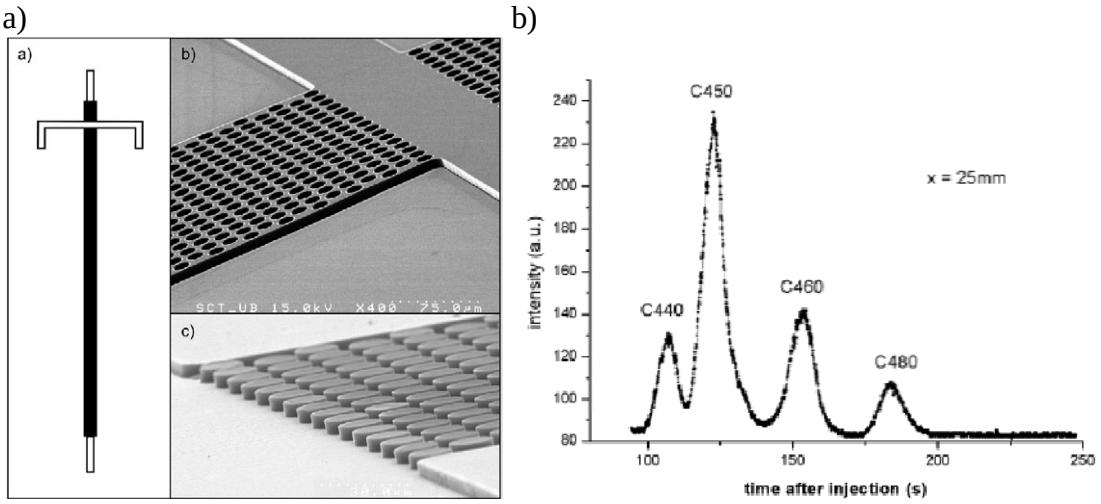

Figure 1.21. a) The design and SEM images of COC chip. **b)** Separation of four coumarins.[93]

As a conclusion, a micropillar array can be used for increasing the surface-to-volume ratio of microchannels in order to enhance reaction rates of surface activated reactions in microreactor applications. Stronger capillary action is produced with higher surface-to-volume ratios of the microchannel. Due to the multiple pathways in a micropillar array, the microflow is not prone to clogging problems. Simulations of various micropillar arrays show a possibility for a better liquid chromatographic separation performance compared to packed particle bed columns or monolithic columns. However, in practice such performance has not been obtained as yet. The micropillar array columns fabricated have been used for separations of coumarins and peptides, using fluorescence detection in most cases, and a micropillar array separation channel was combined with MS in only one study. However, no separations of drug molecules have been presented thus far.

1.5 References

1 J. A. Nollet, Recherches sur les causes particulières des phénomènes électriques, 1ére edn., Chez les fréres Guerin, Paris, 1749.

2 J. Fenn, M. Mann, C. Meng, S. Wong and C. Whitehouse, Electrospray ionization for mass spectrometry of large biomolecules, Science, 246, 67-71, 1989.

3 P. Kebarle and U. Verkerk, Electrospray: From ions in solution to ions in the gas phase, what we know now, Mass Spec. Rev. 28, 898-917, 2009.

4 M. Yamashita and J. Fenn, Electrospray ion source. Another variation on the free-jet theme, J. Phys. Chem. 88, 4451-4459, 1984.

5 M. Yamashita and J. Fenn, Negative ion production with the electrospray ion source, J. Phys. Chem. 88, 4671-4675, 1984.

6 G. Taylor, Disintegration of Water Drops in an Electric Field, Proc. R. Soc. London, Ser. A, 280, 383–397, 1964.

7 J. Iribarne and B. Thomson, On the evaporation of small ions from charged droplets, J. Chem. Phys., 64, 2287-2294, 1976.
8 B. Thomson and J. Iribarne, Field induced ion evaporation from liquid surfaces at atmospheric pressure, J. Chem. Phys. 71, 4451, 1979.
9 Alessandro Gomez and Keqi Tang, Charge and fission of droplets in electrostatic sprays, Phys. Fluids 6, 404, 1994.
10 M. Dole, L.Mack, and R. Hines, Molecular Beams of Macroions, J. Chem. Phys., 49, 2240-2249, 1968.
11 R. King, R. Bonfiglioa, C. Fernandez-Metzlera, C. Miller-Steina and T. Olaha, Mechanistic investigation of ionization suppression in electrospray ionization, J. Am. Soc. MS, 11, 942-950, 2000.
12 T. Annesley, Ion Suppression in Mass Spectrometry, Clinical Chemistry, 49, 7, 1041–1044, 2003.
13 M. Prudent and H. H. Girault, Functional electrospray emitters, Analyst, 134, 2189–2203, 2009.
14 T. Sikanen, S. Franssila, T. J. Kauppila, R. Kostiainen, T. Kotiaho, and R. A. Ketola, Microchip technology in mass spectrometry, Mass Spectrometry Reviews, 29, 351-391, 2010.
15 S. Koster and E. Verpoorte, A decade of microfluidic analysis coupled with electrospray mass spectrometry: An overview, Lab Chip, 7, 1394–1412, 2007.
16 I. M. Lazar, J. Grym and F. Foret, Microfabricated devices: A new sample introduction approach to mass spectrometry, Mass Spectrom. Rev. 25, 4, 573–594, 2006.
17 M. Wilm and M. Mann, Electrospray and Taylor-Cone theory, Dole's beam of macromolecules at last, Int. J. Mass Spectrom. Ion Process, 136, 167–180, 1994.
18 M. Wilm and M. Mann, Analytical Properties of the Nanoelectrospray Ion Source, Anal. Chem., 68, 1–8, 1996.
19 M. Belov, M. Gorshkov, H. Udseth, G. Anderson, R. Smith, Zeptomole-sensitivity electrospray ionization-fourier transform ion cyclotron resonance mass spectrometry of proteins. Anal Chem, 72, 2271–2279, 2000.
20 R. Ramsey, J. Ramsey, Generating electrospray from microchip devices using electroosmotic pumping. Anal Chem, 69, 1174–1178, 1997.
21 A. Desai, Y. Tai, M. Davis, T. Lee, A MEMS electrospray nozzle for mass spectrometry. Proc Transducers ’97 (Chicago, IL), pp. 927–930, 1997.
22 W. Kim, M. Guo, P. Yang, D. Wang, Microfabricated monolithic multinozzle emitters for nanoelectrospray mass spectrometry. Anal Chem, 79, 3703–3707, 2007.
23 S. Arscott, S. Le Gac, C. Rolando, A polysilicon nanoelectrospray-mass spectrometry source based on a microfluidic capillary slot. Sens Actuators B 106, 741–749, 2005.
24 S. Arscott, S. Le Gac, C. Druon, P. Tabourier, C. Rolando, Polysilicon nanoelectrospray emitter tips for mass spectrometry, Sens. and Act. B, 106, 241-249, 2005.

25 S. Le Gac, S. Arscott, C. Rolando, An open design microfabricated nib-like nanoelectrospray emitter tip on a conducting silicon substrate for the application of the ionization voltage, J. Am. Soc. Mass Spectrom., 17, 75-80, 2006.
26 M. Brinkmann, S. Arscott, S. Le Gac, C. Druon, P. Tabourier, C. Rolando, R. Blossey, Microfluidic design rules for capillary-slot based electrospray sources, Appl. Phys. Lett., 85, 2140-2142, 2004.
27 G. Schultz, T. Corso, S. Prosser and S. Zhang, A Fully integrated monolithic microchip electrospray device for mass spectrometry, Anal. Chem. 72, 4058–4063, 2000.
28 J. Dethy, B. Ackermann, C. Delatour, J. Henion, G. Schultz. Demonstration of direct bioanalysis of drugs in plasma using nanoelectrospray infusion from a silicon chip coupled with tandem mass spectrometry. Anal Chem 75, 805–811, 2003.
29 J. McDonald, D. Duffy, J. Anderson, D. Chiu, H. Wu, O. Schueller, and G. Whitesides Fabrication of microfluidic systems in poly(dimetgylsiloxane) Electrophoresis 21. 27–40 2000.
30 S. Le Gac, S. Arscott, and C. Rolando, A planar microfabricated nanoelectrospray tip based on a capillary slot, Electrophoresis, 24, 3640-3647, 2003.
31 S. Le Gac, S. Arscott, and C. Rolando, Two-dimensional microfabricated sources for nanoelectrospray, J. Mass Spectrom., 38, 1259-1264, 2003.
32 S. Arscott, S. Le Gac, C. Druon, P. Tabourier, and C. Rolando. A planar on-chip micro-nib interface for NanoESI-MS microfluidic applications, J. Micromech. Microeng., 14, 310-316, 2004.
33 S. Le Gac, S. Arscott, C. Cren-Olivé, and C. Rolando, A novel nib-like design for microfabricated nanospray tips, J. Am. Soc. Mass Spectrom. 15, 409-412, 2004.
34 S. Arscott, S. Le Gac, C. Druon, P. Tabourier, C. Rolando, A Micro-nib nanoelectrospray source for mass spectrometry, Sens. and Act. B. 98, 140-147, 2004.
35 S. Arscott, S. Le Gac, C. Druon, P. Tabourier, and C. Rolando, A micromachined 2D nanoelectrospray emitter, Electronic letters, 39, 1702-1703, 2003.
36 T. Sikanen, S. Tuomikoski, R. Ketola, R. Kostiainen, S. Franssila, and T. Kotiaho, Analytical characterization of microfabricated SU-8 emitters for electrospray ionization mass spectrometry. J Mass Spectrom. 43, 726–735, 2008.
37 T. Sikanen, S. Tuomikoski, R.A. Ketola, R. Kostiainen, S. Franssila, and T. Kotiaho, Fully microfabricated and integrated SU-8-based capillary electrophoresis-electrospray ionization microchips for mass spectrometry. Anal Chem. 79, 9135–9144, 2007.
38 K. Huikko, P. Östman, K. Grigoras, S. Tuomikoski, V.-M. Tiainen, A. Soininen, K. Puolanne, A. Manz, S. Franssila, R. Kostiainen, and T. Kotiaho, Poly(dimethylsiloxane) electrospray devices fabricated with diamond-like carbon–poly(dimethylsiloxane) coated SU-8 masters, Lab chip, 3, 67–72, 2003.
39 L. Licklider, X Wang, A Desai, Y. Tai, and T. Lee, A micromachined chip-based electrospray source for mass spectrometry. Anal Chem 72, 367–375, 2000.
40 C-H. Yuan and J. Shiea, Sequential Electrospray Analysis Using Sharp-Tip Channels Fabricated on a Plastic Chip, Anal. Chem. 73, 1080-1083, 2001.

41 P. Myers and K. Bartle, Miniaturization in LC-MS, Recent applications in LC-MS, LCGC Europe, Nov 2, 2002
42 J. Abian, A. Oosterkamp, and E. Gelpì, Comparison of Conventional, Narrow-bore and Capillary Liquid Chromatography/Mass Spectrometry for Electrospray Ionization Mass Spectrometry: Practical Considerations, J. Mass Spectrom. 34, 244-254, 1999.
43 J.P. Kutter, Current developments in electrophoretic and chromatographic separation methods on microfabricated devices, Trends. Anal. Chem. 19, p. 352, 2000.
44 K. Tomer, M. Moseley, L. Deterding, and C. Parker, Capillary liquid chromatography/mass spectrometry, Mass Spectrom .Rev . 13, 431, 1994.
45 C. Horvath, B. Preiss, and S. Lipsky. Fast Liquid Chromatography: An Investigation of Operating Parameters and the Separation of Nucleotides on Pellicular Ion Exchangers Anal Chem. 39, 1422, 1967.
46 R. Kennedy and J. Jorgenson, Quantitative Analysis of Individual Neurons by Open Tubular Liquid Chromatography with Voltammetric, Anal. Chem. 61, 436-441, 1989.
47 R. Kennedy and J. Jorgenson, Preparation and Evaluation of Packed Capillary Liquid Chromatography Columns with Inner Diameters from 20 to 50 µm. Anal. Chem. 61, 1128, 1989.
48 F. Yang, Fused-silica narrow-bore microparticle-packed-column high-performance liquid chromatography, Chrom. A. 236, 2, 265-277, 1982.
49 G. Marko-Varga, J. Nilsson, and T. Laurell. New directions of miniaturization within the proteomics research area, Electrophoresis. 24, 352, 2003.
50 S. Le Gac, J. Carlier, C. Cren-Olivé, J.-C. Camart, and C. Rolando, Monoliths for microfluidics devices in proteomics, J. Chrom. B. 808, 3-14, 2004.
51 H. Yin, K. Killeen, R. Brennen, D. Sobek, M. Werlich, and T. Van der Goor. Microfluidic chip for peptide analysis with an integrated HPLC column, enrichment column, and nanoelectrospray tip. Anal Chem. 77, 527–533, 2005.
52 J. Xie, Y. Miao, J. Shih, Y. Tai, T. Lee. Microfluidic platform for liquid chromatography-tandem mass spectrometry analyses of complex peptide mixtures. Anal Chem. 77, 6947–6953, 2005.
53 A. Manz, N. Graber, and H. Widmer, Miniaturized total chemical analysis systems: a novel concept for chemical sensing, Sens. Actuators B, 1, 244-248, 1990.
54 A. Renken and L. Kiwi-Minsker, Microstructured Catalytic Reactors, Advances in Catalysis, 53, 2010.
55 T. Thorsen, S. J. Maerkl, S. Quake, Microfluidic Large-Scale Integration, Science 298, 580-584, 2002.
56 J. McMullen and K. Jensen, Integrated Microreactors for Reaction Automation: New Approaches to Reaction Development, Annu. Rev. Anal. Chem. 3, 19–42, 2010.
57 G. Doku, W. Verboom, D. Reinhoudt, and A. van den Berg, On-microchip multiphase chemistry—a review of microreactor design principles and reagent contacting modes, Tetrahedron 61, 2733-2742, 2005.
58 K. Jensen, Microreaction engineering — is small better?,Chem. Engin. Sci., 56, 293-303, 2001.

59 M. Brivio, R. Oosterbroek,W. Verboom, A. van den Berg, and D. N. Reinhoudt, Simple chip-based interfaces for on-line monitoring of supramolecular interactions by nano-ESI MS, Lab Chip, 5, 1111–1122, 2005.
60 A. Cingöz, F. Hugon-Chapuis, and V. Pichon, Evaluation of various immobilized enzymatic microreactors coupled on-line with liquid chromatography and mass spectrometry detection for quantitative analysis of cytochrome c, J. Chromatogr. A, 1209, 95-103, 2008.
61 D. Peterson, T. Rohr, F. Svec, and J. Fréchet, Enzymatic Microreactor-on-a-Chip: Protein Mapping Using Trypsin Immobilized on Porous Polymer Monoliths Molded in Channels of Microfluidic Devices, Anal. Chem., 74, 4081–4088, 2002.
62 J. Krenkova, Z. Bilkova, and F. Foret, Characterization of a monolithic immobilized trypsin microreactor with on-line coupling to ESI-MS. J. Sep. Sci. 28, 1675-1684, 2005.
63 J. Ji, Y. Zhang, X. Zhou, J. Kong, Y. Tang, B. Liu, Enhanced Protein Digestion through the Confinement of Nanozeolite-Assembled Microchip Reactors. Anal. Chem. 80, 2457-2463, 2008.
64 C. Zhao, H. Jiang, D. Smith, S. Bruckenstein, and T. Wood, Integration of an On-Line Protein Digestion Microreactor and a Nanoelectrospray Emitter for Rapid Peptide Mapping, Anal. Biochem. 359, 167-175, 2006.
65 J. Ma, J. Liu, L. Sun, L. Gao, Z. Liang, L. Zhang, and Y. Zhang. Coupling formic acid assisted solubilization and online immobilized pepsin digestion with strong cation exchange and microflow reversed-phase liquid chromatography with electrospray ionization tandem mass spectrometry for integral membrane proteome analysis, Anal. Chem., 82, 9622–9625, 2010.
66 X. Xu, X. Wang, Y. Liu, B. Liu, H. Wu, and P. Yang, Trypsin entrapped in poly(diallyldimethylammonium chloride) silica sol-gel microreactor coupled to matrix-assisted laser desorption/ionization time-of-flight mass spectrometry, Rapid Commun. Mass Spectrom. 22, 1257-1264, 2008.
67 A. Palm and M. Novotny, Analytical characterization of a facile porous polymer monolithic trypsin microreactor enabling peptide mass mapping using mass spectrometry, Rapid Commun. Mass Spectrom. 18, 1374-1382, 2004.
68 S. Wang, Z. Chen, P. Yang, and G. Chen, Trypsin-immobilized fiber core in syringe needle for highly efficient proteolysis, Proteomics 8, 1785-1788, 2008.
69 K. Nichols, S. Azoz, and H. Gardeniers, Enzyme kinetics by directly imaging a porous silicon microfluidic reactor using desorption/ionization on silicon mass spectrometry, Anal. Chem. 80, 8314-819, 2008.
70 R. Schoenherr, M. Ye, M. Vannatta, and N. Dovichi, CE-microreactor-CE-MS/MS for protein analysis, Anal. Chem. 79, 2230-2238, 2007.
71 C. Wang, R. Oleschuk, F. Ouchen, J. Li, P. Thibault, and D. J. Harrison. Integration of immobilized trypsin bead beds for protein digestion within a microfluidic chip incorporating capillary electrophoresis separations and an electrospray mass spectrometry interface, Rapid Commun. Mass Spectrom. 14, 1377-1383, 2000.

72 P. Hoffmann, U. Häusig, P. Schulze, and D. Belder, Microfluidic Glass Chips with an Integrated Nanospray Emitter for Coupling to a Mass Spectrometer, Angew. Chem. Int. Ed. 46, 4913-4916, 2007.
73 J. Drott, K. Lindström, L. Rosengren, and T. Laurell, Porous silicon as the carrier matrix in microstructured enzyme reactors yielding high enzyme activities, J. Micromech. Microeng. 7, 14-23, 1997.
74 A. Ressine, S. Ekström, G. Marko-Varga, and T. Laurell, Macro-/nanoporous silicon as a support for high-performance protein microarrays. Anal. Chem. 75, 6968-6974, 2003.
75 C. Melander, D. Momcilovic, C. Nilsson, M. Bengtsson, H. Schagerlöf, F. Tjerneld, T. Laurell, C. Reimann, and L. Gorton, Microchip immobilized enzyme reactors for hydrolysis of methyl cellulose, Anal. Chem. 77, 3284-3291, 2005.
76 M. Odijk, A. Baumann, W. Lohmann, F. van den Brink, W. Olthuis, U. Karst, and A. van den Berg. A microfluidic chip for electrochemical conversions in drug metabolism studies, Lab Chip, 9, 1687–1693, 2009.
77 M. De Pra, W. Kok, J. Gardeniers, G. Desmet, S. Eeltink, J. van Nieuwkasteele, and P. Schoenmakers, Experimental Study on Band Dispersion in Channels Structured with Micropillars, Anal. Chem, 78, 6519-6525, 2006.
78 N. Vervoort, J. Billen, P. Gzil, G. V. Baron, and G. Desmet, Importance and Reduction of the Sidewall-Induced Band-Broadening Effect in Pressure-Driven Microfabricated Columns, Anal. Chem. 2004, 76, 4501-4507.
79 J. Vangelooven and G. Desmet, Theoretical optimisation of the side-wall of micropillar array columns using computational fluid dynamics, Journal of Chromatography A, 1217, 8121–8126, 2010.
80 M. De Pra, W. Kok, J. Gardeniers, G. Desmet, S. Eeltink, J. van Nieuwkasteele, and P. Schoenmakers, Experimental Study of Porous Silicon Shell Pillars under Retentive Conditions, Anal. Chem., 2006, 78 (18), pp 6519–6525
81 J. De Smet, P. Gzil, G. Baron, and G. Desmet, On the 3-dimensional effects in etched chips for high performance liquid chromatography-separations, J. Chromatogr. A, 1154, 189–197, 2007.
82 J. Vangelooven, W. De Malsche, J. Op De Beeck, H. Eghbali, H. Gardeniers, and G. Desmet, Design and evaluation of flow distributors for microfabricated pillar array columns, Lab Chip, 10, 349–356, 2010.
83 J. Eijkel, Chip-based HPLC: the quest for the perfect column, Lab Chip, 7, 815–817, 2007.
84 P. Gzil, N. Vervoort, G. V. Baron, and G. Desmet, Advantages of Perfectly Ordered 2-D Porous Pillar Arrays over Packed Bed Columns for LC Separations: A Theoretical Analysis, Anal. Chem., 75, 6244–6250, 2003.
85 P. Gzil, J. De Smet, and G. Desmet, A discussion of the possible ways to improve the performance of silica monoliths using a kinetic plot analysis of experimental and computational plate height data. J. Sep. Sci. 29, 12, 1675–1685, 2006.
86 B. He, N. Tait, and F. Regnier, Fabrication of Nanocolumns for Liquid Chromatography, Anal. Chem., 70, 3790–3797, 1998.

87 B. Slentz, N. Penner, and F. Regnier, Geometric effects of collocated monolithic support structures on separation performance in microfabricated systems, J. Sep. Sci. 25, 1011–1018, 2002.
88 X. Chen, D. Cui, C. Liu, and H. Li, Microfluidic chip for blood cell separation and collection based on crossflow filtration. Sens. Act. B, 130, 1, 216-221, 2008.
89 N. Kaji, Y. Tezuka, Y. Takamura, M. Ueda, T. Nishimoto, H. Nakanishi, Y. Horiike, and Y. Baba, Separation of Long DNA Molecules by Quartz Nanopillar Chips under a Direct Current Electric Field, Anal. Chem. 76, 15-22, 2004.
90 W. De Malsche, H. Eghbali, D. Clicq, J. Vagelooven, H. Gardeniers, and G. Desmet. Pressure-Driven Reverse-Phase Liquid Chromatography Separations in Ordered Nonporous Pillar Array Columns. Anal. Chem. 79, 5915, 2007.
91 E. Mery, F. Ricoul, N. Sarrut, O. Constantin, G. Delapierre, J. Garin, and F. Vinet, A silicon microfluidic chip integrating an ordered micropillar array separation column and a nano-electrospray emitter for LC/MS analysis of peptides. Sens Actuators B, 134, 438–446, 2008.
92 L. Taylor, N. Lavrik, M. Sepaniak. High-aspect-ratio, silicon oxide-enclosed pillar structures in microfluidic liquid chromatography, Anal. Chem. 82, 9549-9556, 2010.
93 X. Illa, W. De Malsche, J. Bomer, H. Gardeniers, J. Eijkel, J. Morante, A. Romano-Rodríguez, and G. Desmet, An array of ordered pillars with retentive properties for pressure-driven liquid chromatography fabricated directly from an unmodified cyclo olefin polymer, Lab.Chip, 9, 511–1516, 2009.

2 Aims of the study

The aim of this research was to develop an analytical microchip platform that can be modified for various analytical purposes in electrospray ionization mass spectrometry. The aims for the analytical platform were simple and rapid usability, high sensitivity, and cost efficient fabrication for disposable use.

The more detailed aims of the research papers (I-VI) were:

1. To demonstrate the usability of the µPESI-chip for electrospray ionization and combine it with mass spectrometry.
2. To show principles that affect on the chip action, such as capillary forces on pillar array.
3. To develop a method for protein analyses that facilitates the chip platform, and show the benefits of direct analyses of on chip made protein digestions.
4. To develop an on-chip method to mimic phase I metabolism for direct ESI/MS analyses
5. To develop a platform for rapid analyses and high throughput screening with ESI/MS.
6. To develop an integrated microchip based liquid chromatographic column-ES ion source for MS.

3 Silicon micropillar array electrospray chip for drug and biomolecule analysis (I)

We have developed a lidless micropillar array electrospray ionization chip (µPESI) combined with mass spectrometry (MS) for analysis of drugs and biomolecules. The µPESI chip, made of silicon, contains a sample introduction spot for a liquid sample, an array of micropillars (diameter, height, and distance between pillars in the range of 15–200, 20–40, and 2–80 µm, respectively), and a sharpened tip for direct electrospray formation. The microchips were fabricated using deep reactive ion etching (DRIE) which results in accurate dimensional control. The chip, providing a reliable open-channel filling structure based on capillary forces and an electrospray emitter tip for ionization, allows an easy operation and reliable, non-clogging liquid transfer. The µPESI chip can be used for a fast analysis using single sampling or for continuous infusion measurements using a syringe pump for sample introduction. The µPESI-MS shows high sensitivity, with a limit of detection of 30 pmol/L (60 amol or 28 fg) for verapamil measured with tandem mass spectrometry (MS/MS) and using a sample volume of 2.5 µL. The system also shows good quantitative linearity ($r^2 > 0.99$) with a linear dynamic range of at least six orders of magnitude and good ion current stability (standard deviation <5%) in 1-hour continuous flow measurement. The µPESI-MS is shown to be a very potent method for direct analysis of drugs and biomolecules.

3.1 Introduction

The trend in analytical chemistry during recent years has been the miniaturization of analytical devices, using microfabrication technology. The goal is to integrate different miniaturized components on a lab-on-a-chip device, allowing faster and cheaper analyses with smaller amounts of sample than with conventional analytical devices. The common means of transferring liquids in microchannels of lab-on-a-chip devices are electro-osmosis or pressure-driven flows. The drawback with both of these techniques is that an additional device, such as a pump or a high-voltage supply, is needed.

Capillary forces provide simple self-filling in microchannels which eliminates the use of external pumps or high-voltage supplies for liquid transfer. The simplicity of both fabrication and operation of capillary-driven devices is very attractive for various fluid transport tasks.[1] Furthermore, uniform pillar arrays can provide high-resolution separation, which has been shown by simulations[2] and with experiments using pumps and closed micropillar channels as a chromatographic column.[3,4,5] These micropillar channels have been applied in the separation of cells[6] and DNA[7] using fluorescence detection. Recently, Desmet and co-workers have introduced silicon non-porous pillar array columns for pressure-driven reversed-phase liquid chromatography.[8,9] Also, micromachined porous SiO_2 pillar arrays have been developed.[10]

The high potential of micropillar chips in bioanalysis can be greatly enhanced by combining them with electrospray ionization mass spectrometry (ESI-MS) which provides both high specificity and sensitivity. The introduction of ESI for analysis of large biomolecules by Fenn et al.[11] has had remarkable impact in the biosciences and was honored with the Nobel Prize in Chemistry in 2002. Both Caprioli et al.[12] (1994) and Wilm and Mann[13] (1994) developed miniaturized ESI sources with low flow rates called microelectrospray or nanoelectrospray devices, which provide high sensitivity and have therefore been widely used in bioanalysis.

Several different microchip-based ESI tips have been developed in the last few years, as shown in recent reviews by Lazar et al.(2006)[14] and Sung et al.(2005)[15] Briefly, these ESI tips are made of either glass[16] or polymers such as PDMS (polydimethylsiloxane),[17] PMMA (polymethyl methacrylate)[18] or SU-8,[19] and they are based either on off-chip spraying microdevices, in which an ESI capillary is separately attached to a microchip or on on-chip spraying microdevices, where the ESI tip is an integral part of the microchip. In these ESI microchips the liquid flow is generated either by means of pumps or electroosmosis. Also, Arscott and co-workers (2004)[20,21] utilized capillary forces in a rectangular capillary slot for liquid transport from a reservoir to a cantilever ESI tip made from SU-8 and polycrystalline silicon (polysilicon). In addition to in-plane tips there are also silicon ESI tips with out-of-plane design.[22,23]

In this paper we present a lidless micropillar array electrospray ionization (µPESI) chip with an in-plane channel and a tip, combined with mass spectrometry (MS). The chip combines self-filling of the channel, based on capillary forces of the micropillar array, and ESI at the tip of the chip. The performance of the µPESI chip is demonstrated, as well as the suitability of µPESI-MS system to a rapid, direct detection of both small molecules and biomolecules.

3.2 Experimental

3.2.1 Chemicals and samples

Acetonitrile was obtained from Rathburn (Walkerburn, Scotland, UK). Acetone was obtained from VWR International AB (Stockholm, Sweden). Methanol was obtained from J.T. Baker (Deventer, The Netherlands). Formic acid and acetic acid was obtained from Sigma-Aldrich (St. Louis, Mo, USA). All solvents were of HPLC grade. Water was purified with Milli-Q water purification system (Millipore, Molsheim, France). Verapamil was purchased from ICN Biomedicals Inc. (Aurora, OH, USA) and tetrabutylammonium iodide from Lancaster Synthesis (Eastgate, White Lund, Morecambe, UK). The peptides (angiotensin I, angiotensin II, and substance P) and horse heart myoglobin were purchased from Sigma-Aldrich. The R-enantiomer of sibutramine hydrochloride (purity >99%) was

obtained from Research Institute for Pharmacy and Biochemistry (Prague, Czech Republic).

3.2.2 Fabrication

The µPESI chips were fabricated on 380-µm-thick n-type <100> silicon wafers with resistivity of 1–14 Ω-cm and diameter of 100 mm. Deep reactive ion etching (DRIE) of silicon was done at cryogenic temperatures using a Plasmalab System 100 reactor (Oxford Instruments, UK). The µPESI chip includes a sample introduction spot, a liquid transfer channel, and a sharp tip for direct ESI (Fig. 3.1). The fabrication process is outlined in Fig. 3.2. A more detailed description of chip fabrication and fluidic behaviour can be found elsewhere.[24,25] Briefly, the two-lithography-step fabrication process utilized nested masks of silicon dioxide (SiO_2) and aluminum (Al), which were both patterned on the wafer prior to any Si etching. SiO_2 and Al have been shown to work well in the DRIE process at cryogenic temperatures.[26] SiO_2 was thermally grown on the wafers (step 2). After the first lithography step, the patterns for the pillar channels were etched into the 520-nm-thick SiO_2 layer using DRIE (step 3). The photoresist was removed and the Al layer (200 nm) was sputtered on top of the SiO_2 structures (step 4). The second lithography step defines the ESI tip. Using the photoresist as an etch mask, the Al and SiO_2 were both wet etched from the tip. The etchings were done using a phosphoric acid based etchant and buffered hydrofluoric acid (BHF), respectively (steps 5 & 6). After the photoresist removal the Al served as a mask during the through-wafer etching (step 7) which defined the sharp ESI tips at the ends of the channels. The angle at the tip was approximately 60 degrees. The Al mask was removed (step 8) and the 40-µm-tall pillars were etched in another silicon etching step, using the previously made SiO_2 pattern as a mask (step 9). Both silicon DRIE steps were done in inductively coupled SF_6/O_2 plasma at cryogenic temperature. After silicon etching the remaining SiO_2 was removed in buffered hydrofluoric acid. Finally, the chips were diced using a wafer saw. Two different chip sizes were fabricated: the small chip (4 mm × 9 mm) had 8-mm-long and 1-mm-wide channels and the large chip (9 mm × 20 mm) 18-mm-long and 2.25-mm-wide channels. Pillar diameters ranged from 15 to 200 µm in different chips and the distances between the pillars varied from 2 to 80 µm. This fabrication procedure produced well-shaped, uniform micropillars with well-defined and accurate distances between them. Also the height of micropillars can be precisely defined, thus increasing the chip-to-chip reproducibility. The fabrication costs per one µPESI chip are low as over 100 chips can be produced on one 100-mm-diameter silicon wafer.

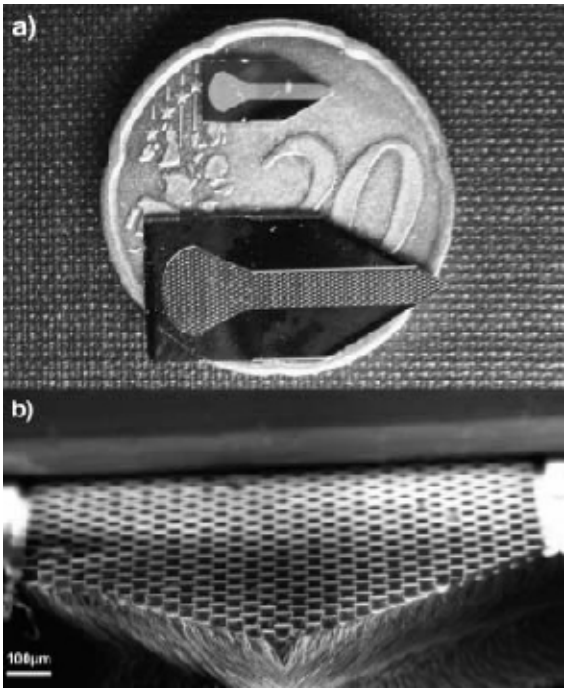

Figure 3.1. a) Overview of two different sized µPESI chips on a 20 euro cent coin. **b)** SEM micrograph of the chip, showing the micropillar array and the electrospray tip.

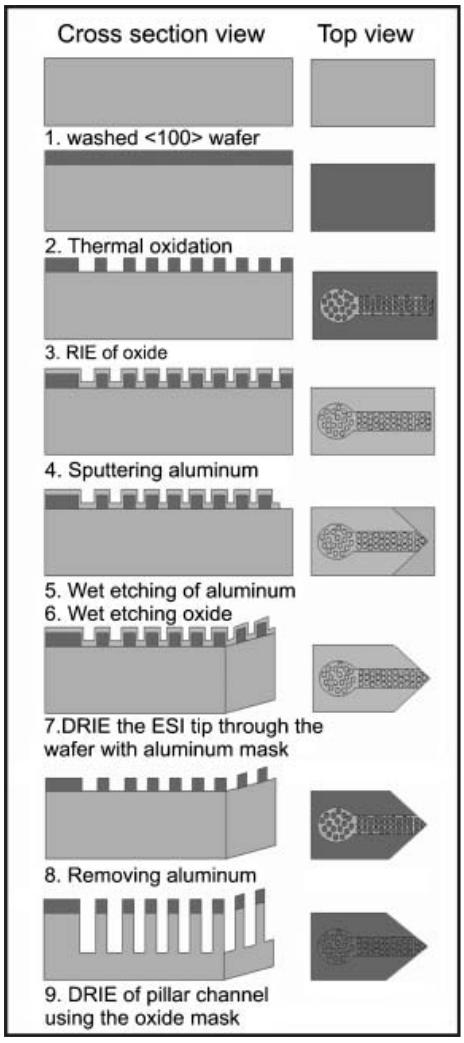

Figure 3.2. Schematic of the cross-sectional and top views of the chip design during fabrication.

3.2.3. Mass spectrometry and methods

The mass spectrometers used were an API300 triple-quadrupole, an API3000 triple-quadrupole (Applied Biosystems/MDS Sciex, Toronto, Canada), and a QTOF Micro quadrupole-time-of-flight instrument (Micromass/Waters, Manchester, UK). Nitrogen produced by a 75-720 nitrogen generator (Whatman Inc., Haverhill, MA, USA) was used as curtain gas. A Microfluidic toolkit voltage supplier from Micralyne Inc. (Edmonton, AB, Canada) was used. The sample droplet injected (0.5–4 µL) into the sample introduction spot filled the chip spontaneously by strong capillary forces to the ESI tip. The high voltage (2 – 4 kV) required for the ESI was applied to the sample introduction spot by a platinum electrode. Since the entire chip was conductive and the voltage drop across the micropillar array was negligible, the 2 – 4 kV voltage provided sufficient electric field for stable ESI. The setup for combining the micropillar array with the mass

spectrometer for ESI-MS measurements is presented in Fig. 3.3(a). The electric current was measured between the high-voltage supply and the platinum electrode by an amperometer (Meterman 38XR, Taiwan).

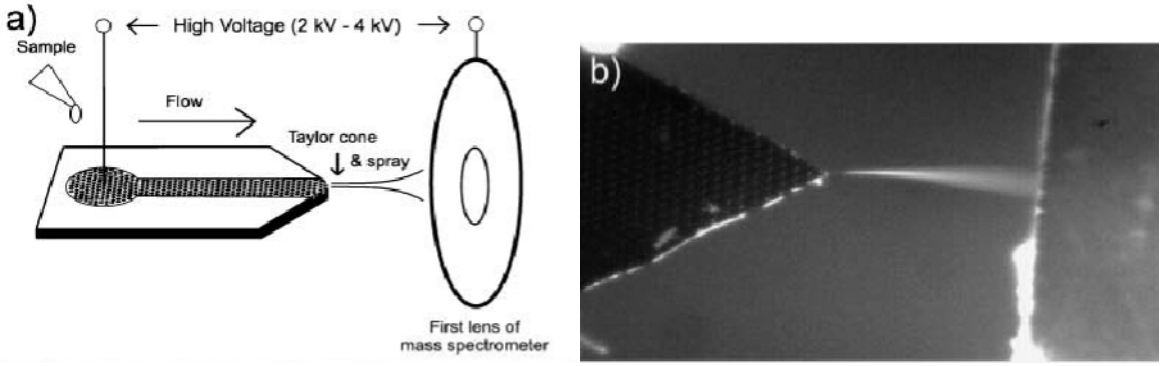

Figure 3.3. (a) Setup of the µPESI measurements. **(b)** Formation of Taylor cone and spray from the small (4 mm x 9 mm) µPESI chip. Diameter of pillars was 60 mm and distance between pillars was 15 mm. Liquid sample contained 95 % acetonitrile, 4.9 % water and 0.1 % formic acid. High voltage applied to the chip was 3 kV.

For bioanalysis experiments verapamil, angiotensin I, angiotensin II, substance P, and horse heart myoglobin were used as test compounds and 2.5 µL of each sample was applied onto the sample introduction spot. For the measurements of linearity and sensitivity verapamil was dissolved in acetonitrile/water (95:5) with 0.1 % formic acid at concentrations of 10 pM to 10 µM. The metabolism sample was prepared by incubating the R-enantiomer of sibutramine hydrochloride (purity > 99 %) with rat hepatocytes for 8 h. The sample preparation was performed according to the method presented in our earlier work.[27] After sample preparation the sample was evaporated to dryness and the residue was diluted to 50 µL of methanol. A volume of 10 µL of sample was dissolved in 500 µL acetonitrile/water (95:5) with 0.1 % formic acid.

In the linearity and sensitivity measurements the selected reaction monitoring (SRM) mode in positive mode was used to measure the verapamil signal and the selected reactions were *m/z* 455 → 165 and *m/z* 455 → 303. Quantitative linearity was measured by applying separately, ten times, 2.5 µL of each concentration of verapamil standard. The average and relative standard deviation (RSD) for signal heights were calculated at each different concentration level.

The peptides (angiotensin I, angiotensin II, and substance P) and the protein (horse heart myoglobin) were diluted into 80 % aqueous methanol containing 1 % acetic acid (two separate samples). The concentrations were 5 µM for the peptides and 300 nM for horse heart myoglobin. Full-scan mass spectra ranging from *m/z* 400 – 750 were measured from the peptide mixture and *m/z* 700 – 950 from the protein in positive mode. The sibutramine

metabolism sample was measured with the QTOF Micro. A mass spectrum of solvent blank sample was subtracted from that of metabolism sample.

A solution of tetrabutylammonium iodide (5 µM) in acetonitrile/water (95:5 v/v) with 0.1 % formic acid was used to test the formation of the electrospray plume at the tip of the chip. A volume of 2.5 µL of the solution was applied onto the sample introduction spot and the formation of electrospray was verified by monitoring the tip of the chip with a CCD camera (Watec camera WAT-502A, Japan) (Fig. 3.3(b)).
In the measurement of long-term stability of the chip the verapamil solution was applied to the sample introduction spot via a fused-silica capillary (i.d. 150 µm, o.d. 250 µm) using a syringe pump (model PDH2000, Harvard Apparatus, Holliston, MA, USA) at a flow rate of 8 µL/min. The end of the silica capillary was positioned just above the introduction spot (the liquid runs freely from the capillary to the spot) to achieve continuous liquid flow inside the micropillar array.

3.3 Results and discussion

The micropillar array provides a liquid transfer by capillary action as was shown previously.[25,28] Briefly, the micropillar array provides a self-filling of the array channel with liquid up to the end of the channel. In this study, the major aim was to provide self-filling with liquids in an open channel and to combine an electrospray (ES) tip to the end of the channel in order to form a continuous flow from the sample introduction spot into a mass spectrometer. The pillar channel structure is not prone to clogging, since the liquid can flow via several routes between the pillars. In these experiments, 15 – 50-µm-diameter pillars with inter-pillar distances of 2 – 25 µm were tested. The exact flow rate of solvents during the self-filling and ESI process could not be measured since the flow channel is open. However, the flow rates were estimated from video recordings with the CCD camera. There were no significant differences in filling rates between microchips with varying pillar dimensions when using normal HPLC solvents such as water, methanol or acetonitrile, since, for example with the chip with small dimension, the liquid moved from the sample introduction spot to the tip in half a second and the differences in filling rates with different liquids were within 0.04 seconds which was the frame speed of the CCD camera used. This also means that hydrostatic pressure and Laplace pressure can increase the overall filling rate to a maximum of 10 %.

The ion current appears as soon as the liquid reaches the tip of the chip and fades away when the liquid runs out due to evaporation and spraying. The signal lasted for about 20 s (with a 2-µL sample using the 8-mm long channel) but, by changing the droplet size, water concentration and dimensions of the chip and pillars, the duration of the signal can be decreased to 5 s or increased to about 30 s. The electric current, measured between the high-voltage supply and the platinum electrode, varied between 20 and 150 nA, depending on the high voltage and solvents used, the microchip dimensions, and the distance between

the chip and the mass spectrometer. The low current values indicate that the spray from the tip is in the nanoES regime, that is nL/min, even when the actual self-filling flow rate is in the low µL/min range. The reason for this difference might be partial evaporation of the solvent during the self-filling stage. It follows from the evaporation that the sample is concentrated and the ES is in the nanoES regime, as mentioned above. This can lead to improved sensitivity but also to memory effect to some extent. It was noticed that at high concentrations (1 – 10 µM) some of the analyte molecules were left on the micropillar array which could be seen in the following analysis of a blank sample. However, this memory effect could be reduced to a negligible level by flushing the chip with a solvent between the analyses from one to three times depending on the concentrations and proton affinities of the analytes. In this way, the same microchip can be easily used for several consecutive samples without carry-over from one sample to another. The memory effect can also induce sample loss; however, at low concentrations this possibility is minimal as the memory effect is negligible and at high concentrations some sample loss can occur but in a repeatable manner according to measurements (see linearity measurements below).

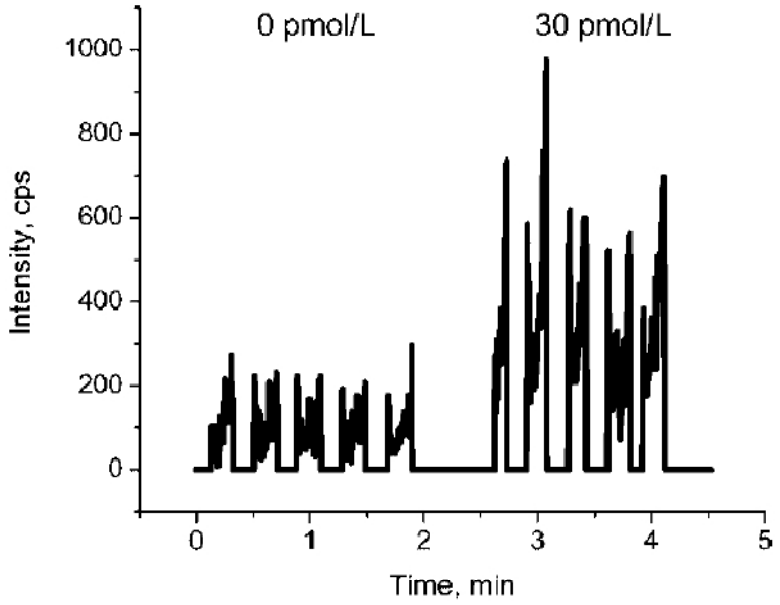

Figure 3.4. The intensity of MS/MS signal in SRM mode of 2.5-µL application of five blank samples and five 30 pM verapamil samples (in acetonitrile/water (95:5) with 0.1% formic acid) onto a µPESI chip.

The µPESI-MS system was shown to be a sensitive technique as the limit of detection measured for verapamil (Fig. 3.4) using the SRM mode (m/z 455 → 165 and 303) was 60 amol (28 fg) with a 2.5-µL sample volume (corresponding to 30 pmol/L or 13.5 pg/mL). This limit of detection was obtained with a micropillar diameter of 60 µm and an inter-pillar distance of 25 µm, but comparable results were also obtained with other diameters and inter-distances. Comparison of the detection limits obtained with our µPESI-MS setup with those obtained by nanospray-MS in the literature showed that the sensitivity was

typically better or at least similar to that obtained with nanospray-MS or microfluidic HPLC-chip-MS.[29,30,31] Similarly, the quantitative linearity of the system was tested with verapamil standard solutions over a concentration range of 100 pM to 10 µM with a 2.5-µL injection (ten times for each concentration) and a correlation coefficient (r^2) of 0.997 was obtained, indicating good quantitative linearity of the system over a range of six orders of magnitude. The relative standard deviation (RSD) of the intensity of the verapamil signal, calculated from those 60 injections, varied between 7 – 17 % at different concentration levels, with an average of 12 %. The linearity measurement was made three separate times, on successive days, using a different individual microchip each time. It was noticed that, even though the absolute signal varied little from day to day, a correlation coefficient r^2 of at least 0.99 was obtained each time within the same concentration range (100 pM to 10 µM).

In addition to self-filling, the µPESI chips can be used in a continuous manner, by applying a continuous flow of liquid with, for example, a syringe pump. This mode can be used in applications where longer ESI signals must be acquired, such as multiple compound analysis using several measurement modes (full-scan MS, SRM, neutral loss scan, etc.). In this study the continuous mode was exploited in the stability measurement, that is the stability of the signal with the microchip was tested by infusing 10-nM and 100-nM solutions of verapamil (separately) with a syringe pump at a flow rate of 8 µL/min for 1 hour (Fig. 3.5). This measurement was repeated three times using different individual microchips (only one measurement is shown in Fig. 3.5). The signal measured with tandem mass spectrometry (MS/MS) was stable throughout the entire experiment, with an RSD of less than 5 % in each measurement, indicating suitability of µPESI-MS for long-term analysis.

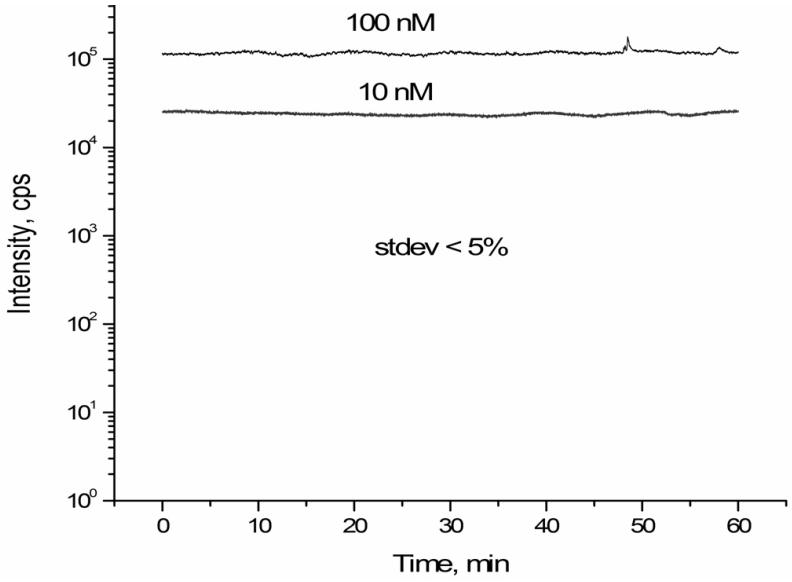

Figure 3.5. Overlaid intensities of MS/MS signal of 10-nM and 100-nM verapamil solutions in 1-h continuous flow analysis, the sample was infused continuously onto the sample introduction spot of the chip with a syringe pump at the flow rate of 8 µL/min.

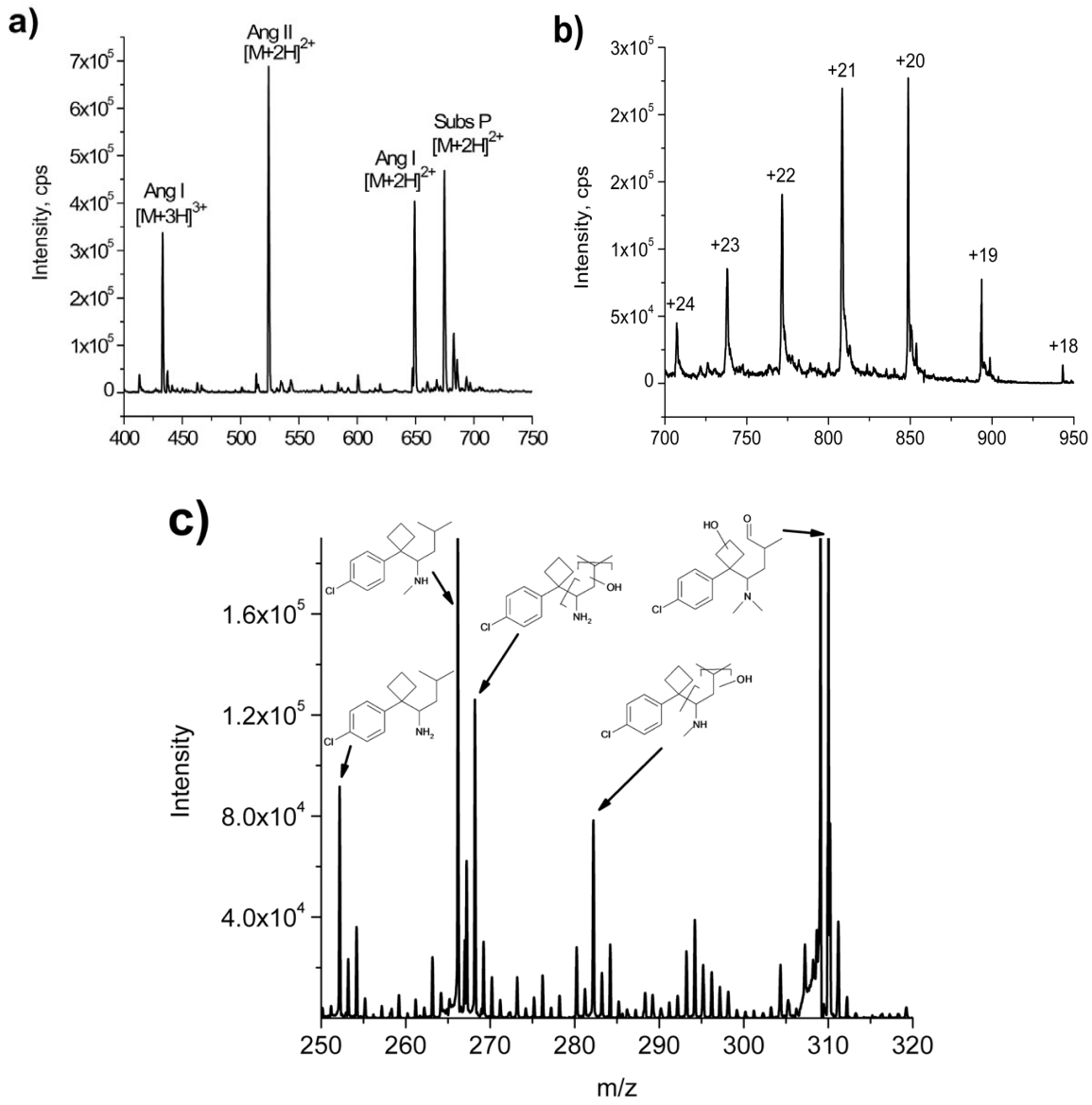

Figure 3.6. µPESI mass spectra of **a)** a peptide mixture (angiotensin I and II, substance P), showing multiply charged ions at a concentration level of 5 µM; **b)** a protein (horse heart myoglobin, molecular weight 16951), showing multiple charged ions at a concentration level of 300 nM; and **c)** sibutramine metabolites produced using rat hepatocytes. Mass spectra were obtained using spectral subtraction of a blank solvent.

High-quality spectra was produced by µPESI-MS for the biomolecules tested, showing multiple charged ions for three peptides (angiotensin I, angiotensin II, and substance P) and a protein (horse heart myoglobin) (Fig. 3.6). All mass spectra were obtained using spectral subtraction of a blank solvent. The usability of the µPESI chip was also tested with a real metabolism sample of sibutramine, produced with rat hepatocytes. A 2.5-µL injection of the metabolism sample showed demethylated (at *m/z* 266), didemethylated (at *m/z* 252), demethylated and hydroxylated (at *m/z* 282), didemethylated and hydroxylated (at *m/z* 268), dihydroxylated and dehydrogenated (at *m/z* 310) sibutramine metabolites.

Small amounts of sibutramine glucuronides were also detected (ions at *m/z* 444 and 458, not shown in Fig. 3.6(c)). The same main metabolites were also found with liquid chromatography/ESI-MS/MS.[27]

3.4 Conclusions

We presented a new silicon-based ESI chip with an array of micropillars and a sharpened ESI tip for the analysis of organic molecules. The µPESI chip provides reliable liquid filling and is stable during the ESI process. The microfabrication of the chip is straightforward providing very accurate and reproducible chip production. The chips are simple, relatively cheap to fabricate and suitable for disposable use. The open micropillar system makes µPESI very easy to use, and it is not prone to clogging, due to multiple pathways for the liquid to move forward to the tip. µPESI provides reliable and quantitative long-term analysis with no clogging problems, and the sensitivity with small molecules is high, similar to or better than that achieved with nanospray or other microfluidic chips. For all these reasons, µPESI-MS is a promising new method for fast analysis of both small molecules and biomolecules.

References

1 P. Ohman, I. Mendel-Hartvig, Patent Application, PCT/SE03/00919, WO 03/103835, 2003.

2 N. Vervoort, J. Billen, P. Gzil, G. Baron, and G. Desmet, Importance and Reduction of the Sidewall-Induced Band-Broadening Effect in Pressure-Driven Microfabricated Columns. Anal. Chem. 76, 4501, 2004.

3 B. He, N. Tait, and F. Regnier, Fabrication of Nanocolumns for Liquid Chromatography, Anal. Chem., 70, 3790–3797, 1998.

4 F. Regnier, Microfabricated Monolith Columns for Liquid Chromatography. Sculpting Supports for Liquid Chromatography, J. High Res. Chromatogr. 23, 19, 2000.

5 B. Slentz, N. Penner, and F. Regnier, Geometric effects of collocated monolithic support structures on separation performance in microfabricated systems J. Sep. Sci. 25, 1011, 2002.

6 N. Panaro, X. Lou, P. Fortina, L. Kricka, P. Wilding. Micropillar array chip for integrated white blood cell isolation and PCR, Biomol. Eng. 21, 157, 2005.

7 O. Bakajin, T. Duke, J. Tegenfeldt, C. Chou, S. Chan, R. Austin, E. Cox, Separation of 100-kilobase DNA molecules in 10 seconds, Anal. Chem. 73, 6053, 2001.

8 W. De Malsche, H. Eghbali, D. Clicq, J. Vangelooven, H. Gardeniers, G. Desmet. Pressure-driven reverse-phase liquid chromatography separations in ordered nonporous pillar array columns, Anal. Chem. 79, 5915, 2007.

9 J. De Smet, P. Gzil, G. Baron, G. Desmet. On the 3-dimensional effects in etched chips for high performance liquid chromatography-separations, J. Chromatogr. A 1154, 189, 2007.

10 R.C. Costa, K. Mogensen, J. Kutter. Microfabricated porous glass channels for electrokinetic separation devices, Lab Chip 5, 1310, 2005.
11 J. Fenn, M. Mann, C. Meng, S. Wong, C. Whitehouse, Electospray ionization for mass spectrometry of large biomolecules, Science, 246, 64, 1989.
12 R. Caprioli, M. Emmett, P. Andren. Proc. 42nd ASMS Conf. Mass Spectrometry and Allied Topics, Chicago, IL, May 29–June 3, 754, 1994.
13 M. Wilm, M. Mann, Proc. 42nd ASMS Conf. Mass Spectrometry and Allied Topics, Chicago, IL, May 29–June 3, 770, 1994.
14 I. Lazar, J. Grym, F. Foret. Microfabricated devices: A new sample introduction approach to mass spectrometry, Mass Spectrom. Rev. 25, 573, 2006.
15 W-C. Sung, H. Makamba, S-H. Chen. Chip-based microfluidic devices coupled with electrospray ionization-mass spectrometry, Electrophoresis 26, 1783, 2005.
16 R. Ramsey, J. Ramsey. Generating electrospray from microchip devices using electroosmotic pumping. Anal. Chem. 69, 1174, 1997.
17 K. Huikko, P. Östman, K. Grigoras, S. Tuomikoski, V. Tiainen, A. Soininen, K. Puolanne, A. Manz, S. Franssila, R. Kostiainen, T. Kotiaho. Poly(dimethylsiloxane) electrospray devices fabricated with diamond-like carbon-poly(dimethylsiloxane) coated SU-8 masters. Lab Chip, 3, 67-72, 2003.
18 A. Muck, A. Svatos, Atmospheric molded poly(methylmethacrylate) microchip emitters for sheathless electrospray, Rapid Commun. Mass Spectrom. 18, 1459, 2004.
19 S. Tuomikoski, T. Sikanen, R. Ketola, R. Kostiainen, T. Kotiaho, S. Franssila, Fabrication of enclosed SU-8 tips for electrospray ionization-mass spectrometry, Electrophoresis 26, 4691, 2005.
20 M. Brinkmann, R. Blossey, S. Arscott, C. Druon, P. Tabourier, S. Le Gac, C. Rolando. Microfluidic design rules for capillary slot-based electrospray sources, Appl. Phys. Lett. 85, 2140, 2004.
21 S. Arscott, D. Troadec, A nanofluidic emitter tip obtained by focused ion beam nanofabrication. Nanotechnology 16, 2295, 2005.
22 W. Deng, J. Klemic, L. Xiaohui, M. Reed, A. Gomez. Increase of electrospray throughput using multiplexed microfabricated sources for the scalable generation of monodisperse droplets, Aerosol Sci. 37, 696, 2006.
23 S. Zhang, C. van Pelt, J. Henion, Automated chip-based nanoelectrospray-mass spectrometry for rapid identification of proteins separated by two-dimensional gel electrophoresis, Electrophoresis 24, 3620, 2003.
24 L. Sainiemi, T. Nissilä, T. Sikanen, T. Kotiaho, R. Kostiainen, R.A. Ketola, S. Franssila, High sensitivity micropillar electrospray ionization chip fabricated of silicon. Proc. IEEE Transducers, Lyon, 1789–1792, 2007.
25 L. Sainiemi, T. Nissilä, V. Jokinen, T. Sikanen, T. Kotiaho, R. Kostiainen, R.A. Ketola, S. Franssila, Fully polymeric integrated microreactor/electrospray ionization chip for on-chip digestion and mass spectrometric analysis. Sensors and Actuators B, 143, 1, 414-420, 2009.
26 L. Sainiemi, S. Franssila, Mask material effects in cryogenic deep reactive ion etching. J. Vacuum Sci. Technol. B, 25, 801, 2007.

27 K. Hakala, M. Link, B. Szotakova, L. Skalova, R. Kostiainen, R.A. Ketola, Metabolite profile of sibutramine in human urine: a liquid chromatography-electrospray ionization mass spectrometric study. J. Mass Spectrom. 41, 1171, 2006.
28 M. Zimmermann, H. Schmid, P. Hunziker, E. Delamarche, Capillary pumps for autonomous capillary systems. Lab Chip, 7, 119, 2007.
29 L. Alfazema, D. Richards, S. Gélébart, J. Mitchell, M. Snowden. Rapid, accurate and precise quantitative drug analysis: comparing liquid chromatography tandem mass spectrometry and chip-based nanoelectrospray ionisation mass spectrometry, Eur. J. Mass Spectrom. 11, 393, 2005.
30 J-M. Dethy, B. Ackermann, C. Delatour, J. Henion, G. Schultz, Demonstration of direct bioanalysis of drugs in plasma using nanoelectrospray infusion from a silicon chip coupled with tandem mass spectrometry. Anal. Chem. 75, 805, 2003.
31 F. Mandel, L. Côté, M. Vollmer, Determination of low femtogram drug levels in serum by HPLC-Chip MS. Proc. 53rd ASMS Conf.Mass Spectrometry and Allied Topics, San Antonio, TX, June 5–9, 2005.

4 Fabrication and fluidic characterization of silicon micropillar array electrospray ionization chip (II)

Herein, the design, fabrication, and characterization of a silicon electrospray ionization chip for mass spectrometric analysis is described. The chip has three parts: a sample introduction spot, a flow channel, and a sharp electrospray ionization tip. A regular micropillar array is micromachined inside the whole channel. The chip has no lid, which makes the sample application and chip fabrication easier. A two photomask level fabrication process utilizes nested masks of silicon dioxide and aluminum oxide. A combination of anisotropic and isotropic plasma etching steps allows formation of a truly three-dimensional electrospray ionization tip without double-sided lithography. The filling properties of the lidless micropillar channel are studied. Because of the capillary forces facilitated by the micropillar array, the sample applied onto the sample introduction spot spontaneously fills the whole flow channel including the electrospray ionization tip, without external pumping. Besides reliable self-filling, the chip offers stable electrospraying and high sensitivity chemical analysis when coupled to a mass spectrometer.

4.1 Introduction

There is a constant demand for faster, more selective, and more sensitive analysis methods of drug and biomolecules using smaller and smaller sample volumes. A microfluidic device coupled to a mass spectrometer (MS) has potential to respond to these demands.[1] Electrospray ionization (ESI) has been the most studied method for miniaturized mass spectrometer interfaces. The most popular fabrication materials of ESI chips have been glass[2,3] and polymers, such as parylene[4], PDMS[5], and SU-8.[6] However, these materials set limits to chip designs. Glass microfabrication techniques are cumbersome compared to silicon micromachining and through-wafer processing is inaccurate. Polymer microfabrication is generally easy and fast, but at the moment it does not match silicon in fabrication of robust high aspect ratio structures and complex three-dimensional features.

Silicon ESI chips[7,8,9] have also been realized because of the well-explored microfabrication techniques of silicon, however the conductivity of silicon limits its use, because it excludes the use of electro-osmotic flow in sample transport. Pressure driven flow has been the other popular method used for sample transportation in previous ESI chips.[2] However, both of these methods require an external actuator, such as a high-voltage supply or a pump. Pressure driven flows also require the use of troublesome fluidic connectors. Some ESI chips exploit capillary forces to transport the sample, but narrow or enclosed channels are usually required in order to achieve sufficiently strong capillarity.[9,10]

We present a micropillar array electrospray ionization (μPESI) chip, where the sample is transported through a 1-mm wide lidless flow channel by capillary forces facilitated by micropillars. No external pumping is required and the only high voltage source needed is the one necessitated by MS. The whole chip is made out of silicon, which allows the fabrication of high aspect ratio micropillars inside the channel and the accurate definition of a truly three-dimensional, in-plane tip. We also investigated how the pillars contribute to capillary filling properties of a lidless channel. The μPESI source was coupled to MS to demonstrate its analytical potential.

4.2 Device design and fabrication

The μPESI chips were fabricated on 300-μm thick <100> silicon wafers that had resistivity of 1-50 Ohm-cm. Both p and n-type wafers were used. The chip has a 2.5-mm wide circular sample introduction spot and a 5.5-mm long and 1-mm wide straight flow channel, which ends with a sharp, in-plane ESI tip. The chip has no lid. Both the sample introduction spot and the flow channel contain a perfectly ordered array of micropillars. Two different sets of geometrical parameters for pillar dimensions and pillar packing were used. These geometrical parameters are presented in Figure 4.1. Similar chips without the pillar array were also fabricated for reference. The depth of the channels was varied between 20 and 40 μm. A photograph of a fabricated chip is shown in Figure 4.2.

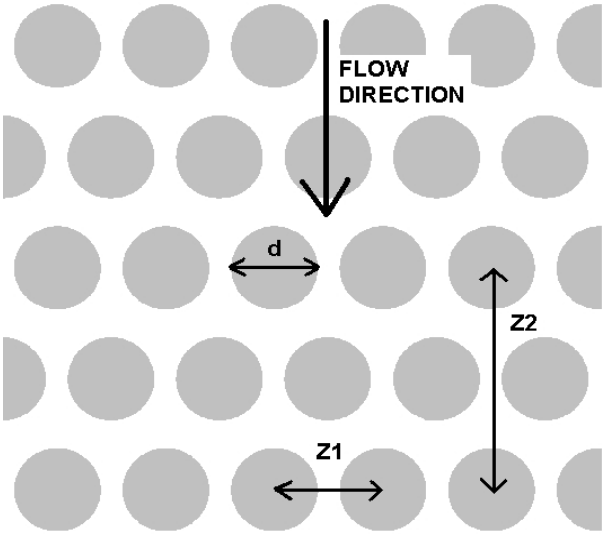

Figure 4.1. Packing of the pillars inside the channel. In the first set-up (denser packing) the pillar diameter d was 10 μm and the pillar centre-to-centre distances Z1 and Z2, were 12 μm and 22 μm, respectively. In the second design d = 60 μm, Z1 = 75μm and Z2 = 160 μm.

Figure 4.2 A μPESI chip on a 10-euro-cent coin.

The fabrication process had two mask levels and utilized nested masks of silicon dioxide (SiO_2) and aluminum oxide (Al_2O_3), which were both patterned on the wafer prior to any silicon etching. First, SiO_2 was thermally grown on the wafers. The SiO_2 mask for pillar channels was etched by CHF_3/Ar reactive ion etching (RIE) using a photoresist mask (Fig. 4.3a). After photoresist removal, an amorphous Al_2O_3 layer was deposited on top of the patterned SiO_2 mask using atomic layer deposition (ALD). The deposition took place at 220 °C, trimethylaluminum and water vapor being the source gases. The second lithography defined the sharp ESI tip at the end of the flow channel. Both Al_2O_3 and SiO_2 were etched away from tip area, by phosphoric acid and CHF_3/Ar RIE, respectively (Figs. 4.3 b, c). Aluminum oxide served as an etch mask during the through-wafer deep reactive ion etching (DRIE) (Fig. 4.3d).

If a three-dimensionally sharp ESI tip is desired, the through-wafer etching has to be done in two parts. First, fairly shallow anisotropic silicon DRIE step is performed. Then, a 250-nm thick SiO_2 passivation layer is deposited using plasma enhanced chemical vapor deposition (PECVD). Deposited PECVD SiO_2 is removed from horizontal surfaces using CHF_3/Ar RIE again, but vertical sidewalls remain passivated because of the anisotropic nature of the RIE step. The rest of the through-wafer etching is also done with DRIE, but using a more isotropic etching process. Isotropic etching causes undercutting and because of the passivation layer a three-dimensionally sharp tip is formed. This two-step anisotropic-isotropic sharpening process of the tip is not included in Fig. 4.3.

After the through-wafer etching, the Al_2O_3 mask was removed in phosphoric acid (Fig. 4.3e) and the pillar channels were created in another anisotropic silicon DRIE step, using the revealed SiO_2 pattern as a mask. All silicon etchings were done in inductively coupled SF_6/O_2 plasma at cryogenic temperature [11] (Plasmalab System 100, Oxford Instruments, UK). After the last silicon DRIE step, the remaining SiO_2 was removed using buffered hydrofluoric acid (Fig. 4.3f). The channels can be transformed to more hydrophilic using

short oxygen plasma treatment or Piranha treatment. Because the channel is lidless, no bonding is required in the fabrication process.

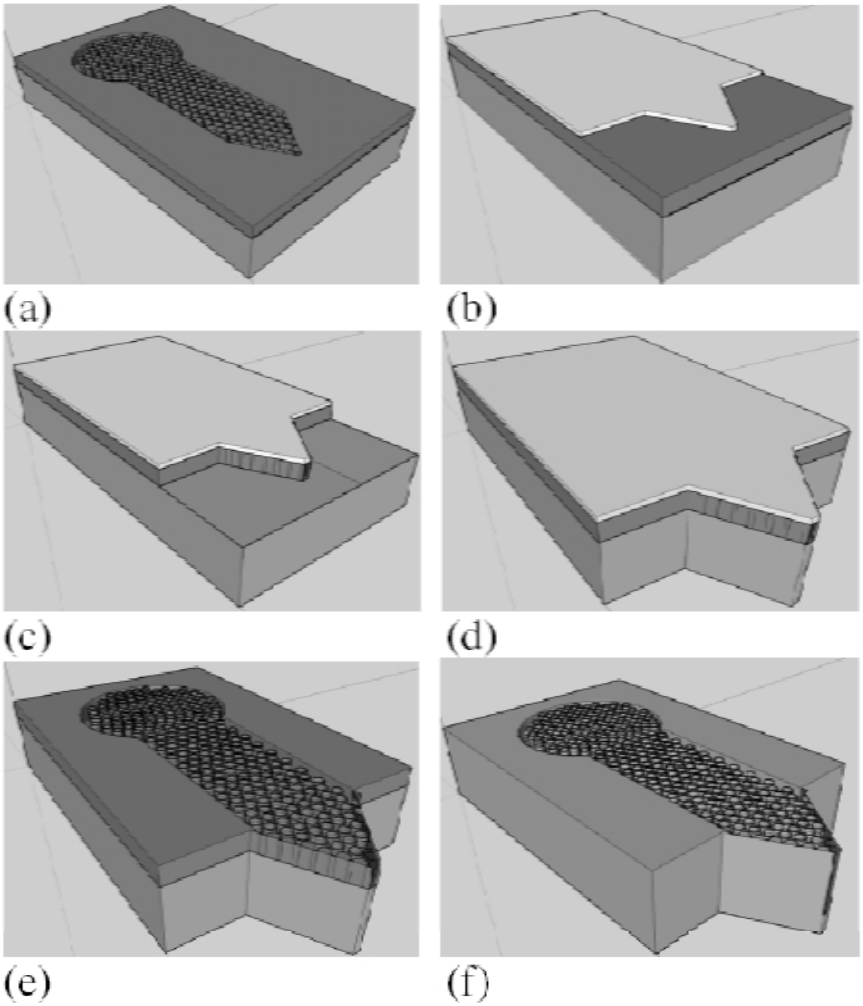

Figure 4.3. The fabrication process of the μPESI chip without the sharpening process. The light gray bottom layer is silicon substrate (300 μm); the dark gray middle layer SiO_2 (1020 nm) and white top layer Al_2O_3 (96 nm). Photoresist layers are not shown in the figure. See text for details.

4.3 Results and discussion

4.3.1 Fabrication

In ESI-MS a strong electric field at the tip of the ESI chip forms a Taylor cone and the liquid breaks into small droplets that are ionized. The ionized molecules are analyzed using a MS. The voltage needed to create an electric field that is sufficiently strong for formation of electrospray is known to be dependent on the sharpness of the ESI tip.[12] The

sharper the tip, the lower the onset voltage of electrospraying is. Therefore, it is desirable to have a three-dimensionally sharp ESI tip. The ESI tip fabricated without the sharpening process is shown in Fig. 4.4. The width of the 100 μm wide ESI tip is defined by the second lithography step and therefore easily adjusted. The thickness control of the tip is not as easy, because it cannot be determined by lithography. The tip presented in Fig 4.4. has the thickness of 300 μm, which is determined by the wafer thickness.

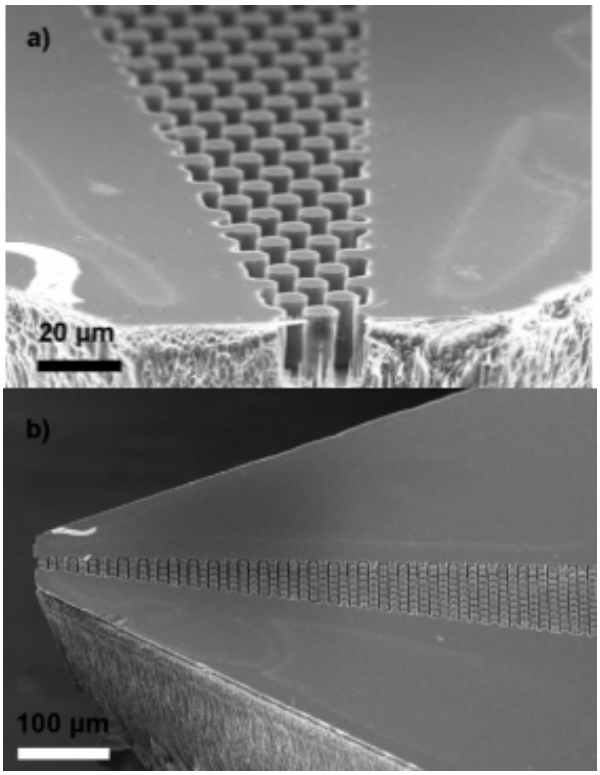

Figure 4.4. (a) Front and (b) side views of the ESI tip of the μPESI chip fabricated without sharpening process.

The thickness control of ESI tip without double-sided lithography requires an adequate combination of anisotropic and isotropic plasma etching steps. Combining the sharpening process, discussed in the previous section with a narrow tip, results in a three-dimensionally sharp ESI tip. The shorter the first anisotropic etching step during the sharpening process is, the sharper the tip becomes. However, the depth of the first anisotropic etching during the sharpening process must always be greater than that of the pillar channel. The tradeoff of an extremely sharp tip is poorer mechanical strength. The ESI tip of the μPESI chip where the sharpening process was utilized is presented in Fig 4.5.

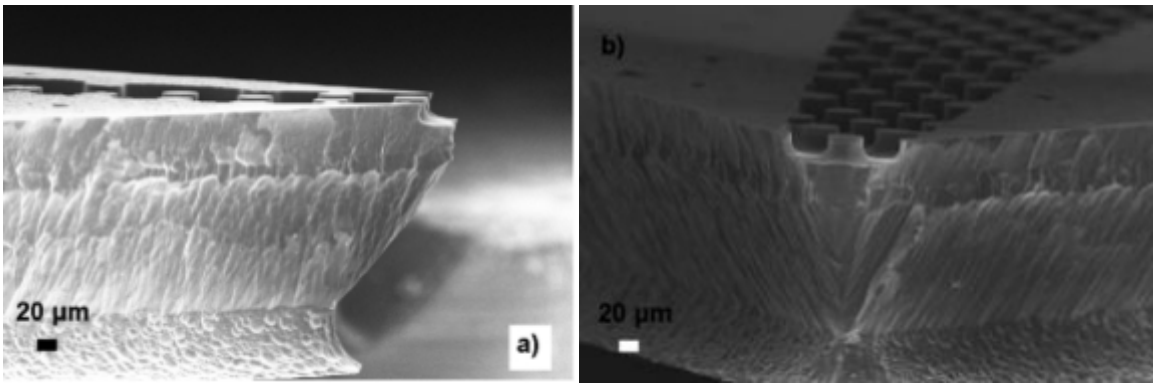

Figure 4.5. (a) Cross-section and (b) tilted top view of ESI tip of the µPESI chip. The sharpening process was utilized in through-wafer etching. Passivation layer protects the top part of the chip during isotropic etching.

An ALD Al_2O_3 layer was used as a mask during the through wafer-etching process, because of its exceptionally high selectivity in cryogenic DRIE.[13,14] The selective removal of Al_2O_3 after the through-wafer etching process is also important. The Al_2O_3 can be removed using phosphoric acid without affecting the underlying SiO_2 layer and silicon surface. The aluminum etch mask was also tested for the through wafer etching, but in fluorine based plasmas sputtering and redeposition of aluminum results in rough etched surfaces.[15]

4.3.2 Capillary Filling

The cross-section of the flow channel of the fabricated µPESI chip is shown in Fig. 4.6. It was found out that both sets of geometrical parameters presented in Fig. 4.1 provided reliable capillary filling, even at relatively high contact angles. Similar pillar channels with different pillar shapes and geometrical parameters have already been utilized in capillary pumps to tailor the capillary pressure and flow resistance of the channel,[16] but these experiments have been made in PDMS sealed channels.

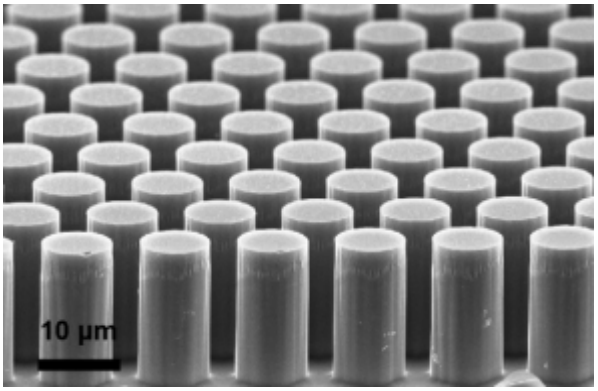

Figure 4.6. The cross-section of the flow channel of the µPESI chip.

Capillary filling of microchannels is based on the surface energetics of the system. A liquid will fill a microchannel spontaneously if this leads to a decrease of the total surface free energy. The surface energies of the system and the contact angle are linked by the Young-Dupré equation:

$$\gamma_{sv} - \gamma_{sl} = \gamma_{lv} \cos\theta, \qquad (1)$$

where θ is the contact angle, γ_{lv}, γ_{sl}, and γ_{sv} are the surface energies of the liquid-vapor, solid-liquid and the solid-vapor phases respectively.

The capillary pressure in a microchannel with a rectangular cross section has been given as:[17,18]

$$P = \gamma_{lv}\left(\frac{\cos\theta_t + \cos\theta_b}{d} + \frac{\cos\theta_l + \cos\theta_r}{w}\right), \qquad (2)$$

where θ_t, θ_b, θ_l, and θ_r are the contact angles at the top, bottom, left, and right channel walls respectively, d is the depth of the channel and w is the width of the channel. In the absence of other driving forces, a microchannel will fill spontaneously if the capillary pressure is positive. Other forces that are present in our experimental setup include forces generated by hydrostatic pressure and Laplace pressure of the droplet, but their contribution is usually small.

We investigated the filling properties of similar channels with and without a micropillar array. A 2.5-µl de-ionized water droplet was applied onto the sample introduction spot and capillary filling was observed under an optical microscope. Typical filling experiments are presented in Figs. 4.7 and 4.8. Both channels were 22.5 µm deep and 1 mm wide. The contact angle of the etched silicon with de-ionized water was measured immediately after the experiment by sessile drop method (CAM 101 from KSV Instruments, Finland) and it was 47° ± 2°. The contact angle of the top wall was taken to be 180° since the material of the top wall was air.

Inserting these values into the equation (2) gives approximately -930 Pa as the capillary pressure in the channels without pillars, which means that the channels should not fill spontaneously by capillarity. This is also what was observed in the experiments (Fig. 4.7). Instead, the channels filled only at the corners and even there the flow was very slow. Capillary flow in corners is well known and for a 90° corner, it should happen spontaneously when the contact angle is less than 45°.[19] Since the measured contact angle was slightly higher than this, it is possible that in this experiment the vertical sidewalls were more hydrophilic than the horizontal areas.

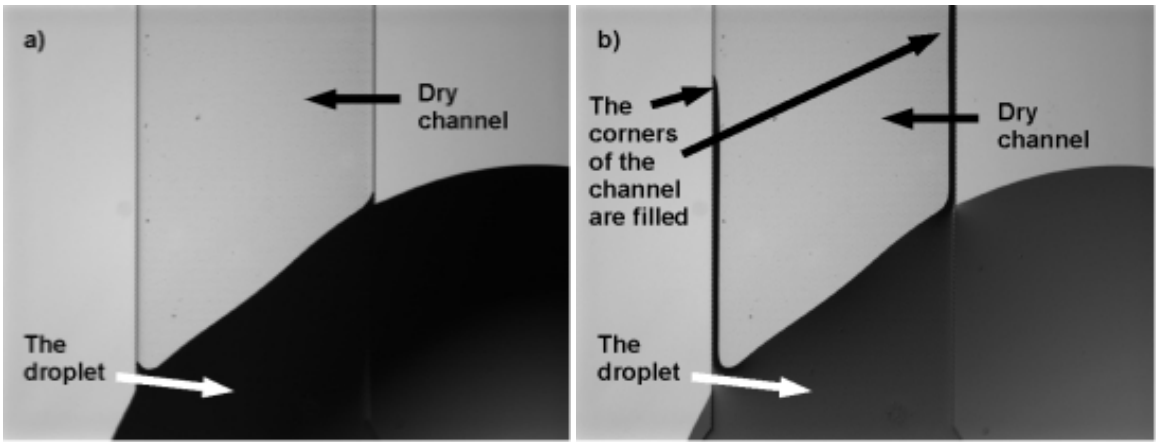

Figure 4.7. a) A water droplet is applied onto the channel without micropillars and **b)** the water proceeds only at intersection of bottom and sidewalls.

The channels with a micropillar array filled spontaneously as shown in Fig. 4.8. The sidewalls of the pillar channel were most conductive to capillary flow and the flow often proceeded to a new pillar row first at the edgemost pillar and then filled rest of the row. Qualitatively, the difference in capillary properties of a channel with and without a micropillar array is that the channel with the micropillar array has more hydrophilic surface area per unit length, which makes the pillar channels more conductive to capillary flow.

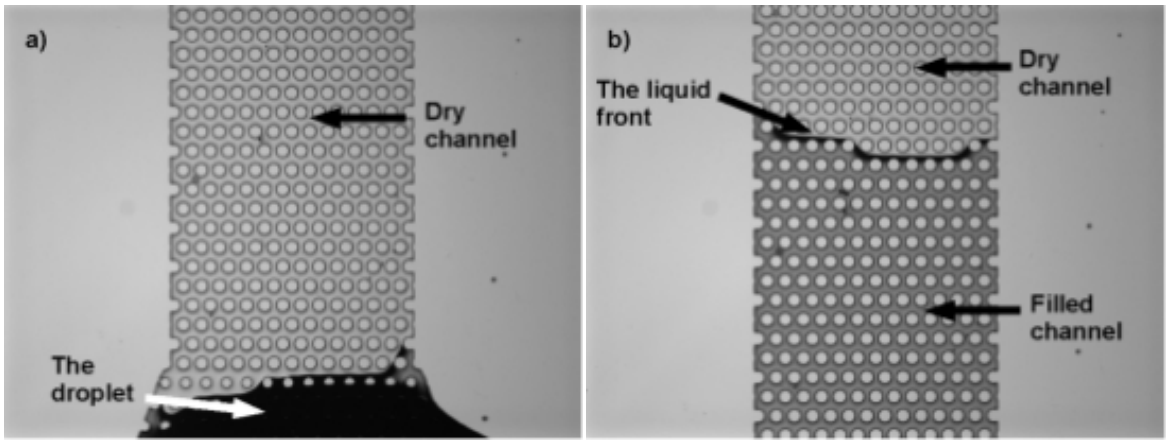

Figure 4.8. a) The water droplet is applied onto the micropillar channel. **b)** The micropillars facilitate the capillary forces and the whole channel is filled without other driving forces.

Contact angles in the 45°-50° range started to be near the limit of capillary filling even for both pillar channel geometries (see Fig. 4.1). At these contact angles the filling was very slow (approximately 1 mm/min) and the sample spot droplet evaporated before the entire channel had filled. At more hydrophilic contact angles, in the 20°-35° range, both pillar channels filled quickly (approximately 1 mm/s) and the channels without pillars still filled only at the edges. At extremely low contact angles (<10°), capillary pressure (2) becomes

positive even for the channels without micropillars and the droplet quickly wetted the channels without pillars also. At all contact angles that were investigated, both pillar channel geometries used in this work produced similar flow rates, but in general the geometrical parameters of the pillar channel also affect the filling rate.

The reasons why we prefer wide pillar channels to narrow channels without pillars include sufficient sample capacity and low clogging probability. The wide pillar channels provide sufficient volume for sample, and therefore sample supply to the ESI tip is continuous, which is essential for stable electrospraying. The clogging of the pillar channel is highly improbable because the sample flow is not stopped if one or even a few gaps between pillars are blocked.

4.3.3 μPESI/MS

The analytical potential of the μPESI chip was demonstrated by mass spectrometric measurements. The early results presented here were obtained using the chips fabricated without the sharpening process. The μPESI chip was coupled to a mass spectrometer (Applied Biosystems/MDS Sciex API-3000, Concord, Ontario, Canada) and tested for the detection of drug molecules. The sample volume applied onto the sample introduction spot was varied between 0.5 and 4.0 μl. The application of the sample onto the chip is extremely easy because the chip is lidless. The sample was driven through the flow channel by capillary forces. When the sample reached the ESI tip of the chip it was sprayed out forming a Taylor cone in the electrospray ionization process. No auxiliary gas or liquid flow was required to produce stable spraying. The voltage needed for ionization depended on the distance between the chip and the first lens of MS. When the distance was 1.5 – 2.0 cm, the voltage needed was 4.0 – 4.5 kV, while the first lens of MS was kept at the potential of 1 kV.

The μPESI chip offers high sensitivity and good stability. The limit of detection for verapamil measured with MS/MS using selected reaction monitoring (SRM) mode (m/z 455 → m/z 165 and 303) was 30 pmol/l (75 amol) as seen in Fig. 4.9. The system also shows quantitative linearity (r^2=0.997) with a linear dynamic range of at least 6 orders of magnitude (Fig. 4.10) and good stability (standard deviation < 4%) at a measurement of 10 μM verapamil lasting for sixty minutes (Fig. 4.11). A more thorough evaluation of analytical performance of μPESI/MS is presented elsewhere.[20]

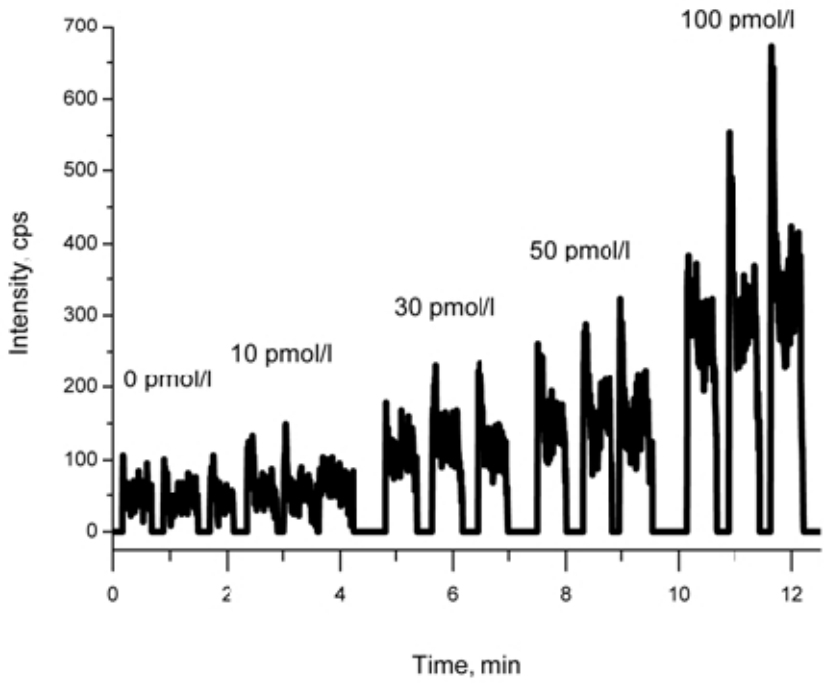

Figure 4.9. The sensitivity of the measurement using the μPESI chip. A blank sample and four different concentrations of verapamil (each injection 2.5 μl) were measured.

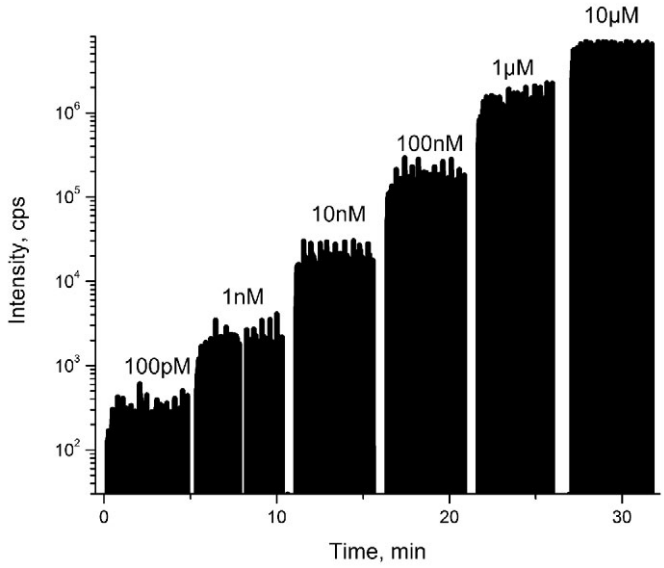

Figure 4.10. Linearity of the measurement with the μPESI chip. Verapamil was measured 60 times (injected amount 2.5 μl), ten times with each of six different concentrations.

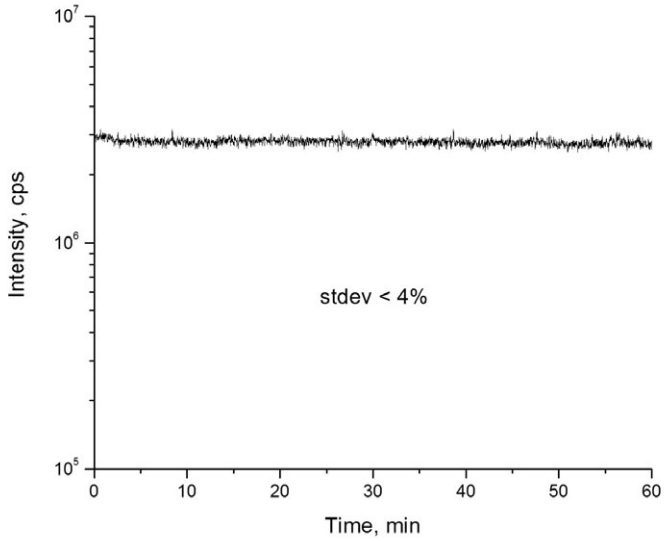

Figure 4.11. Stability of the measurement using the μPESI chip. Measurement of 10 μM verapamil with MS/MS using SRM mode with continuous injection.

4.4 Conclusions

We fabricated and characterized an ESI chip for mass spectrometric analysis. Using silicon as a fabrication material gives more freedom to chip design than other materials. Therefore, a truly three-dimensional in-plane ESI tip and a flow channel filled with an array of perfectly ordered high aspect ratio micropillars could be fabricated. Because there is no need to seal the channel, no bonding is required in the fabrication process. Application of the sample onto the μPESI chip is easy because it does not have a lid. The sample transport from the sample introduction spot to the ESI tip of the chip is spontaneous because of the capillary forces facilitated by the micropillar array. This filling method circumvents the use of pumps and cumbersome fluidic connectors. The micropillar array inside the channel is shown to have an essential role in the sample transport. Without the pillar array, wide lidless channels cannot be filled without external pumping. The μPESI chip also offers sensitive and stable analysis when coupled to a mass spectrometer. This combination of ease of use and high sensitivity is expected to be very useful in chemical analysis.

References

1 F. Foret, P. Kusy, Microfluidics for multiplexed MS analysis, Electrophoresis 27, 4877-4887, 2006.

2 Q. Xue, F. Foret, Y. M. Dunayevskiy, P. M. Zavracky, N. E. McGruer, B. L. Karger, Multichannel microchip electrospray mass spectrometry, Anal. Chem. 69, 426-430, 1997.
3 R. S. Ramsey, J. M. Ramsey, Generating electrospray from microchip devices using electroosmotic pumping, Anal. Chem. 69,1174-1178, 1997.
4 X.-Q. Wang, A. Desai, Y.-C. Tai, L. Licklider, T. D. Lee, Polymer-based electrospray chips for mass spectrometry, Tech. Digest, IEEE MEMS, Orlando, 1999 pp. 523-528.
5 C.-H. Chiou, G.-B. Lee, H.-T. Hsu, P.-W. Chen, P.-C., Liao, Micro devices integrated with channels and electrospray nozzles using PDMS casting techniques, Sens. Actuators, B, Chem. 86, 1-7, 2002.
6 S. Tuomikoski, T. Sikanen, R. A. Ketola, R. Kostiainen, T. Kotiaho, S. Franssila, Fabrication of enclosed SU-8 tips for electrospray ionization-mass spectrometry, Electrophoresis 26, 4691-4702, 2005.
7 A. Desai, Y.-C. Tai, M. T. Davis, T. D. Lee, A MEMS electrospray nozzle for mass spectrometry", Tech. Digest, IEEE Transducers, Chicago, 927-930, 1997.
8 S. Zhang, C. K. Van Pelt, J. D. Henion, Automated chip-based nanoelectrospray-mass spectrometry for rapid identification of proteins separated by two-dimensional gel electrophoresis, Electrophoreses 24, 3620-3632, 2003.
9 S. Arscott, S. Le Gac, C. Rolando, A polysilicon nanoelectrospray-mass spectrometry source based on a microfluidic capillary slot, Sens. Actuators, B, Chem. 106, 741-749, 2005.
10 M. Brinkmann, R. Blossey, S. Arscott, C. Druon, P. Tabourier, S. Le Gac, C. Rolando, Microfluidic design rules for capillary slot-based electrospray sources, Appl. Phys. Lett. 85, 2140-2142, 2004.
11 M. J. de Boer, J. G. E. Gardeniers, H. V. Jansen, E. Smulders, M-J. Gilde, G. Roelofs, J. N. Sasserath, M. Elwenspoek, Guidelines for etching silicon MEMS structures using fluorine high-density plasmas at cryogenic temperatures, J. Microelectromech. Syst. 11, 385-401, 2002.
12 S. Arscott, D. Troadec, Electrospraying from nanofluidic capillary slot, Appl. Phys. Lett. 87, 134101, 2005.
13 L. Sainiemi, S. Franssila, Mask material effects in cryogenic deep reactive ion etching, J. Vac. Sci. Technol., B 25, 801-807, 2007.
14 K. Grigoras, L.Sainiemi, J. Tiilikainen, A. Säynätjoki, V-M. Airaksinen, S. Franssila, Application of ultra-thin aluminium oxide etch mask made by atomic layer deposition technique, J. Phys: Conf. Ser. 61, 369-373, 2007.
15 T. H. Fedynyshyn, G. W. Grynkewich, T. B. Hook, M.-D. Liu, T.-P. Ma, The effect of aluminum vs. photoresist masking on the etching rates of silicon and silicon dioxide in CF4/O2 plasmas, J. Electrochem. Soc. 134, 206-209, 1987.
16 M. Zimmermann, H. Schmid, P. Hunziker, E. Delamarche, "Capillary pumps for autonomous capillary systems", Lab Chip 7, 119-125, 2007.

17 E. Delamarche, A. Bernard, H. Schmid, A. Bietsch, B. Michel, H. Biebuyck, Microfluidic networks for chemical patterning of substrates: design and application to bioassays, JACS 120, 500-508, 1998.
18 H. Anderson, W. van der Wijngaart, P. Griss, F. Niklaus, G. Stemme, Hydrophobic valves of plasma deposited octafluorocyclobutane in DRIE channels, Sens. Actuators, B, Chem. 75, 136-141, 2001.
19 L. Romeo, F. Yost, Flow in an open channel capillary, J. Fluid Mech. 322,109-129, 1996.
20 T. Nissilä, L. Sainiemi, T. Sikanen, T. Kotiaho, S. Franssila, R. Kostiainen, R. A. Ketola, Silicon micropillar array electrospray chip for drug and biomolecule analysis, Rapid commun mass spectr. 21, 3677-3682, 2007.

5. Fully polymeric integrated microreactor/electrospray ionization chip for on-chip digestion and mass spectrometric analysis (III)

We have developed, fabricated and tested a lidless polymeric microchip which integrates a microreactor with an electrospray ionization (ESI) tip for mass spectrometric (MS) analysis. The microchip contains a microreactor spot, a micropillar-filled channel and an electrospray tip, all made of an SU-8 epoxy polymer. The fabrication process of the microchips required just two lithographic steps, making it simple, cost-effective, rapid, and well-suited for mass production. The lidless structure of the chip provides easy sampling of reagents and samples. On-chip trypsin protein digestion of bovine heart cytochrome c (CytC) and bovine serum albumin (BSA) was performed in the microreactor in a solvent drop without the need for immobilization of the enzyme to the microreactor. The digestion was accomplished in the microreactor within eight minutes, after which the digestion products were measured directly by an integrated on-chip ESI combined to MS. The whole procedure was rapid as the total time for on-chip digestion and measurement was less than ten minutes. An average sequence coverage obtained with CytC was 90 % and with BSA it was 82 %. The microchip can also be used as a stand-alone electrospray ionization tip for mass spectrometric analysis.

5.1 Introduction

The goal of microfluidics has been the integration of several functions such as sample concentration, separation, and analysis on a single microchip. [1] The integration would reduce the number of laborious manual steps currently used in analytical procedures. Therefore, such microfluidic chips would make the analysis of samples faster and more cost-effective. At the time being, only a few microchips that are capable of performing multiple functions exist.[2] Another major advantage of miniaturized fluidic chips is the reduced size because at the microscale, diffusion-limited reactions occur faster. The sample volumes required are also much smaller, which is advantageous, especially when dealing with difficult-to-obtain or otherwise expensive samples.

The most common material used in microtechnology is silicon, due to its well-characterized material properties and sophisticated fabrication techniques developed for the microelectronics industry. However, in microfluidics, glass and polymers are often utilized instead of silicon because of electrical and thermal insulation and transparency in the visible wavelengths. Polymer microfabrication has developed rapidly and various fabrication procedures for elaborate devices have been published.[3] While poly(dimethylsiloxane) (PDMS) has been extensively used, photoactive polymers are gaining more popularity because they are directly patternable using UV light. The most commonly used photopolymer is an epoxy-based polymer SU-8 which is mechanically strong, electrically insulating, biocompatible, flexible, visually transparent, and it also

supports electro-osmotic flow (EOF).[4] All of these properties are advantageous in most fluidic devices. SU-8 has been previously used, for example in the fabrication of a closed, straight channel ESI tip,[4] of an integrated capillary electrophoretic-ESI (CE-ESI) chip,[5] and of an integrated microfabricated system containing a purification module and nanoESI interface.[6]

Electrospray ionization (ESI) is a common method in analytical chemistry to form ions into a gas phase for mass spectrometric (MS) analysis. As an analytical technique ESI-MS has high specificity and sensitivity, especially when combined with separation methods such as liquid chromatography or capillary electrophoresis. ESI-MS is commonly used for rapid detection and identification of polar organic compounds from a variety of sample matrices. The simple structure and easy usefulness of ESI forms an ideal platform for miniaturization, and various forms of ESI tips have been fabricated during the last decade.[7,8] Most of the chips use external mechanical pumps or electro-osmotic pumping to provide sample transportation. Both methods require additional equipment such as a pump or a voltage source in addition to the chip. Capillary forces can also be used for sample transportation, as exemplified with the use of micropillar arrays. [9,10,11,12,13,14] Recently, we presented a micropillar array electrospray ionization (μPESI) chip made of silicon.[15] A hydrophilic microchannel that has a regular pillar array facilitates capillary forces even in a wide and lidless channel.[16,17]

Microreactors have been made of silicon, glass, and polymers, for various chemical and biological reactions, as previously reviewed.[18] Most of the microreactors used for trypsin digestion of proteins have utilized immobilized enzymes on the walls of the reactions spot or along the reaction channel.[19] The microreactor has been connected to a mass spectrometer with a liquid junction microelectrospray interface,[20] an off-line nanoESI,[21] an on-line nanoESI,[22] an off-line MALDI-TOF interface,[23,24,25] an on-line HPLC [19], a DIOS interface [26] or a CE interface [27,28]. On-line digestion in a confluence of two liquid flows has also been performed and the digestion products have been analyzed with a CE-ESI microchip.[29] In some studies porous silicon has been utilized as a carrier matrix for immobilization of enzymes [30,31,32].

Here we present a novel polymeric microreactor integrated with an electrospray ionization chip for mass spectrometric measurement. The fabrication process of the chip is straight-forward, and well-suited for mass production without the need for immobilization of enzymes to the microreactor. The chip contains a microreactor spot, a channel with perfectly ordered micropillars and an in-plane electrospray tip. Reactions on the chip are fast due to micro scale in the microreactor spot. The hydrophilic micropillar channel provides strong capillary forces, therefore reaction products are spontaneously transported from the microreactor to the electrospray tip. Direct electrospray at the tip facilitates specific and sensitive analysis with mass spectrometers. The integrated microchip is applied to on-chip protein digestion experiments and its use as a stand-alone ESI tip is also demonstrated.

5.2 Experimental

5.2.1 Fabrication

Single-side-polished <100> oriented silicon wafers, purchased from Okmetic (Vantaa, Finland), were used as substrates for microreactor/electrospray ionization chips. The diameter of the wafers was 100 mm with a thickness of 381 ± 15 μm. SU-8 50 negative tone photoresist and a developer mr-Dev 600 were purchased from Micro Resist Technologies GmbH (Berlin, Germany). The SU-8 layers were exposed using a Karl Süss MA6/BA6 (München, Germany) i-line mask aligner.

The silicon wafers were thermally wet oxidized at 1050 ºC in a horizontal furnace to create a 650-nm-thick sacrificial SiO_2 layer for releasing the chips from the silicon substrate. The first layer of SU-8, which created a 70-μm-thick floor, was spun on the oxidized substrate and exposed to form the bottom part of the sharp electrospray tip using the first photomask. Before the development of non-cross linked SU-8, another 70-μm-thick SU-8 layer was spun on top of the first one. The second photomask defines the microreactor, the micropillar channel and the ESI tip. The microreactor is circular with a diameter of 2.5 mm. The channel is 5.5 mm long and 1 mm wide and it contains a regular array of 10-μm-diameter micropillars in hexagonal packing. The channel narrows to a 100-μm-wide ESI tip. After the second exposure, both SU-8 layers were simultaneously developed. The SU-8 chips were released from the substrate by etching the sacrificial SiO_2 layer in 50 % hydrofluoric acid. Finally, the chips were treated with oxygen plasma in a Plasmalab 80 System reactive ion etcher (Oxford Instruments, Bristol, UK), in order to decrease the water contact angle of SU-8 surface below 45º. The silicon substrate is reusable. The process flow is schematically depicted in Figure 5.1.

5.2.2 Digestion and measurement

All solvents used were HPLC grade. Methanol was from J.T. Baker (Deventer, The Netherlands). Water was purified with a Milli-Q water purification system (Millipore, Molsheim, France). Formic acid, methanol, ammonium bicarbonate, trifluoroacetic acid (TFA), angiotensin I and II and substance P, bovine heart cytochrome c (CytC), and bovine albumin serum (BSA) were obtained from Sigma-Aldrich. Verapamil was purchased from ICN biomedicals Inc. (Aurora, OH, USA) and sequencing grade modified trypsin was from Promega (Madison, WI, USA).

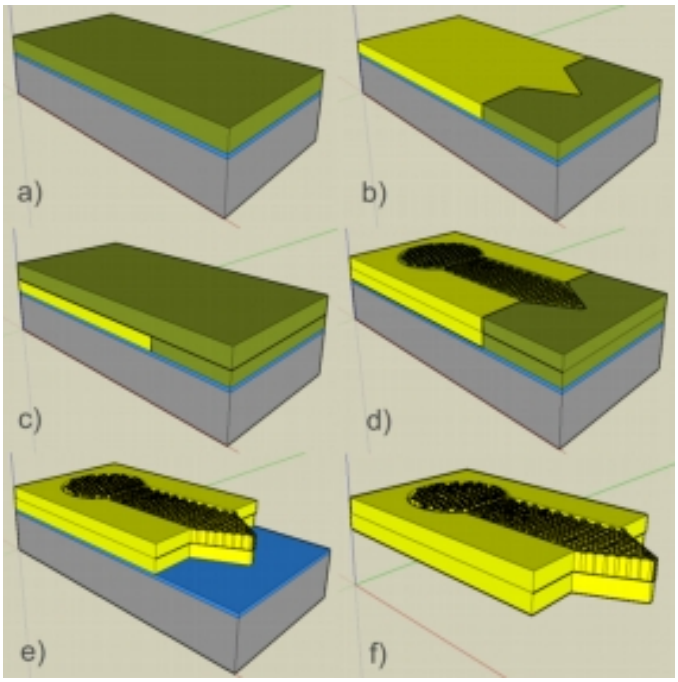

Figure 5.1. Fabrication of SU-8 microreactor/electrospray ionization chip. a) Spinning of the first layer of SU-8 on top of an oxidized silicon substrate. b) Exposure of the first SU-8 layer. c) Spinning of the second SU-8 layer. d) Exposure of the second SU-8 layer. e) Development of both SU-8 layers simultaneously. f) Release of the SU-8 chips by sacrificial etching of SiO_2.

The mass spectrometers used were an API3000 triple-quadrupole (Applied Biosystems/MDS Sciex, Concord, Canada), an ion trap 6330 (Agilent, Santa Clara, CA, USA) and a QTOF Micro quadrupole-time-of-flight instrument (Waters/Micromass, Manchester, UK).

The setup for all measurements was similar. The microchip was positioned in front of the MS on a plastic, non-conductive plate with the tip of the chip just over the edge of the plate. The position of the chip was adjusted using a xyz-controller (Proxeon, Odense, Denmark). The voltage between the chip and the MS was applied using a platinum electrode and a high voltage source of the MS. Spraying voltage applied depended on the distance between the chip and MS (5 – 7 mm) and the geometry of the first plate of the MS, being usually about 3 kV. When a sample solution was pipetted onto the chip, capillary forces drove the sample to the tip of the chip. A typical sampling volume was 2 – 3 µL. The chip electrosprayed solution to the MS while there was solution at the microtip and the voltage was set on.

On-chip digestion was performed on the microreactor spot of the chip. 20 µg of trypsin was diluted with 57 µL of 50 mM acetic acid to give a concentration of 0.35 µg/µL. The buffer used was 100 mM ammonium bicarbonate at pH 8. The concentration of proteins (bovine heart cytochrome c (CytC) and bovine albumin serum (BSA)) in solutions used for digestion was 10 µg/µL (in water). The on-chip digestion experiments were performed using the QTOF Micro mass spectrometer for the detection of digestion products. The

QTOF Micro MS was externally calibrated using sodium iodide solution at a mass range from *m/z* 100 to 2500. The high voltage for ESI was 3250 V and the cone temperature was 80 ºC. The voltage of the sample cone was tuned to 40 V, the extraction cone to 2 V, the ion energy to 2.0 V, the collision energy to 10.0 eV and the mass range measured was from *m/z* 100 to 1500. Samples of blank solution (90 % of methanol, 9.9 % water and 0.1 % TFA) were analyzed before the digestion experiments. While the voltage between the chip and MS was turned off, 1 µL of the trypsin solution and 1 µL of the protein solution were pipetted onto the chip and incubated for one minute at 36 ºC (the temperature of the microchip caused by heating from the cone of the mass spectrometer) before adding 3 µL of the buffer solution. The reaction mixture was incubated for about 8 minutes until the buffer solution evaporated (a flow of nitrogen was used to assist the evaporation). The high voltage was turned on and the digestion products were flushed with 3 µL of the blank solution to the tip of the microchip and consequently electrosprayed and deteced with the MS. This procedure was repeated five times in order to clean the microchip before the next digestion experiment. A background mass spectrum (the mass spectrum of a blank sample) was subtracted from the acquired MS data. The *m/z* values of peaks obtained were entered to the MASCOT search engine at www.matrixscience.com, MSDB database was used and identification criteria of ± 50 mDa were used. The digestion experiments were repeated four times with BSA and three times with CytC.

5.2.3 Stand-alone ESI tip

Performance of the chip as an ESI tip was evaluated using verapamil (a drug substance) and a mixture of peptides as test samples. For verapamil, the limit of detection (LOD), linearity range and stability of the signal were determined with the API3000 triple-quadrupole mass spectrometer. Verapamil was dissolved into 95 % aqueous methanol containing 0.1 % formic acid. Approximately 2.5 µL of a blank solution (95 % aqueous methanol containing 0.1 % formic acid) was introduced ten times to the chip and 1nM verapamil solution ten times after that. Selected reaction monitoring (SRM) was used in LOD measurements. The SRM pairs *m/z* 455 (protonated verapamil) → 303 and *m/z* 455 → 165 were followed. Background was defined by averaging the signal from ten collected and integrated blank sample replicates. LOD was defined as the signal-to-noise ratio (≥ 3) where the signal was background subtracted average of collected and integrated signals from ten verapamil samples and the noise was the standard deviation of integrated signals from blank samples. The linearity was tested in the range of 1 nM to 10 µM, using ten replicates of sampling of 2.5 µL for each concentration. Determination was made using the same solvent composition and SRM method as in LOD measurements. In the stability experiments the sample solution was continuously injected to the chip using a syringe pump Harvard PHD2000 (Harvard Apparatus, Holliston, MA, USA) and a fused silica capillary (i.d. 150 µm, o.d. 250 µm). The end of the capillary was positioned to the microreactor spot of the chip to achieve a continuous liquid flow in the micropillar array, and the flow rate used was 7 µL/min. Selected ion monitoring (SIM) mode was used for the measurements of verapamil signal (ion at *m/z* 455). The mixture of peptides

(angiotensin I, II, and substance P) was used to test the performance of the polymeric chip for the analysis of peptides with the Agilent ion trap MS. Peptides were measured with an aqueous solution containing 90 % methanol and 0.1 % formic acid, and the sample volume applied to the chip was 3 µL.

5.3 Results and discussion

5.3.1 Fabrication

The strength of the fabrication process presented is in its simplicity. The oxidized silicon wafer serves only as a mechanical support and the microchips are fully made of SU-8. The two lithographic processes define the device on the substrate. In our case, the development of unexposed SU-8 is easy because the channels do not have a coverlid. Development of enclosed channels is diffusion-limited and in the case of long channels, very slow. Extremely long development times can also inflict cracking.[4] The lidless chip design also circumvents the use of a cumbersome bonding process. The sacrificial etching of silicon dioxide releases the chips from the substrate and has been used before in fabrication of SU-8 ESI tips.[4]

Fabrication of similar micropillar channel-ESI tips from silicon has been published previously.[15] Figure 5.2a shows the SU-8 chip inside a staple. The fabrication process of silicon chips requires two deep reactive ion etching (DRIE) steps. Through-wafer etching to define the tip is especially time consuming. Both DRIE steps require hard masks. Typically a metal mask is required for through-wafer etching and the pillar channel is etched using a silicon dioxide mask. Lithography and etching steps are required for patterning of hard masks. Fabrication of SU-8 devices requires only two lithographic steps and the resulting device geometries are similar (pillar spacing is different due to the different photomask fabrication processes, and the pillar height is variable depending on SU-8 thickness and silicon DRIE depth). No etching is needed in the SU-8 version, except for the non-critical release etch. The processing time required for the fabrication of the SU-8 microreactor/ESI chips is considerably shorter compared with that of the silicon version.

Well-established silicon micro and nanofabrication techniques enable fabrication of robust high-aspect-ratio micro and nanostructures. The mechanical properties of silicon are in many cases superior to those of SU-8. Still, due to low price and easy fabrication of SU-8 devices, the use of SU-8 is feasible in applications where its mechanical properties are adequate. Unlike silicon, SU-8 is a flexible material, which renders pillars and the whole chip more durable and shock-resistant. The pillars in the SU-8 chip are not as well defined as those in a silicon chip. Still, the form of the pillar array is adequate to enable the spontaneous filling of the chip. The tip of the SU-8 chip is presented in Figure 5.2b.

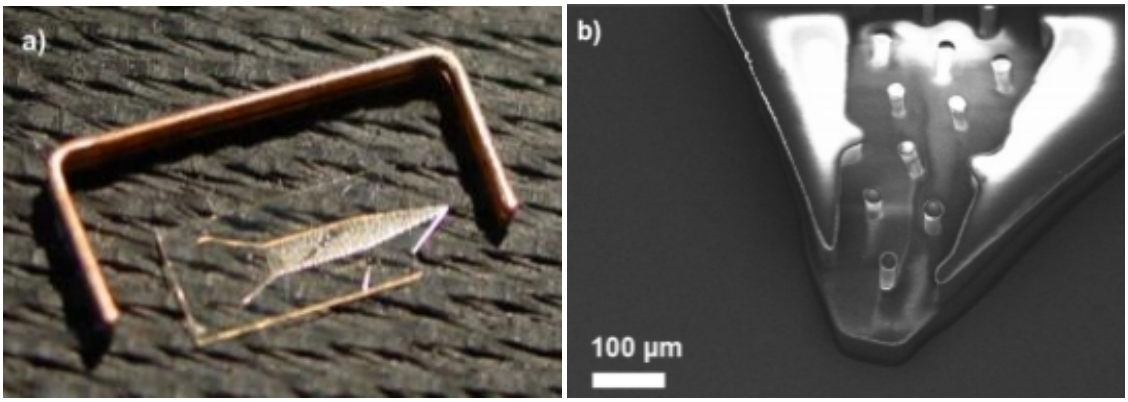

Figure 5.2 a) A photograph of a SU-8 microreactor/electrospray chip side by side with a staple. **b)** A scanning electron microscopic image of the electrospray tip of the SU-8 chip.

5.3.2 Performance of stand-alone ESI chip

The performance of the SU-8 microchip as a pure ES ionization tip was tested using verapamil as the test compound and a triple-quadrupole MS in SRM mode. The observed LOD was 1 nmol/L, corresponding to an absolute amount of 2.5 fmol when 2.5 µL of sample solution was applied. The quantitative linearity range was observed to be 4 orders of magnitude, from 10 nM to 10 µM with 2.5-µL-sampling, the correlation coefficient r^2 being 0.990 (the linearity curve is presented in Fig. 5.3a). The LOD of verapamil obtained in the analysis with the SU-8 chip is somewhat higher than that with the silicon chip: 2.5 fmol vs. 60 amol.[7] This discrepancy is probably caused by differences in the electric field at the proximity of the electrospray tip because silicon is conductive whereas SU-8 can be considered as an insulator. The stability of the verapamil signal during ES ionization was determined with a continuous application of the sample solution to the chip. A relative standard deviation (RSD) of the peak height of the signal during a 25-min-long measurement for verapamil at a concentration level of 1 µM, 100 nM , and 10 nM was 0.6 %, 2.5 %, and 2.2 %, respectively. The extracted ion chromatograms from the measurement of stability are shown in Figure 5.3b. RSD values were of the same order as those previously obtained for the silicon µPESI [15] and for a closed, straight channel ESI tip made of SU-8.[33]

The performance of the polymeric chip was also tested with other compounds and with another mass spectrometric instrument, namely with peptides using an ion trap MS. A mixture of angiotensin I, II and substance P (at a concentration level of 100 µg/mL of each peptide) was analyzed, and a typical mass spectrum obtained from the peptide mixture is presented in Figure 5.4. It shows that the peptides were ionized in a manner comparable to that with a normal-sized ESI source, showing multiple charge states for each peptide and only a few intensive background peaks. As shown, the polymeric microchip can be used as an ESI tip for both small molecules and biomolecules. The linearity and stability tests show that the microchip is applicable also for quantitative analysis, which was not the aim

of this study however. It is possible to form multispray ionization (i.e., several plumes from the tip at the same time) by increasing the high voltage, but it was observed that ionization was most stable and sensitive when only one plume sprays from the tip (data not shown).

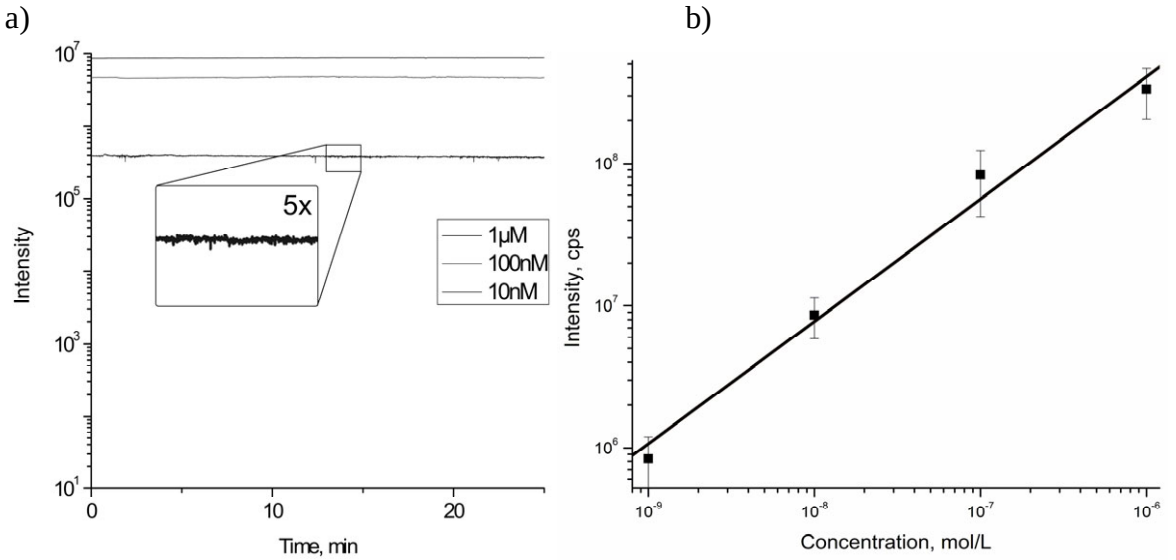

Figure 5.3 a) Linearity of the measured signal for verapamil with the SU-8 chip. **b)** Stability of the verapamil signal at three concentration levels using the SU-8 ESI chip, measurement by a triple-quadrupole MS in SRM mode, and a continuous application of the sample solution to the microchip.

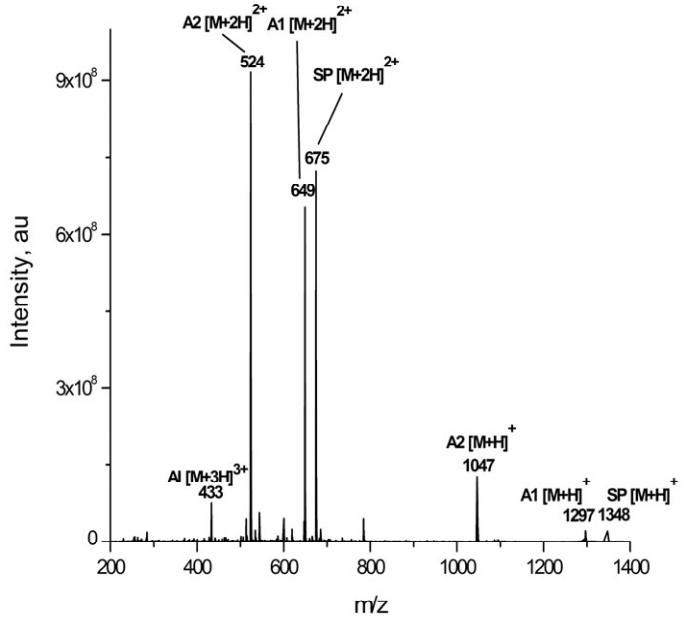

Figure 5.4. A mass spectrum of a peptide mixture (angiotensin I (A1), angiotensin II (A2), and substance P (SP)) measured with the polymeric ESI chip and an ion trap MS.

5.3.3 On-chip trypsin digestion

The polymeric chip was tested as an integrated microreactor/electrospray ionization device using a well-known protein digestion with trypsin as a test case. Trypsin, protein, and buffer solutions were pipetted into the microreactor and the reaction mixture was incubated for eight minutes in order to ensure a complete digestion of the protein molecules. The total volume of the reaction mixture was 5 µL. After incubation the digestion products were flushed from the ESI tip with the buffer solution, ionized, and analyzed with a QTOF mass spectrometer. The total time of the digestion and analysis was approximately ten minutes. A mass spectrum measured for the reaction products from bovine heart cytochrome C digestion (the amount of protein digested was 10 µg) is shown in Figure 5.5. The digestion experiments of CytC were repeated three times. The peptides detected (an average number of peptides observed in the mass spectra was 23 ± 3) after CytC digestion covered 90 ± 10 % of the CytC amino acid sequence. The sequence of CytC is shown in Figure 5.5. Some peaks from the background were also observed but they did not interfere with the analysis of peptides because high resolution of the QTOF mass spectrometer was utilized. With more complex samples the non-identified peaks from autolysis of trypsin can interfere with the data analysis if the resolution of the mass spectrometer is inadequate. The same kind of digestion experiments were conducted for another protein, bovine serum albumin (BSA). A total number of 108 digested peptides were found, covering 87% of the BSA sequence as shown for one sample in Figure 5.6. With four replicate digestion experiments the sequence coverage ranged from 76 to 87 %, with an average of 82 %. A typical mass spectrum measured from the sample showing the detected peptides is presented in Figure 5.6. It is well-known that surfaces can adsorb peptides and proteins.[34,35,36] In this research the number of peptides observed and the high magnitude of sequence coverage obtained show that the surface adsorption was not a major concern in the analysis. This was also confirmed with analyses of blank samples which did not show any traces of proteins or digested peptides after cleaning the microchip.

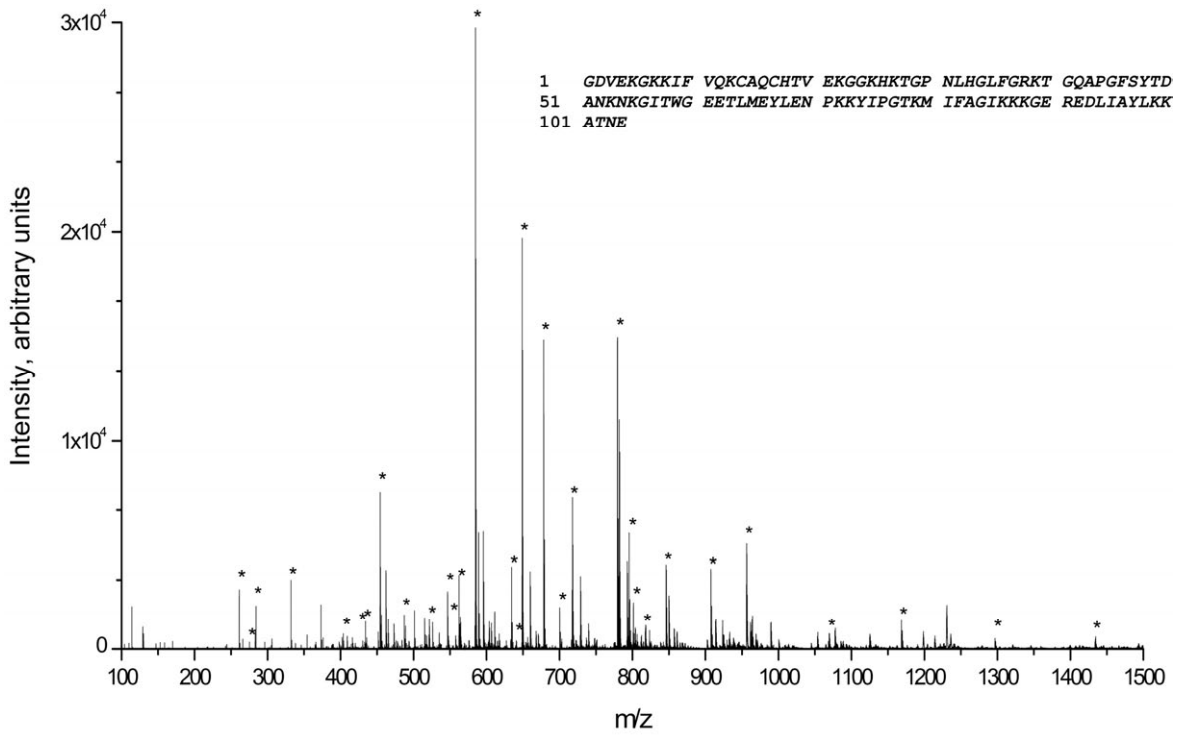

Figure 5.5. A mass spectrum of a tryptic digestion of bovine heart cytochrome C protein, measured after on-chip digestion using the SU-8 ESI chip and QTOF/MS. The peptides detected from the mass spectrum are marked with an asterisk after the subtraction of the mass spectrum of a blank sample. The amino acid sequence of cytochrome C is shown, as well as the sequence coverage observed, marked with bold and italics.

The polymeric microreactor combined with direct electrospray ionization seems to be an efficient combination to analyze the products from protein digestions. The total amounts of proteins used in the microreactor were 14 pmol (BSA) and 86 pmol (CytC) but smaller amounts could be used if needed. The sequence coverage with this method was similar to or better than those obtained with other microreactors using immobilized trypsin [20,25,37] or without the immobilization of trypsin.[38] The major benefit of this method is its simplicity because there is no need for external devices (for example pumps, syringes, or high voltage sources) for sample transportation or for sample treatment (for example the addition of a matrix as in matrix-assisted laser desorption/ionization (MALDI) analysis) during the on-chip digestion and subsequent MS analysis. The same microchip could be used for digestion experiments for several days without reduced sensitivity or reduced spontaneous liquid transfer (data not shown).

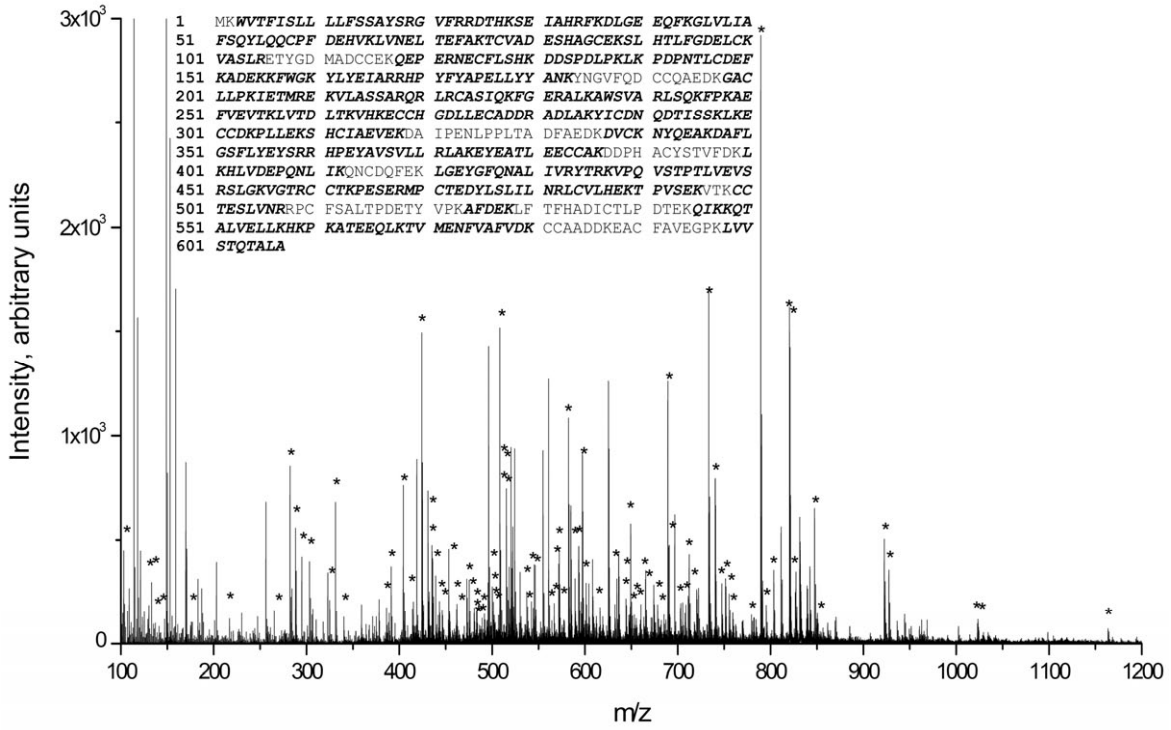

Figure 5.6. A mass spectrum of a tryptic digestion of bovine serum albumin protein, measured after on-chip digestion using the SU-8 chip and QTOF/MS. The peptides detected from the digestion are marked with an asterisk after the subtraction of the mass spectrum of a blank sample. The amino acid sequence of BSA is shown, as well as the sequence coverage observed, marked with bold and italics.

5.4 Conclusions

We have presented a lidless microreactor/electrospray ionization chip made completely of SU-8 polymer with a self-filling structure. The microchip provides an on-chip microreactor, a spontaneous liquid transfer, and a stable ES ionization. The chip can be easily connected to various mass spectrometers that have an atmospheric pressure ion source, such as QTOF, triple-quadrupole, and ion trap instruments. The open micropillar array structure of the chip provides easy sampling of digestion solutions and reliable liquid transportation due to multiple pathways between the micropillars. The benefits of the polymeric chip are its straightforward, simple fabrication process and low price. Therefore, the microchips are well-suited for disposable use. In digestion experiments there is no need for an external device for sample transfer or sample treatment before the direct ESI/MS measurement. The on-chip digestion and measurement can be conducted in ten minutes, making the system ideal for rapid screening of proteins. The simplicity of the digestion process and the high digestion efficiency show that the current method could be applicable to automated high-throughput protein analysis, using a platform of multiple microreactor-ESI chips. Due to the lack of immobilization of trypsin the same microreactor chip could be used, after cleaning, for digestion experiments using a variety of different enzymes, thus making it cost-effective. For that reason, the microreactor could

also be used for performing other chemical or biochemical reactions. In addition to the instantaneous analysis of microreactor products, the microchip can be used for direct ESI/MS analysis of small and biomolecules.

References

[1] A. Manz, N. Graber, H. M. Widmer, Miniaturized total chemical analysis systems: a novel concept for chemical sensing, Sens. Actuators B, 1, 244-248, 1990.

[2] T. Thorsen, S. J. Maerkl, S. R. Quake, Microfluidic Large-Scale Integration, Science 298, 580-584, 2002.

[3] C-C. Lee, G. Sui, A. Elizarov, C.J. Shu, Y-S. Shin, A.N. Dooley, J. Huang, A. Daridon, P. Wyatt, D. Stout, H.C. Kolb, O.N. Witte, N. Satyamurthy, J.R. Heath, M.E. Phelps, S.R. Quake, H-R. Tseng, Multistep Synthesis of a Radiolabeled Imaging Probe Using Integrated Microfluidics, Science 310, 1793-1796, 2005.

[4] S. Tuomikoski, T. Sikanen, R.A. Ketola, R. Kostiainen, T. Kotiaho, S. Franssila, Fabrication of enclosed SU-8 tips for electrospray ionization mass spectrometry, Electrophoresis 26, 4691-4702, 2005.

[5] T. Sikanen, S. Tuomikoski, R.A. Ketola, R. Kostiainen, S. Franssila, T. Kotiaho, Fully microfabricated and integrated SU-8-based capillary electrophoresis-electrospray ionization microchips for mass spectrometry, Anal. Chem. 79, 9135-9144, 2007.

[6] J. Carlier, S. Arscott, V. Thomy, J-C. Camart, C. Cren-Olive, S. Le Gac, Integrated microfabricated systems including a purification module and an on-chip nano electrospray ionization interface for biological analysis, J. Chromatogr. A 1071, 213-222, 2005.

[7] S. Koster, E. Verpoorte, A decade of microfluidic analysis coupled with electrospray mass spectrometry: An overview, Lab Chip 11, 1394-1412, 2007.

[8] T. Sikanen, S. Franssila, T. J. Kauppila, R. Kostiainen, T. Kotiaho, R. A. Ketola, Microchip technology in mass spectrometry, Mass Spectrom. Rev. 29, 351-391, 2010.

[9] S. Arscott, B. Legrand, L. Buchaillot, A. E. Ashcroft, A silicon beam-based microcantilever nanoelectrosprayer, Sens. Actuators B 125, 72-78, 2007.

[10] V. Jokinen, S. Franssila, Capillarity in microfluidic channels with hydrophilic and hydrophobic walls, Microfluid. Nanofluid. 5, 443-448, 2008.

[11] N. Vervoort, J. Billen, P. Gzil, G.V. Baron, G. Desmet, Importance and reduction of the sidewall-induced band-broadening effect in pressure-driven microfabricated columns, Anal. Chem. 76, 4501-4507, 2004.

[12] J. De Smet, P. Gzil, G.V. Baron, G. Desmet, On the 3-dimensional effects in etched chips for high performance liquid chromatography-separations, J. Chromatogr. A 1154 189-197, 2007.

[13] R. de Andrade Costa, K. Mogensen, J. Kutter**,** Microfabricated porous glass channels for electrokinetic separation devices, Lab Chip 5, 1310-1314, 2005.

[14] A. Saha, S. Mitra, M. Tweedie, S. Roy, J. McLaughlin, Experimental and numerical investigation of capillary flow on SU8 and PDMS microchannels with integrated pillars, Microfluid. Nanofluid. 7, 451-465, 2009

[15] T. Nissilä, L. Sainiemi, T. Sikanen, T. Kotiaho, S. Franssila, R. Kostiainen, R. A. Ketola, Silicon micropillar array electrospray chip for drug and biomolecule analysis, Rapid Commun. Mass Spectrom. 21, 3677-3682, 2007.

[16] L. Sainiemi, T. Nissilä, V. Jokinen, T. Sikanen, T. Kotiaho, R. Kostiainen, R. A. Ketola, S. Franssila, Fabrication and fluidic characterization of silicon micropillar array electrospray ionization chip Sens. Actuators B Chem. 132, 380-387, 2008.

[17] N. Suni, M. Haapala, A. Mäkinen, L. Sainiemi, S. Franssila, E. Färm, E. Puukilainen, M. Ritala, R. Kostiainen, Selective Surface Patterning with an Electric Discharge in the Fabrication of Microfluidic Structures, Angew. Chemie Int. Ed. 47, 7442-7445, 2008.

[18] G.N. Doku, W. Verboom, D.N. Reinhoudt, A. van den Berg, On-microchip multiphase chemistry—a review of microreactor design principles and reagent contacting modes, Tetrahedron 61, 2733-2742, 2005.

[19] A. Cingöz, F. Hugon-Chapuis, V. Pichon, Evaluation of various immobilized enzymatic microreactors coupled on-line with liquid chromatography and mass spectrometry detection for quantitative analysis of cytochrome c, J. Chromatogr. A 1209, 95-103, 2008.

[20] J. Krenkova, Z. Bilkova, F. Foret, Characterization of a monolithic immobilized trypsin microreactor with on-line coupling to ESI-MS J. Sep. Sci. 28, 1675-1684, 2005.

[21] J. Ji, Y. Zhang, X. Zhou, J. Kong, Y. Tang, B. Liu, Enhanced Protein Digestion through the Confinement of Nanozeolite-Assembled Microchip Reactors, Anal. Chem. 80, 2457-2463, 2008.

[22] Zhao, H. Jiang, D.R. Smith, S. Bruckenstein, T.D.Wood, Integration of an on-line protein digestion microreactor and a nanoelectrospray emitter for rapid peptide mapping, Anal. Biochem. 359, 167-175, 2006.

[23] X. Xu, X. Wang, Y. Liu, B. Liu, H. Wu, P. Yang, Trypsin entrapped in poly(diallyldimethylammonium chloride) silica sol-gel microreactor coupled to matrix-assisted laser desorption/ionization time-of-flight mass spectrometry, Rapid Commun. Mass Spectrom. 22, 1257-1264, 2008.

[24] A. Palm, M. Novotny, Analytical characterization of a facile porous polymer monolithic trypsin microreactor enabling peptide mass mapping using mass spectrometry, Rapid Commun. Mass Spectrom. 18, 1374-1382, 2004.

[25] S. Wang, Z. Chen, P. Yang, G. Chen, Trypsin-immobilized fiber core in syringe needle for highly efficient proteolysis, Proteomics 8, 1785-1788, 2008.

[26] K. Nichols, S. Azoz, H. Gardeniers, Enzyme kinetics by directly imaging a porous silicon microfluidic reactor using desorption/ionization on silicon mass spectrometry, Anal. Chem. 80, 8314-819, 2008.

[27] R. Schoenherr, M. Ye, M. Vannatta, N. Dovichi, CE-microreactor-CE-MS/MS for protein analysis, Anal. Chem. 79, 2230-2238, 2007.

[28] C. Wang, R. Oleschuk, F. Ouchen, J. Li, P. Thibault, D. Harrison., Integration of immobilized trypsin bead beds for protein digestion within a microfluidic chip

incorporating capillary electrophoresis separations and an electrospray mass spectrometry interface, Rapid Commun. Mass Spectrom. 14, 1377-1383, 2000.

[29] P. Hoffmann, U. Häusig, P. Schulze, D. Belder, Microfluidic Glass Chips with an Integrated Nanospray Emitter for Coupling to a Mass Spectrometer, Angew. Chem. Int. Ed. 46, 4913-4916, 2007.

[30] J. Drott, K. Lindström, L. Rosengren, T. Laurell, Porous silicon as the carrier matrix in microstructured enzyme reactors yielding high enzyme activities, J. Micromech. Microeng. 7, 14-23 1997.

[31] A. Ressine, S. Ekström, G. Marko-Varga, T. Laurell, Macro-/nanoporous silicon as a support for high-performance protein microarrays, Anal. Chem. 75, 6968-6974, 2003.

[32] C. Melander, D. Momcilovic, C. Nilsson, M. Bengtsson, H. Schagerlöf, F. Tjerneld, T. Laurell, C.T. Reimann, L. Gorton, Microchip immobilized enzyme reactors for hydrolysis of methyl cellulose, Anal. Chem. 77, 3284-3291, 2005.

[33] T. Sikanen, S. Tuomikoski, R.A. Ketola, R. Kostiainen, S. Franssila, T. Kotiaho, Analytical characterization of microfabricated SU-8 emitters for electrospray ionization mass spectrometry, J. Mass Spectrom. 43, 726-735, 2008.

[34] S-F. Sui, H. Wu, J. Sheng, Y. Guo, Conformational changes of proteins at an interface induced by a supported planar phosphatidic acid monolayer, J. Biochem. 115, 1053-1057, 1994.

[35] P. Turbill, T. Beugeling, A.A. Poot, Proteins involved in the Vroman effect during exposure of human blood plasma to glass and polyethylene, Biomaterials 17, 1279-1287, 1996.

[36] M. Lindblad, M. Lestelius, A. Johansson, P. Tengvall, P. Thomsen, Cell and soft tissue interactions with methyl- and hydroxyl-terminated alkane thiols on gold surfaces, Biomaterials 18, 1059-1068, 1997.

[37] D.S. Peterson, T. Rohr, F. Svec, J.M.J. Fréchet, Dual-function microanalytical device by *in-situ* photolithographic grafting of porous polymer monolith: integrating solid phase extraction and enzymatic digestion for peptide mass mapping, Anal. Chem. 75 5328-5335, 2003.

[38] D. Finnskog, K. Jaras, A. Ressine, J. Malm, G. Marko-Varga, H. Lilja, T. Laurell, High-speed biomarker identification utilizing porous silicon nanovial arrays and MALDI-TOF mass spectrometry, Electrophoresis 27, 1093-1103, 2006.

6 Integrated Photocatalytic Nanoreactor Electrospray Ionization Microchip for Mimicking Phase I Metabolic Reactions (IV)

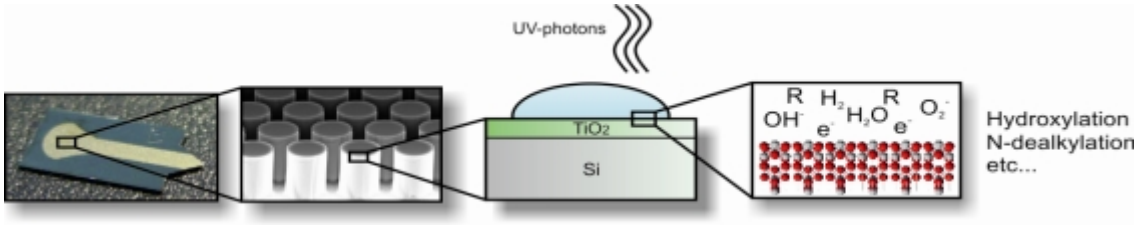

We developed a nanoreactor chip based system to mimic phase I metabolic reactions of small organic compounds. The microchip, made of silicon, has an anatase-phase titanium dioxide (TiO_2) nanolayer coating for photocatalysis and an integrated electrospray ionization (ESI) tip for direct mass spectrometric (MS) analysis. This novel method for mimicking phase I metabolic reactions uses an on-chip TiO_2-nanolayer and an external UV-lamp to induce photocatalyzed chemical reactions of drug compounds in aqueous solutions. The reactions of selected test compounds (verapamil, metoprolol, propranolol, lidocaine, 2-acetamidofluorene, and S-methylthiopurine) produced mostly the same main products as phase I metabolic reactions induced by human liver microsomes, rat hepatocytes, or cytochrome P enzymes, showing hydroxylation, dehydrogenation, and dealkylations as the main photocatalytic reactions. With this method it is possible to detect reactive and toxic products (mimicking reactive metabolites) due to the absence of biological matrices and to an immediate analysis. The method used is sensitive: only 20 – 40 pmol (1 – 10 ng) of a substrate was needed for the experiment, thus it provides an inexpensive method for screening possible metabolites of new drug candidates. Due to small dimensions of the microchip, diffusion lengths are suitable for the high reaction rates, thus providing a rapid analysis as the reaction products can be detected and identified directly after the photoinduced reactions have occurred. The method shows a similar performance to that of electrochemistry, a commonly used technique for mimicking phase I metabolism.

6.1 Introduction

In drug discovery it is important to know as early as possible whether the drug candidate is forming toxic metabolites or not. The most important active site for drug metabolism is the liver where phase I metabolic enzymes such as cytochrome P450 biotransform xenobiotics into polar metabolites. If toxic metabolites are formed, this usually takes place in phase I metabolism and therefore it is important to establish the metabolism studies as early as possible in the preclinical stage of drug discovery. In drug discovery, the metabolism of each drug candidate must be evaluated and these *in vitro* metabolism

experiments are extensive, time consuming, and expensive. Metabolites, formed *in vitro* by using hepatocytes, microsomes, or CYP450 enzymes, are usually analyzed with high-performance liquid chromatography combined with tandem mass spectrometry (HPLC-MS/MS).[1] This procedure is comprehensive and selective but also time-consuming and laborious.

Electrochemistry (EC) has been shown to be able to mimic phase I oxidative reactions of compounds when compared with cytochrome P450 reactions. EC can be used to form small amounts of reaction products starting from the drug or drug candidate.[2,3] There is also a commercial EC/LC system available which can be combined with MS. Mimicking of metabolism with EC is done in an electrochemical cell where a variety of oxidation products can be obtained by applying different voltages to the cell. Electrolyte solution has shown to affect the reaction efficiency of organic compounds[3] and by varying the electrolyte composition, different kinds of products are able to form. When the EC system is directly combined with MS, without LC, the electrolyte solution has also been shown to affect the ionization process in MS, lowering the signal-to-noise ratio of the measurement, thus decreasing the sensitivity. The main oxidation products observed in pure EC experiments are allylic and aliphatic hydroxylation, benzylic hydroxylation (low yield), N-dealkylation, dealkylation of ethers (low yield), hydroxylation of aromatics, N- and S-oxidation, and dehydrogenation.[4,5] Electrochemical conversions of drug molecules have also been performed on a microfluidic chip, where a 9.6-nL cell with palladium and platinum electrodes was used to mimic oxidative metabolism of amodiaquine, [6] and also on an integrated 3-electrode chip, which provides stable conditions for EC experiments and was successfully applied to metabolism studies of procainamide.[7]

Titanium dioxide (TiO_2) is capable of catalyzing both reductive and oxidative reactions in solutions when exposed to ultraviolet (UV) light.[8,9] When TiO_2 absorbs a photon with adequate energy, an electron is excited from its valence band to the conduction band, thereby producing an electron-hole pair and being able to participate in chemical reactions. TiO_2 has two crystal structures: anatase and rutile, with bandgaps of 3.2 and 3.0 eV, corresponding to 385 and 410 nm wavelengths, respectively.[10] UV light, with a shorter wavelength than these, is thus needed to create electron-hole pairs in TiO_2, which then can react with water and organic compounds to produce radicals and other reaction products thereafter. In an aqueous solution common chemical reactions are a production of hydrogen (H_2), oxygen (O_2), hydroxyl (OH), and superoxide (O_2^-).[11,12] Reduction products are formed with electrons, oxidation products with holes, and degradation products with the presence of hydroxyls.[12] In an addition to electron, hole, and hydroxyl reactions, superoxide is very reactive to organic compounds, such as small drugs, present in the solution. TiO_2 have been used for successful degradation of different kind of materials, such as environmental pollutants, pesticides, and dyes, and various methods, such as HPLC, GC-MS, LC-MS, ^{1}H NMR, FTIR, and ESR, were used to detect organic intermediates in these experiments.[12]

Microchip technology has shown several advantages over conventional methods, especially when combined with MS.[13] Rapid reactions are possible due to high surface area of the microchip with short distances in small volumes so the diffusion lengths are adequately short to provide high reaction rates. Small volumes also mean lower solvent consumption and a lower amount of substrate needed for the reactions. For example, atmospheric pressure ionization microchips can increase ionization efficiency and thereby the sensitivity of measurements, minimize the use of organic solvents and also speed up the analysis. A nanoreactor combined with MS gives the possibility for a direct analysis of reaction products. Nanoreactors and microreactors have been fabricated on silicon, glass, and polymers, for diverse chemical and biological reactions, as previously reviewed.[14] We recently published a study of protein analysis with on-chip trypsin digestion in a microreactor combined with MS via an electrospray ionization (ESI) interface.[15] The chip contained a microreactor spot, a pillar channel for spontaneous filling of the chip, and an electrospray tip for ionization.

The aim of this work was to develop a microchip to mimic phase I metabolic reactions of low-molecular weight organic compounds. The purpose was to investigate the feasibility of an integrated TiO_2 nanoreactor/ionization chip with UV radiation and a direct MS analysis for production and identification of photocatalyzed reaction products of selected drug molecules. Furthermore, a comparison of the results obtained with common phase I metabolic reaction products, with those obtained by electrochemical reactors, was made.

6.2 Experimental

6.2.1 Fabrication of the microchip

The fabrication process of an open uncoated ESI microchip has been published previously,[16,17] where the microchip is fabricated on a p-type silicon wafer. There are two mask levels in the fabrication process and it utilizes nested masks of silicon dioxide (SiO_2) and aluminum oxide (Al_2O_3). Both silicon dioxide and aluminum oxide masks are patterned on the wafer before any silicon etching. The first lithographic step using a SiO_2 mask defines the nanoreactor chamber and the fluidic micropillar channel. The second mask (Al_2O_3) defines the sharp electrospray ionization tip. Al_2O_3 was used as an etch mask in through-wafer deep reactive ion etching (DRIE). After through-wafer etching the SiO_2 masked reactor and channel are etched, also by DRIE. The microchip was coated with a 100-nm-thick TiO_2-nanolayer using an atomic layer deposition (ALD).[18] The TiO_2 layer has a considerable amount of anatase phase, which in general is considered photocatalytically more active than the rutile phase. The nanolayer coated reactor contains micropillars (diameter 60 µm, space between the pillars 20 µm, height 25 µm) to increase the active surface area and thereby to speed up the reaction rates. The channel is filled with micropillars to induce capillary flow, and a sharp tip for ESI for MS.

6.2.2 Chemicals and samples

HPLC-grade methanol was obtained from J.T. Baker (Deventer, Netherlands). Formic acid, lidocaine, and 2-acetamidofluorene were obtained from Sigma (St. Louis, Mo, USA). Water was purified with a Milli-Q purification system (Millipore, Molsheim, France). Verapamil hydrochloride, metoprolol, and propranolol hydrochloride were obtained from ICN Biomedicals Inc. (Aurora, OH, USA). S-methylthiopurine was available from Astatech (Chengdu, China). A solvent used for flushing the microchip between measurements consisted of 90 % methanol and 1 % formic acid in water. Human liver microsomes were obtained from BD (New Jersey, USA) Gentest LOT 18888, HLM pool 1008. 100 mM sodium phosphate buffer pH 7.4 was made from Sigma's sodium phosphate monobasic dihydrate and disodium hydrogen phosphate dihydrate. NADP, glucose 6-phosphate and glucose 6-phosphate dehydrogenase were also from Sigma. Magnesium chloride was obtained from Merck (New Jersey, USA). NADPH-regenerating solution contained 1.3 mM NADP, 1.0 mg/ml glucose 6-phosphate, 400 mU/ml glucose 6-phosphate dehydrogenase and 0.31 mg/ml of $MgCl_2$.

6.2.3 On-chip photocatalytic experiments with on-line mass spectrometric analysis

A QTOF Micro quadrupole-time-of-flight mass spectrometer (Waters / Micromass, Manchester, UK) was used in all chip experiments. The mass spectrometer was calibrated using a sodium formate solution in external calibration. The microchip (Fig. 6.1a) with a nanoreactor and an electrospray tip (Fig.6.1b) was positioned in front of the cone of a mass spectrometer as shown in Figure 6.2. The microchip was positioned a distance of 5 mm from the cone with an angle of 90 degrees. Nitrogen produced by a high-purity nitrogen generator was used as a cone gas (flow 40 L h^{-1}, cone temperature 80 ºC) and to stop reactions by evaporating of water-based on-chip reaction buffer (flow 200 L h^{-1}). A platinum electrode connected the high voltage source of the MS to the microchip. A high voltage of 3.5 kV was used to produce stable electrospray. An UV lamp (TEK-Lite, Union Bridge, MD, USA, maximum at peak 365 nm, intensity of 100 mW cm^{-2}) was positioned on the upper side of the microchip at a distance of 2 cm. The microchip was washed by applying flushing solvent (3 µL) several times to the microchip before background measurements. Before the reaction solution was deposited on the microchip the high voltage of the chip was switched off. An aqueous sample solution (a volume of 3 µL and a concentration of 10 µM) was deposited onto the nanoreactor spot of the chip. UV light was switched on, and the reactor was kept wet by applying suitable amounts of water to the open reactor spot while a part of the water was evaporated during the UV exposure. The reactions were completed in the nanoreactor within 15 minutes, after which time the reaction spot was dried thoroughly by nitrogen and the high voltage was switched on. Reaction products were eluted and spontaneously transported via the micropillar channel to the tip at the end of the microchip by depositing 3 µL of a flushing solvent to the reactor spot. The sample was ionized by ESI and the ions were measured in the positive ion mode at a mass range of *m/z* 100 to 800 with a mass resolution of approximately 5000. A mass

spectrum of a blank flushing solvent was subtracted from that of reaction products to obtain a better signal-to-noise ratio. MS/MS analysis was performed for selected precursor ions (either protonated molecules or radical cations) to verify suggested chemical structures of the reaction products. The MS and MS/MS spectra of the original substrate were used to assist the characterization of the reaction products. An uncoated silicon microchip (with a silicon dioxide layer) was used similarly to the TiO_2-nanolayer microchip to verify that the reaction products were not produced in the electrospray ionization process or photocatalytically without TiO_2 coating (Fig 6.3).

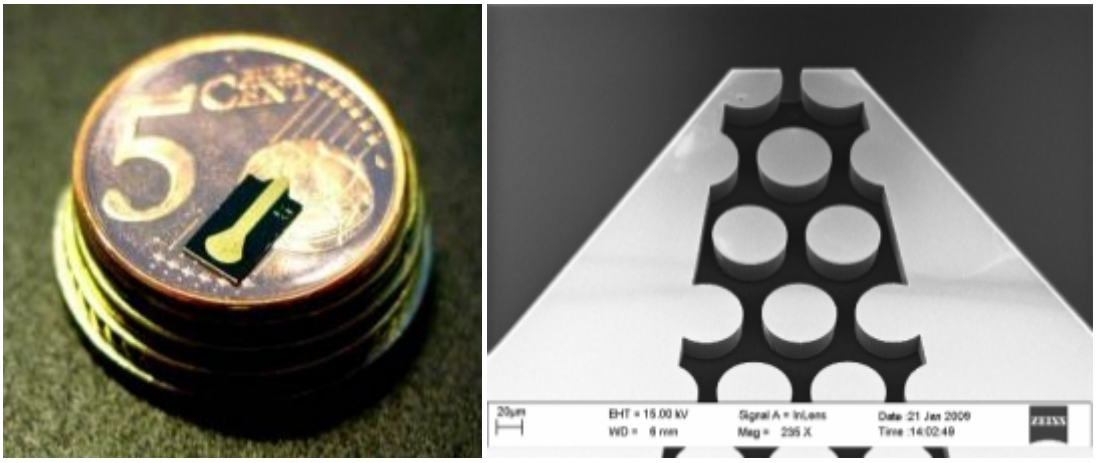

Figure 6.1. a) A TiO_2 nanoreactor / electrospray ionization chip on a 5 euro cent coin. The color of the chip is due to the interference of light in the 100-nm-thick TiO_2-nanolayer. b) A micrograph from an electrospray tip of a microchip.

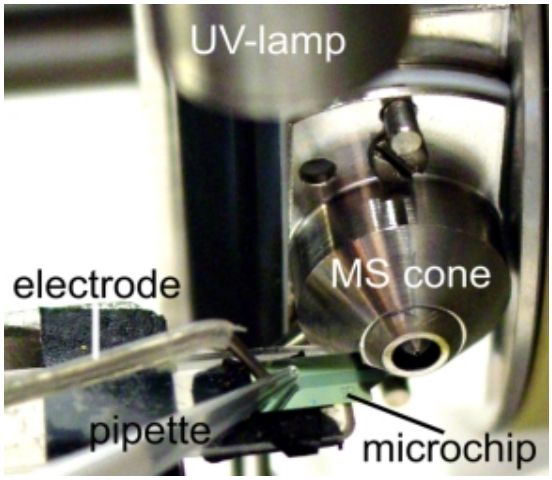

Figure 6.2. A setup of a TiO_2 nanoreactor-µPESI microchip with a Waters QTOF Micro mass spectrometer.

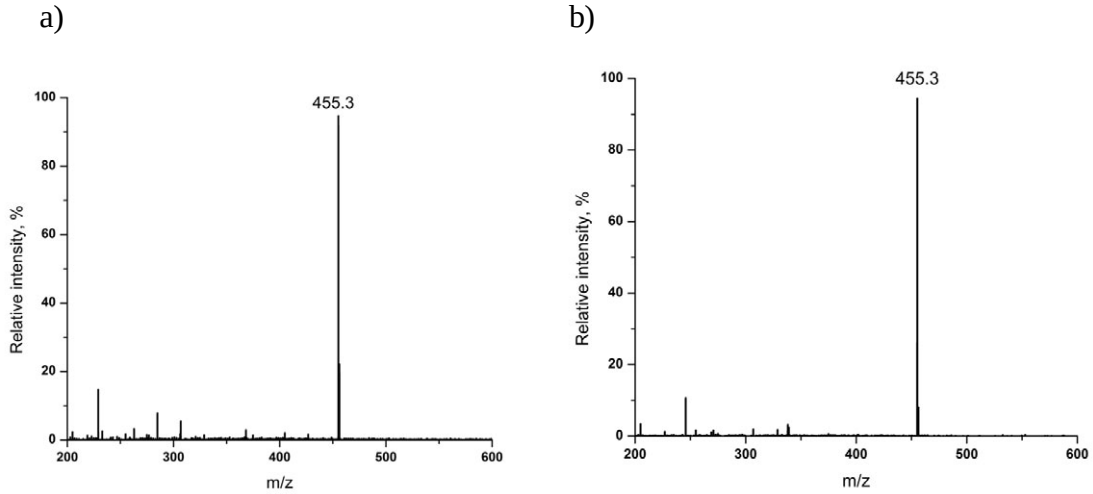

Figure 6.3. a) A mass spectrum of verapamil, measured after keeping it for 15 min on an uncoated silicon µPESI microchip (containing a native SiO_2-nanolayer) and **b)** a mass spectrum of verapamil and its possible reaction products formed within 15 min UV illumination on the uncoated silicon µPESI microchip.

6.2.4 Human liver microsome experiments and off-line LC-MS analysis

HLM experiments were made in 100 mM phosphate buffer at pH 7.4. 10 µL of 1 mM substrate was added to 90 µL of NADPH-regenerating solution to obtain a 100 µM solution. Exactly 5 µL of 20 mg/mL human liver microsomes was added to the solution to obtain about 1 mg/mL concentration. The solution was incubated in 37 ºC and the incubation time was varied between 1 and 48 hours. The first sample (20 µL) was collected after 60 min incubation, the second (20 µL) after 120 min, the third (20 µL) after 24 hours and the fourth (40 µL) after 48 hours. After incubation, the reaction was stopped by adding 100 µL of acetonitrile to the sample directly from the -20 ºC freezer. The four sub-samples were pooled together in order to detect all possible metabolites, including intermediate metabolites, in one analysis. The solution was centrifuged (Eppendorf 5415D, Eppendorf, Hauppauge, NY, USA) for 10 min at 16100 x g. Then, 180 µL of the supernatant was diluted with 820 µL of milli-Q water. Solid-phase extraction (SPE) was made with Waters Oasis 30 mg 1mL cartridges. The cartridge was conditioned with 1 mL of methanol and 1 mL of 0.1 % formic acid. After that, 1 mL of sample was loaded into the cartridge which was then washed with 1 mL of 0.1 % formic acid and dried with nitrogen. Then, 1 mL of methanol was used to elute the compounds from the cartridge. UPLC (Waters) with the Agilent Ion Trap 6330 (Agilent Technologies, Walbronn, Germany) was used for the LC-MS analysis of the extracts. The column used was Acquity UPLC HSS T3 (100 x 2.1 mm, particle size 1.8 µm), injection volume was 10 µL, flow rate was 300 µL/min, and a gradient started after one minute from 0.1 % formic acid containing 5 % B eluent which was methanol. A linear gradient lasted 23 min ending with 90 % of B. After one minute the eluent composition was restored to the starting

composition during one minute. The column was stabilized for four minutes before the next injection. Electrospray ionization was used in positive ion mode. Ion trap was used in enhanced scan mode with a scan range of *m/z* 70 – 500.

6.3 Results

6.3.1 Evaluation of performance of the TiO_2 nanoreactor chip

The performance of the TiO_2-nanoreactor chip was evaluated using verapamil, a common drug acting as a calcium influx inhibitor, as a test compound. The nanoreactor utilizes small sample volumes (100 nL – 4 µL), demanding high sensitivity from the analytical detection. Verapamil at a concentration of 10 µM produced main reaction products with an adequate signal intensity, however, the concentration was low enough to preventing overloading of the nanoreactor which was then easily washable between separate experiments. This setup formed a sensitive experimental protocol because the absolute amount of the substrate needed was 20 - 40 pmol, corresponding to about 1 - 10 ng of the substrate. The UV irradiation time was varied from 0 to 15 minutes, and it was observed that the relative intensities of ion peaks of reaction products at *m/z* 196, 277, 291, 441, 469, and 471 (the reaction products and the reactions are shown in Table 1) in a measured ESI mass spectrum increased until 10 min after which the intensity remained constant, whereas the intensity of the mass peak of protonated verapamil at *m/z* 455 decreased at the same time (Fig. 6.4). To assure that all substrates have a sufficient time to react, the UV exposure time of 15 min was used in the latter experiments. One reason for fast reactions was the high ratio of active surface area to volume because the side walls of the micropillars were also coated with active TiO_2. An obvious risk of a longer UV exposure time is that the organic compounds are completely decomposed by the photocatalytic processes. The experiments with verapamil were repeated in two other ways: without the UV exposure and with an uncoated silicon microchip. In both cases only the ion of protonated verapamil was detected in the mass spectra, thus proving that the reaction products were produced in photocatalytic reactions induced by the UV radiation and the TiO_2 coating (Fig. 6.3). After flushing pure methanol a 3-5 times, the microchip showed no memory effects (i.e., contamination from the photocatalytic experiment), thus the microchip was reusable for several experiments with other compounds.

Table 6.1. The molecular weights (MW) of detected reaction products with TiO_2-µPESI chip compared with metabolites produced *in vitro* by human liver microsomes (HLMs) and rat hepatocytes, or *in vivo*. Reaction products of propranolol with rat hepatocytes are from articles ref. 25–27. Human in vivo metabolites are from articles ref. 19–21,24. Metabolites formed with CYP450 enzymes are from article ref. 23 and with electrochemistry are from paper ref. 2.

Compound	MW	Reactions	TiO_2 µPESI	HLM	CYP450	Rat hepatocytes	Human in vivo	EC
Propranolol	216	N-dealkylation, oxidation	x	x		x	x	
	217	N-dealkylation	x	x	x	x	x	
	218	N-dealkylation, hydroxylation		x			x	
	232	N-dealkylation, carboxylation	x	x	x		x	No
	233	N-dealkylation, hydroxylation					x	data
	234	N-dealkylation, dihydroxylation					x	found
	248	N-dealkylation, carboxylation, hydroxylation	x				x	
	273	Hydroxylation, dehydrogenation	x	x				
	275	Hydroxylation	x	x	x	x	x	
	289	Dihydroxylation, dehydrogenation	x	x				
	291	Dihydroxylation	x	x	x			
	305	Hydroxylation, methoxylation					x	
Metoprolol	225	N-dealkylation	x	x	x			x
	237	Oxidation to benzaldehyde	x	x				x
	239	Dealkylation, hydroxylation		x			x	
	240	N-dealkylation, carboxylation					x	
	242	N-dealkylation, dihydroxylation	x					
	251	Dehydroxylation	x	x		No data		
	253	Demethylation	x	x	x	found	x	x
	267	Oxidation to carboxylic acid		x			x	x
	269	Hydroxylation, demethylation	x	x			x	
	281	Dehydrogenation, hydroxylation	x	x				
	283	Hydroxylation	x	x	x		x	x
Verapamil	182	Dealkylation, oxidative deamination		x			x	
	195	N-dealkylation	x	x			x	
	196	Dealkylation, oxidative deamination					x	
	262	N-dealkylation, demethylation				x		No
	276	N-dealkylation	x	x	x	x	x	data
	290	Dealkylation	x	x	x	x	x	found
	304	Dealkylation					x	
	318	Dealkylation, aldehyde formation					x	
	412	Tridemethylation				x		
	426	Didemethylation		x	x	x	x	
	440	Demethylation	x	x	x	x	x	
	456	Demethylation, hydroxylation		x		x		
	468	Formation of aldehyde	x	x		x		
	470	Hydroxylation	x	x		x		
Lidocaine	73	N-dealkylation	x					x
	74	Two N-dealkylations		x				
	121	N-dealkylation	x	x			x	
	130	N-dealkylation	x	x		No data		
	137	N-dealkylation, hydroxylation		x		found	x	
	178	Two N-deethylations	x	x	x		x	
	206	N-deethylation	x	x	x		x	x
	222	N-deethylation, hydroxylation					x	
	248	Hydroxylation, dehydrogenation	x	x				
	250	Hydroxylation	x	x	x		x	
S-methyl-thiopurine	182	Hydroxylation	x	x	No data found	No data found	No data found	x
2-acetamido-fluorene	181	N-deacetylation				x	No	
	237	Oxidation	x		x		data	
	239	N- or ring-hydroxylation	x	x	x	x	found	x

x denotes that the reaction product has been detected.

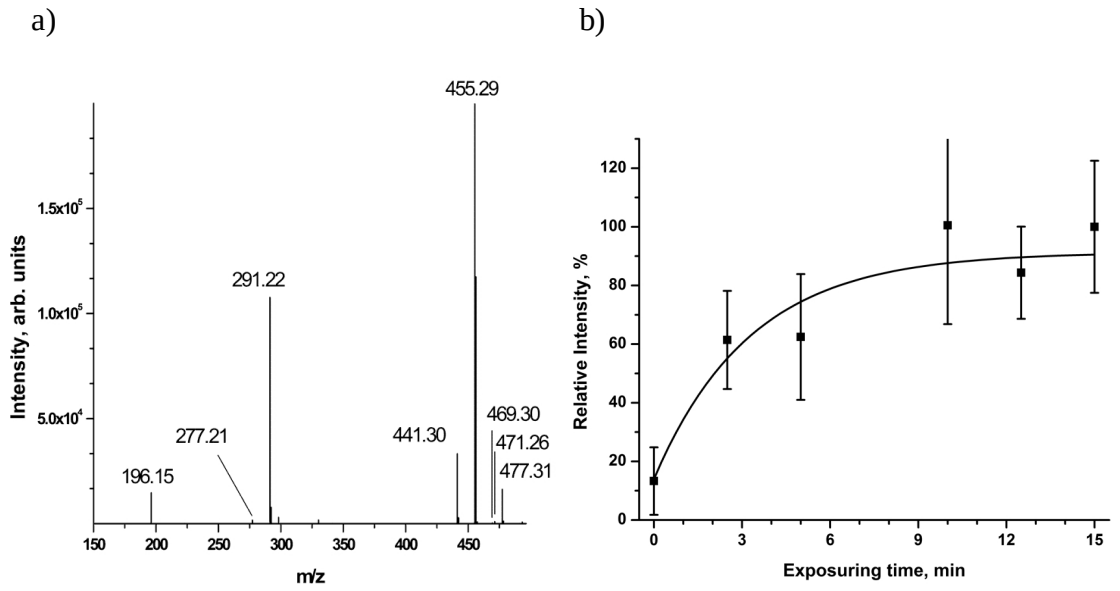

Figure 6.4: a) Mass spectrum of verapamil reaction products formed with TiO_2-nanoreactor-µPESI chip. b) Relative intensity of verapamil reaction products versus a protonated verapamil ion as a function of UV exposure time.

6.3.2 Identification of photocatalytic reaction products of selected drugs

The integrated nanoreactor/ionization microchip combined with MS was applied to study photocatalytic oxidation/reduction reactions of six selected compounds, namely verapamil, propranolol, metoprolol, lidocaine, S-methylthiopurine, and 2-acetamidofluorene, whose metabolic reactions (either *in vitro* or *in vivo* metabolism) or electrochemical reactions are well-known. The photocatalytic reactions observed with the TiO_2-coated microchip are shown in Table 1. All detected reaction products were protonated or with sodium adduct. The main reaction products and suggested reaction pathway of propranolol are shown in Figure 6.3, as an example**.** The spectra and suggested reaction pathways for other compounds, showing several reaction products, are presented in Figures 6.4-6.8. Metabolites from human liver microsome incubations in our experiments as well as the products detected in *in vitro* experiments with rat hepatocytes[19] and CYP450 enzymes,[20] *in vivo* experiments with humans,[21] and with EC presented in literature are shown in Table 1.

a)

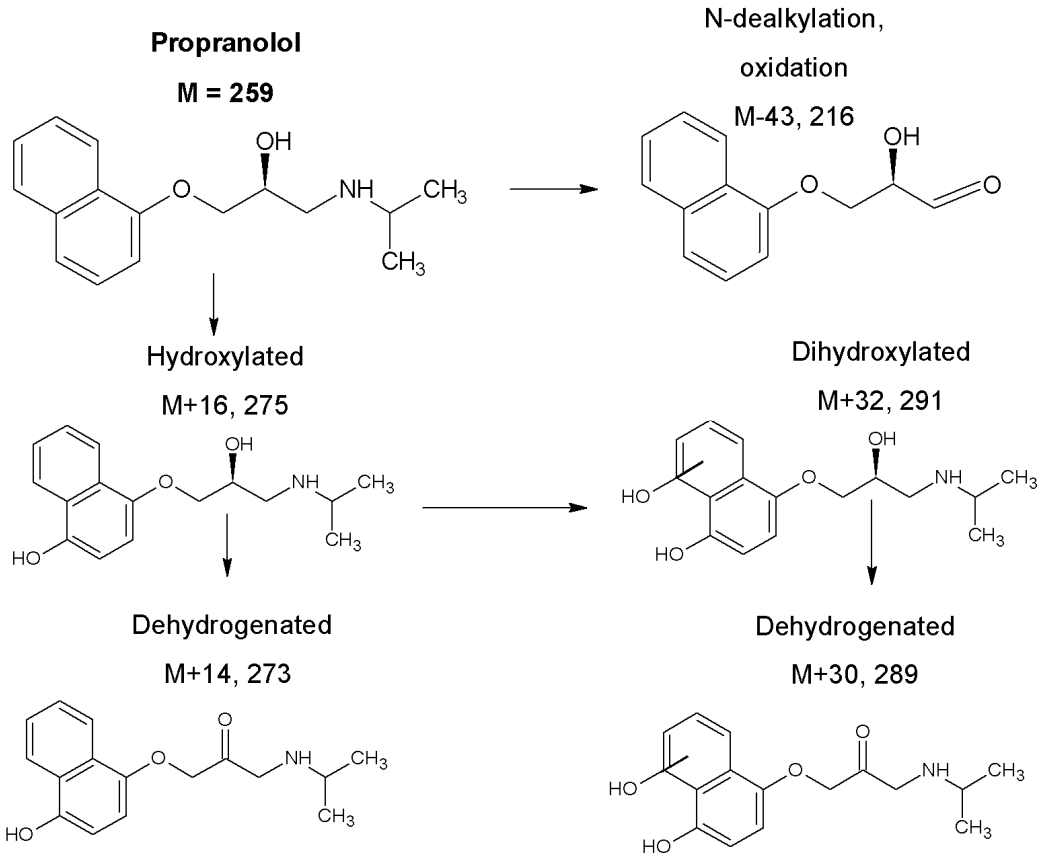

b)

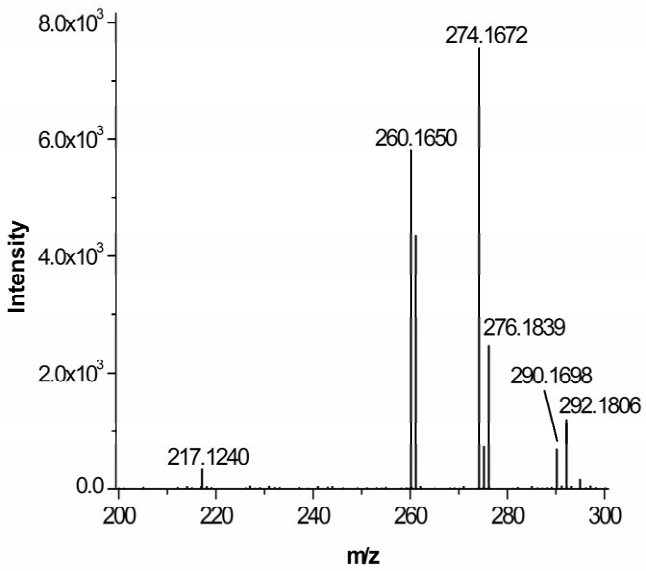

Figure 6.5. a) The chemical structures of propranolol and its reaction products produced with a TiO_2 nanoreactor µPESI microchip and analyzed with MS and MS/MS. All reaction positions were not verified. Arrows show the suggested pathways. **b)** A mass spectrum of reaction products of propranolol measured in a positive ion mode.

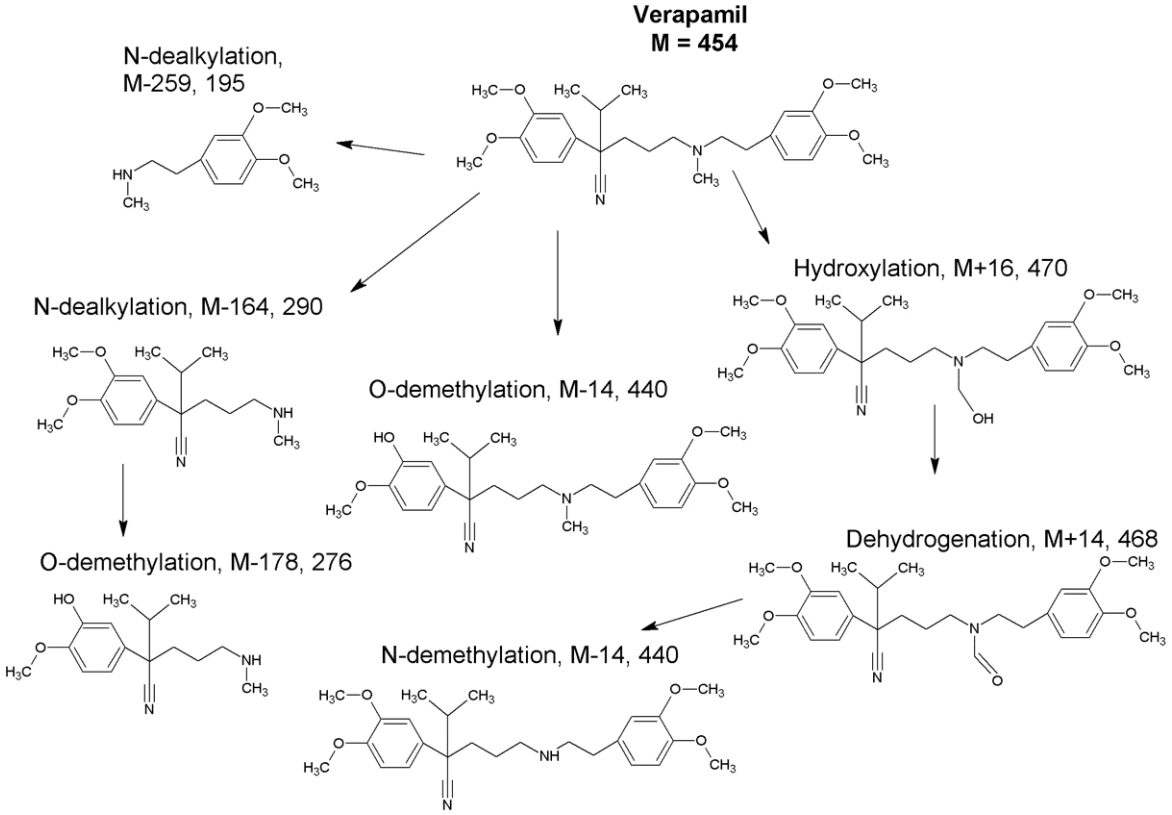

Figure 6.6. Verapamil and reaction products produced with TiO_2-nanoreactor-µPESI method. Arrows shows the suggested verapamil metabolism pathway.

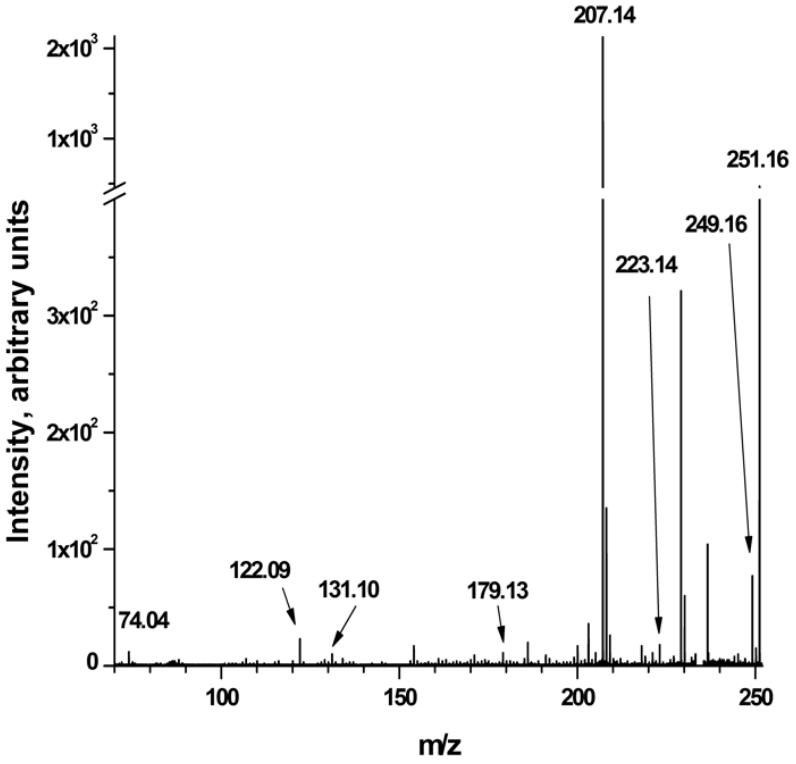

a)

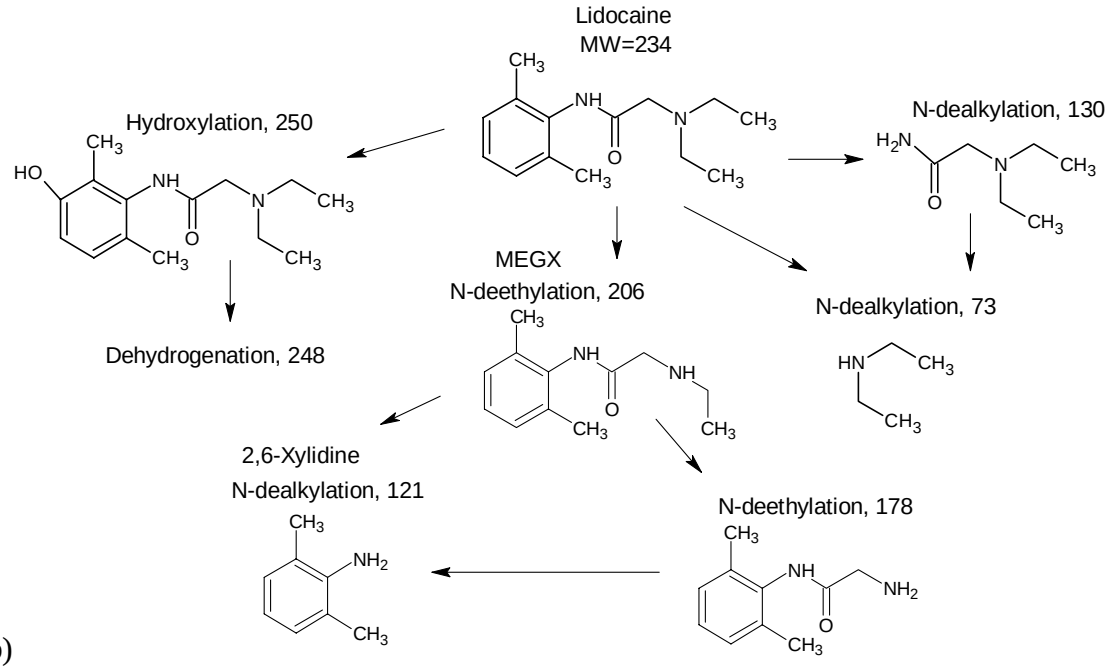

b)

Figure 6.7. a) A mass spectrum of lidocaine reaction products analyzed with TiO_2-nanoreactor-µPESI-MS. **b)** Suggested metabolism pathway of lidocaine.

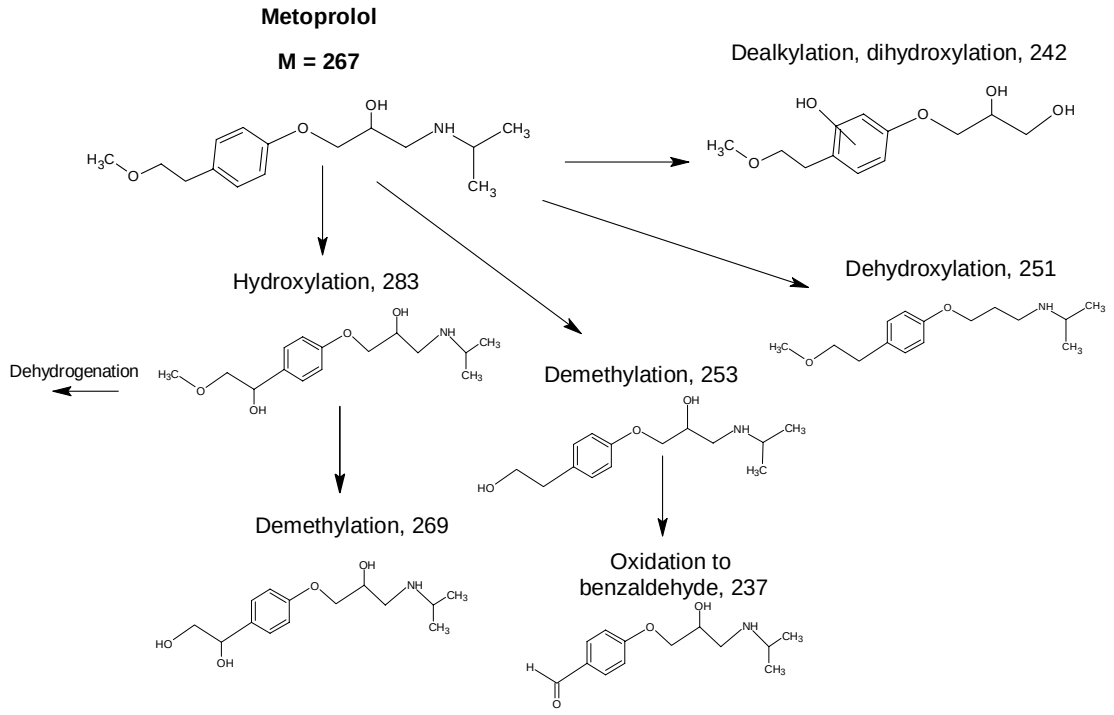

a)

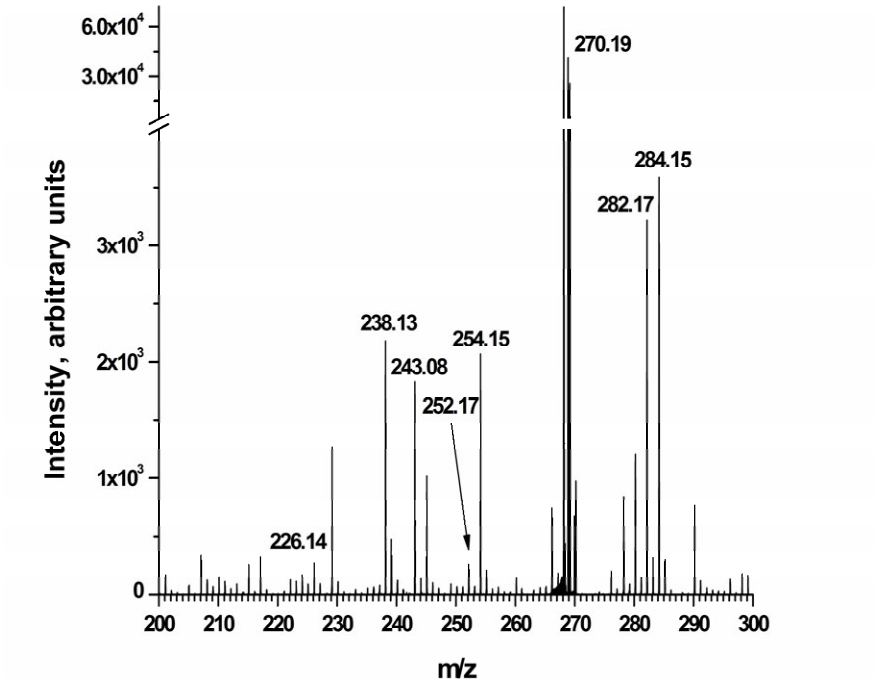

b)

Figure 6.8. a) A suggested metabolism pathway of metoprolol. **b)** A mass spectrum of metoprolol reaction products analyzed with TiO_2 nanoreactor-µPESI-MS.

6.4 Discussion

The experimental results obtained with the TiO_2-µPESI-MS setup cover 80 % of phase I metabolites of the substrates obtained in *in vitro* experiments with HLMs. A very important aspect of the TiO_2-µPESI microchip based method is that the main phase I metabolic reactions, such as hydroxylation, oxidation, N-, O-dealkylation, and dehydrogenation, were observed with the compounds tested. One special property of the method was the number of dehydrogenated reaction products when compared to those observed with CYP450 and EC. HLM reaction products were more similar with our method. In cases, where hydroxylated reaction products were detected, their dehydrogenated analogs were also usually detected, which means that dehydrogenation happens very effectively or the products are oxidated directly with superoxide and hydrogenated thereafter. Dealkylation reactions were common in photocatalytic TiO_2 processes. We assume that the dealkylation happens when the substrate is reduced by the electron-reaction product. N-dealkylations with verapamil and lidocaine were also observed. However, multiple reactions, such as dealkylation together with hydroxylation, were seldom observed in the photocatalytic reaction, whereas as they were rather common in *in vitro* experiments.

The experiments with the test compounds and CYP450 enzymes,[20] rat hepatocytes, [22, 23, 24] and *in vivo* human studies [21, 25, 26] show a large diversity in the metabolites detected. Therefore, it is not surprising that the results obtained with the photocatalytic TiO_2-µPESI microchip do not totally correlate with any of them. *In vivo* metabolism studies of 2-acetamidofluorene in rats[27] have revealed regioisomeric hydroxylated metabolites (3-, 5-, and 7-hydroxy-2-acetamidofluorene) but with the MS used in our study we could not identify the exact position of the hydroxyl group in the reaction product(s) with the TiO_2-µPESI microchip. A direct comparison of photocatalytic reactions with *in vivo* metabolism in humans is not straightforward because *in vivo* metabolism covers also phase II metabolism with all co-factors, whereas the TiO_2-nanoreactor was meant to mimic only phase I metabolism.

The reaction products of four compounds obtained by EC[2] for the comparison of those obtained with the photocatalytic TiO_2-µPESI microchip are also presented in Table 1. It has been previously observed that reactions which are initiated via a single electron transfer step, such as N-dealkylation and dehydrogenation, can be successfully mimicked by EC, whereas reactions that are initiated by direct hydrogen atom abstraction, such as O-dealkylation and hydroxylation, are seldom observed in EC experiments.[3] However, the comparison shows that with the TiO_2-µPESI-MS method it is possible to detect even more dealkylated and dehydrogenated products than with EC.

The main benefits of using the TiO_2-µPESI microchip compared with other *in vitro* methods are speed, high sensitivity, and low cost. It is possible to produce measurable amounts of reaction products with a 2-min UV irradiation of 30 pmol of a substrate and to analyze the reaction products on-line with mass spectrometry with the same experimental

setup. In the experiments we used longer irradiation times, 8-15 min to obtain a maximum amount of reaction products, but for example 50 % of the maximum signal of verapamil metabolites was reached during the first two minutes (see Fig. S1). Characterization of photodegradation products of propranolol with sole UV irradiation has been previously described,[28] and the comparison of photodegradation products with the reaction products observed in this study demonstrates that the reaction products are different, thus showing that the mechanism of UV irradiation with TiO_2 is not photodegradation, but indeed photocatalyzed reactions. The nanoreactor chip is designed for mass production: hundreds of TiO_2-µPESI nanoreactor chips can be microfabricated on a single 100-mm diameter silicon wafer. The nanoreactor chips are disposable, but after proper cleaning, for example washing with organic solvents or Piranha cleaning (sulphuric acid-hydrogen peroxide mixture), they can be reused. There is no chromatographic separation in the pillar microchannel but the lack of separation can be overcome in most cases by using a high resolution mass spectrometer or a hyphenated MS instrument with MS/MS capabilities. On the other hand, the lack of a chromatographic part also means much faster analyses, which could enable monitoring of reaction kinetics.

6.5 Conclusions

In summary, we developed, fabricated, and characterized a TiO_2 nanoreactor/ESI microchip for the production, detection, and identification of the photocatalytic reaction products of selected drugs by mass spectrometry to mimic phase I metabolic reactions. The integration of nanoreactor and ESI source on the same microchip enables rapid on-line analyses with MS. The correlation between the reaction products observed on the microchip and the metabolites detected with *in vitro* and *in vivo* methods was remarkable. The TiO_2 nanoreactor/ESI microchip can therefore be used for a rapid prediction of phase I metabolites in the early preclinical stage of drug research and it has the potential to speed up the discovery of new potential drug candidates.

References

1 M. Holčapek, L. Kolářová, M. Nobilis, Anal. Bioanal. Chem. 2008, 391, 59–78

2 U. Jurva, H. Wikström, L. Weidolf, A. P. Bruins, Rapid Commun. Mass Spectrom. 2003, 17, 800-810

3 U. Jurva, H. Wikström, A. P. Bruins, Rapid Commun. Mass Spectrom, 2000, 14, 529-533

4 T. Johansson, L. Weidolf, U. Jurva, Rapid Commun. Mass Spectrom, 2007, 21, 2323-2331.

5 W. Lohmann, U. Karst, A. Baumann, LCGC ASIA PACIFIC, 2010, 13, 1.

6 M. Odijk, A. Baumann, W. Lohmann, F.T.G. van den Brink, W. Olthuis, U. Karst, A. van den Berg, Lab Chip, 2009, 9, 1687-1693.

7 M. Odijk, A. Baumann, W. Olthuis, A. van den Berg, U. Karst, Biosens. Bioelectron., 2010, , DOI:10.1016/j.bios.2010.07.102.

8 A. Linsebigler, L. Guangquan, J. T. Yates, Chem. Rev., 1995, 95, 735-758
9 M. Addano, V. Augugliaro, A. Di Paola, E. Garci'a-Lo' Pez, V.Loddo, G. Marci', L. Palmisano, J. Appl. Electrochem., 2005, 35, 765-774
10 A. Agrios and P. Pichat, J. Appl. Electrochem, 2005, 35, 655-663
11 J. Tang, J. R. Durrant, D. R. Klug, J. Am. Chem. Soc., 2008, 130, 13885-13891.
12 I. Konstantinou and T. Albanis, Applied Catalysis B: Environmental, 2004, 49, 1-14.
13 T. Sikanen, S. Franssila, T. J. Kauppila, R. Kostiainen, T. Kotiaho, R. A. Ketola, Mass Spectrom. Rev., 2010, 29, 351-391.
14 G.N. Doku, W. Verboom, D.N. Reinhoudt, A. van den Berg, Tetrahedron, 2005, 61, 2733–2742.
15 T. Nissilä, L. Sainiemi, S. Franssila, R.A. Ketola, Sens.Actuators B, 2009, 143, 414–420.
16 L. Sainiemi, T. Nissilä, V. Jokinen, T. Sikanen, T. Kotiaho, R. Kostiainen, R. A. Ketola, S. Franssila, Sens. Actuators B, 2008, 132, 380-387
17 T. Nissilä, L. Sainiemi, T. Sikanen, T. Kotiaho, S. Franssila, R. Kostiainen, R. A. Ketola, Rapid Comm. Mass Spectrom., 2007, 22, 3677-3682
18 M. Ritala, M. Leskelä, L. Niinistö, P. Haussalo, Chem. Mater., 1993, 5, 1174-1181
19 M. Eichelbaum, M. Ende, G. Rememberg, M. Schomerus, H. J. Dengler, Naunyn-Schmiedeberg's Arch. Pharmacol., 1993, 348, 332-337
20 S. Rendic, Drug Metab. Rev., 2002, 34, 83-448
21 M. Eichelbaum, M. Ende, G. Rememberg, M. Schomerus, H. J. Dengler, Drug Metab. Dispos., 1979, 7, 145-148
22 T. Baughman, C. Talarico, J. Soglia, Rapid Commun. Mass Spectrom., 2009, 23, 2146-2150
23 M. Walles, T. Thum, K. Levsen, J. Borlak, J. Chromatogr. B, 2003, 798, 265-274
24 E. Dybing, E. Søderlund, L. Haug, S. Thorgeirsson, Cancer Research, 1979, 39, 3266-3275
25 T. Walle, U. Walle, L. Olanoff, Drug Metab. Dispos., 1984, 13, 204-209
26 J. McGourty, J. Silas, M. Lennard, G. Tucker, H. Woods, Br. J. Clin. Pharmacol, 1985, 20, 555-566.
27 P. Lotlikar, M. Gruenstein, Biochem. J., 1970, 119, 921-923.
28 K. Uwaia, M. Tania, Y. Ohtakea, S. Abea, A. Marukoa, T. Chibab, Y. Hamayab, Y. Ohkuboa , M. Takeshita, Life Sci., 2005, 78, 357– 365

7 Rotating multitip micropillar array electrospray ion source for rapid analyses and high throughput screening with mass spectrometry (V)

A rotating multitip electrospray ionization (ESI) source for mass spectrometry (MS) is presented here. The ESI tips are based on lidless micropillar array ESI (µPESI) sources where the transfer of liquid is based on capillary forces without external pumping. A single silicon wafer contains 60 separate µPESI tips which can be individually used by rotating the whole wafer by six degrees each time from tip to tip using a computer control. This enables rapid, repeatable, and contamination-free ionization and analysis with mass spectrometry as 60 samples (one by each tip) can be analyzed in less than 15 minutes. The rotating multitip µPESI chip with an ion trap mass spectrometer was successfully applied to rapid identification and monitoring of intermediates and final products in one chemical synthesis within ten minutes. The system was also applied to high throughput screening of benzodiazepines from urine samples. Urine samples were extracted with solid-phase extraction (SPE) using C_{18} phase ZipTip™ pipettes, enabling the use ofurine sample volumes as low as 50 µL. Therefore the whole sample treatment and the analysis with the rotating multitip µPESI-MS took only eight minutes per sample.

7.1 Introduction

A current trend in analytical chemistry has been the miniaturization and microfabrication of analytical instruments and integration of different kinds of functionalities on the same microchip. Similarly, an important research field in analytical chemistry has been miniaturization of ion sources for mass spectrometry.[1,2] For example, various miniaturized electrospray ionization (ESI) sources have been developed from glass,[3,4] silicon,[5] and different types of polymers.[6,7] The miniaturized ion sources can increase ionization efficiency and thereby the sensitivity of measurements, minimize the use of organic solvents and also speed up the analysis.[8] Most of the microchip-based ion sources, just like conventional ion sources, are individual separate devices which are connected between sample introduction devices, such as a chromatograph or an infusion pump and a mass spectrometer. Due to low manufacturing costs, the microchip ion sources can be replaced, when their performance is no longer acceptable in terms of sensitivity and stability. To speed up analysis cycle time and to diminish contamination risks, multi ion sources have been recently developed, Nanomate™ being the most common of them.[9] The Nanomate system contains an array of nanoelectrospray needles etched in a silicon wafer. Typical flow rates used in Nanomate systems range from 20 to 300 nL/min. It has three operation modes, namely chip-based infusion, LC-MS fraction collection, and liquid extraction surface analysis[10] (LESA™). These modes can be used for example, in rapid analysis of proteins[11] and lipids,[12] drug and metabolite analysis,[13,14] and surface analysis of tissues[15] and dried blood spots. Other multiarray ion source systems are, for example, a multichannel device with an array of ESI tips,[16] chemically etched fused-silica ESI emitter

for improved sensitivity,[17] an array of enclosed ESI tips made from an SU-8 polymer,[18] and a micromachined silicon-based ultrasonic ejector array.[19]

A rotating sample surface for desorption electrospray ionization MS (DESI/MS) has been previously published.[20] In this system suitable surface spots for DESI were printed on the edge of a CD disc (a total of 50 spots), and after introduction of a sample to the sampling spot, DESI/MS was applied for a rapid analysis of the sample. In this way a rapid quantitative determination of caffeine in two diet sport drinks using isotopically labeled caffeine as an internal standard was demonstrated. The total analysis time of seven calibration standards and two sport drink samples (45 separate analyses) was 7.5 min.

We have previously shown that an open silicon micropillar array channel can induce a spontaneous sample transfer to a sharp tip where an electrospray plume is formed.[21,22] The open channel enables very easy placement of liquid samples onto the microchip as well as rapid and repeatable ESI from the tip. The open micropillar array channel made of SU-8 polymer can also be used as a microreactor for protein digestion studies.[23] When a silicon based µPESI microchip is covered with titanium dioxide (TiO_2) it can be used for photocatalytic reactions and mimicking phase I metabolism with an UV lamp, and a direct analysis of reaction products with MS.[24] The main benefit of nano- and microreactors is that they are more efficient due to shorter diffusion lengths and higher surface-to-volume ratios, thus providing faster reactions when compared to conventional *in vitro* methods. The reaction and analysis are performed on the same microchip, minimizing loss of analytes in sample transfer from microreactor to ESI-MS analysis.

The aim of this study was to design and fabricate a multitip micropillar array electrospray ionization (µPESI) source and to study its performance in rapid analyses. The feasibility of the multitip-µPESI was studied in the rapid follow-up analysis of synthesis processes and in high throughput screening analysis of abused drugs in urine samples using a quick sample preparation method of ZipTip^{TM} solid-phase extraction.[14,25,26] This multitip µPESI system was combined with ion trap and time of flight mass spectrometers.

7.2 Experimental

7.2.1 Fabrication of the rotating µPESI multitip chip

Analytical properties[21] and fabrication process[22] of the single µPESI chips have already been published. In brief, the microchips are fabricated on double sided polished (DSP) silicon wafers. The fabrication process uses two mask levels: nested masks of silicon dioxide (SiO_2) and aluminum (Al). Both masks are patterned on the wafer before etching of silicon. The SiO_2 mask defines the microreactor chamber and the fluidic channel embedded with micropillars while the aluminum mask defines the sharp thru-wafer etched

ESI-tip. Silicon etching is done in two parts: the first deep reactive ion etching (DRIE) step creates the ESI-tip and the second DRIE step the microreactor and flow channel. Both the microreactor and the flow channel contain micropillars (diameter 60 µm, space between the pillars 15 µm, height 15 µm) to provide large surface areas for the reaction and to support spontaneous sample flow towards the electrospray tip. There are 60 tips on one chip and the angles between the tips are 6 degrees (Fig 7.1).

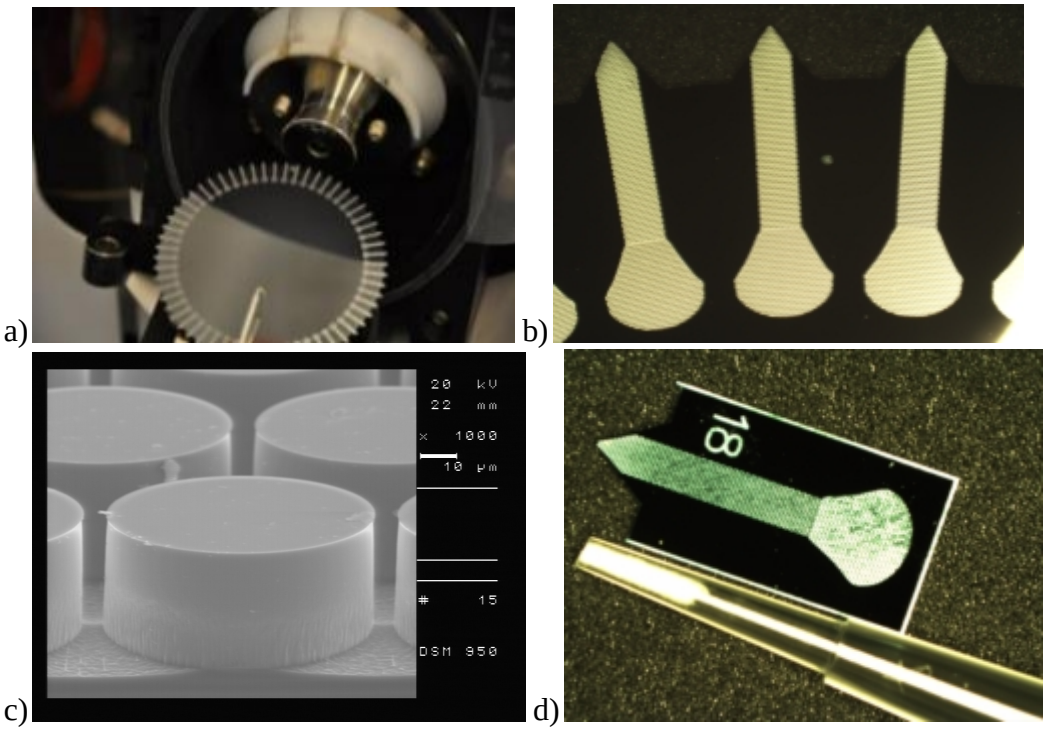

Figure 7.1. a) A rotating µPESI multitip ion source containing 60 individual tips combined with MS. **b)** Three individual µPESI tips on a rotating multitip ion source. Width of the pillar array channel is 1 mm. **c)** A scanning electron micrograph of a micropillar array of the chip. **d)** A single micropillar electrospray ionization chip (µPESI-chip) with a ZipTip solid phase extraction pipette.

7.2.2 Chemicals and samples

HPLC-grade acetonitrile (ACN), methanol (MeOH), and formic acid (FA) were obtained from Sigma (St. Louis, Mo, USA). Water was purified with Milli-Q purification system (Millipore, Molsheim, France). A solvent used for flushing the microchip before measurements consisted of 95 % ACN or MeOH and 1 % FA in water. 1 mL of 100 µM samples of benzodiazepines in MeOH, namely nordiazepam, oxazepam, temazepam, α-hydroxyalprazolam, and α-hydroxymidazolam were obtained from United Medix Laboratories Ltd. (Helsinki, Finland). The structures of the compounds are shown in Figure 7.2. Pooled urine and authentic positive urine sample, analyzed previously with immunological and GC-MS methods, were obtained from United Medix Laboratories Ltd.

Spiked urine sample was prepared to a have all benzodiazepines with cut-off concentration 200 ng/mL in pooled urine.

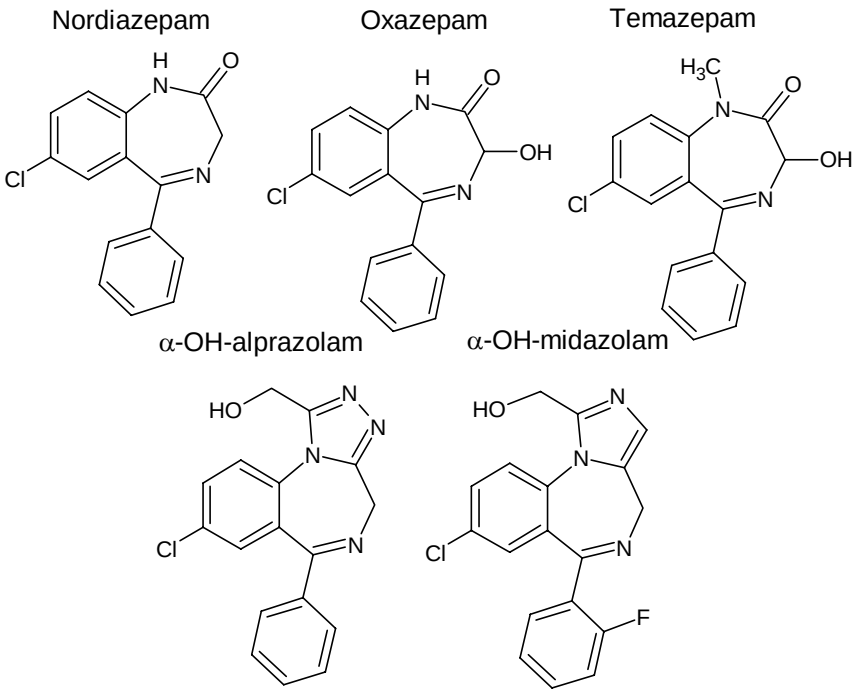

Figure 7.2. Chemical structures of the benzodiazepines studied.

7.2.3 Mass spectrometry

QTOF Micro (Waters, UK), Bruker MicroTOF (Bruker Daltonics, Germany), and Agilent 6330 Ion trap (Agilent Technologies, Santa Clara, CA, US) were used in MS experiments. The QTOF and MicroTOF were calibrated using a sodium formate solution in external calibration. The microchip positioned in front of the cone of a mass spectrometer to the distance of 5 mm. Nitrogen produced by a high-purity nitrogen generator was used as a cone gas (flow 40 L/h, cone temperature 80 ºC). A platinum electrode connected the high voltage source of the MS to the microchip. The high voltage of 3.5 kV was used in experiments for electrospray ionization in positive ion mode. A mass range of *m/z* 80 to 800 was monitored. With Agilent 6330 ion trap mass spectrometer, the chip was positioned to the same 5 mm distance from an electrospray shield. Ultra scan and positive ion mode were used and drying gas temperature was set to 150 ºC and flow rate was 2.0 L/min. No nebulizer gas was used. A multitip ion source chip was attached to a rotating platform (Thorlabs CR1-Z7/M, Thorlabs Sweden AB, Göteborg, Sweden). The rotating platform was controlled by Thorlabs computer software APT motor controller.

7.2.4 Urine sample treatment

Spiked pooled urine sample was prepared so that the added nordiazepam, oxazepam, temazepam, α-OH-alprazolam, and α-OH-midazolam were each present at a concentration of 200 ng/mL. Solid-phase extraction of urine sample was done with 10 µL C_{18} ZipTips^{TM} (Millipore, Molsheim, France). First, the tips were conditioned three times with 10µL of acetonitrile and three times with 10 µL of 10% acetonitrile keeping the tip wet the whole time. After conditioning, the tip was loaded five times with 10 µL of the sample, washed ten times with 10 µL of 10% acetonitrile and after the last washing step the tip was left to dry. Elution straight onto the chip was made with 2 µL of 95% MeOH/ 1% FA / 4% H_2O.

Preparation of authentic positive benzodiazepine urine sample started with hydrolysis. Approximately 500 µL of 800 mM sodium phosphate buffer (pH 7.0) with 20 µL of β-glucuronidase (*E. coli*, Roche Diagnostics GmbH, Mannheim, Germany) enzyme was added to 2 mL of urine sample and vortexed. The sample was incubated in a 55 ºC water bath for 30 minutes. Afterwards the ZipTip-solid phase extraction method was used for pretreatment as described for spiked urine sample.

7.2.5 Organic synthesis and sampling

The synthesis of tropones from heptafulvenes has been previously described.[27] Briefly, the oxidative cleavage of the semicyclic carbon-carbon double bond of the starting heptafulvene (A, see Fig. 7.4a) was studied. The purity of starting heptafulvene was checked with NMR before the reaction and no impurities were found. The reaction was carried out in a round-bottomed flask placed in an acetone–ice bath (–15 °C). Heptafulvene A (6.00 mg, 1.0 equiv) was dissolved in dichloromethane (2.0 mL), producing a 10 mM reaction solution of *m*-Chloroperoxybenzoic acid (*m*-CPBA, Aldrich, 77%, 11.0 mg, 2.5 equiv) to initiate the oxidation reaction. From the magnetically stirred reaction mixture, a 10-µL aliquot was taken and diluted with 1 mL of 0 °C (ice cold) 95% MeOH / 1% FA / 4% H_2O. Consequently, 1.5 µL of the diluted sample was introduced to the µPESI tip for immediate analysis of the remaining starting materials, reaction intermediates and products. The first four samples were taken with a rate of one sample per minute and the last one was taken after ten minutes of adding the oxidizing agent to a reaction mixture.

7.3 Results and discussion

7.3.1 Performance of the multitip chip

The performance of the multitip µPESI chip for rapid analysis was tested using a verapamil solution (500 nM) and the ion trap MS. Approximately 1.5 µL (750 fmol) of the

same sample solution was introduced into a µPESI sample spot and the peak height of the protonated verapamil (ion at *m/z* 455) was recorded. After measurement, the chip was rotated by six degrees and the next sample was analyzed. In this manner 60 samples were analyzed twice (120 times in total) with the multitip µPESI chip (Fig. 7.3). From 60 individual µPESI tips only three were not functional, that is the electrospray was not formed, or the signal of ESI was negligible when compared with those of other tips. The main reason for this was that the micropillars right at the tip were badly formed or missing, thus disabling the formation of electrospray plume even though the micropillar channel was filled to the tip. The relative standard deviation of the peak height of the extracted ion chromatogram of *m/z* 455 was 32 %, showing that the tips could be used for semiquantitave analysis as such. One of the reasons for the observed deviation can be manual injection which was noted to affect both signal intensity and also duration of the signal (varying from 3 to 7 s). Therefore, automatic and precise sampling together with the use of an internal standard could substantially increase repeatability. The multitip µPESI microchip was shown to be reusable, after cleaning with either a Piranha solution (H_2SO_4 : 30% H_2O_2, v/v 3:1) or by ultrasonication with acetone, toluene and methanol. The washed chip showed no memory effects (data not shown) and thus could be utilized for new analyses.

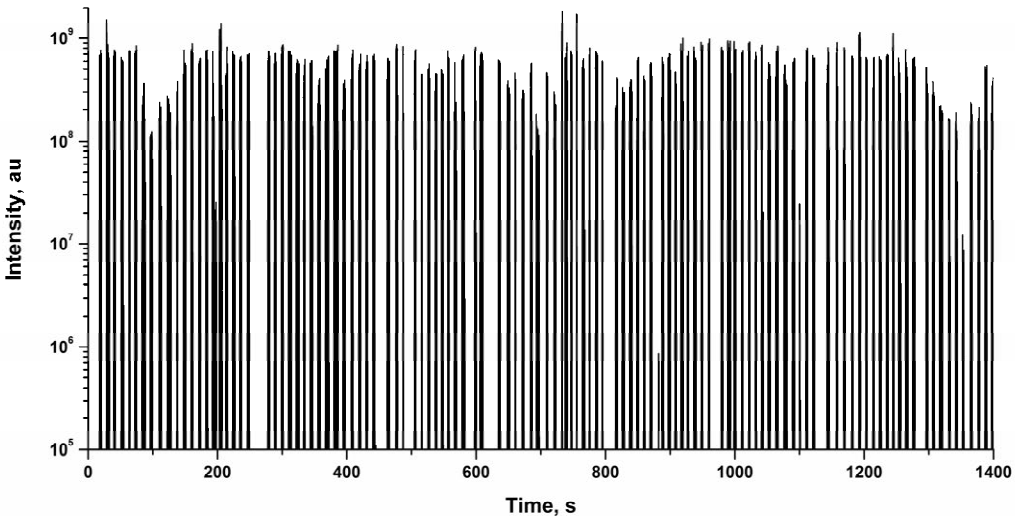

Figure 7.3. Intensities of ion *m/z* 455 recorded from the analyses of 500 nM verapamil sample with 120 times 1.5 µL injections to 60 individual tips (changing the tip each time after injection).

The measurement itself with one tip is very rapid as it takes about 5 seconds to spray the whole liquid sample (1.5 µL) out from the tip to the MS. With manual sampling it was possible to introduce a sample into the sampling spot once in about 10 seconds, taking into account the 5-second measurement, rotating the chip to a new position, and the sampling (pipetting) itself. This high frequency enables the use of the multitip chip for rapid and high throughput analysis as 60 samples from one chip can be analyzed in about 11-12

minutes. The sampling frequency can be further increased by automation of the sampling and rotation procedures. The performance and the speed of the analysis can be improved by an automated instrumentation.

7.3.2 Rapid analysis of reaction products from organic synthesis

The multitip µPESI-MS was applied to the monitoring of reaction products from a synthesis of tricyclic tropones from heptafulvenes. The synthesis is rather rapid, as the whole synthesis is completed in 10 minutes. However, despite being carried out as a "one-pot" process, it consists of several chemical reaction steps, thus yielding intermediate products whose structures have not been confirmed so far with any analytical methods. Therefore, the new multitip µPESI chip was found to be a suitable choice for the analysis as it provides rapid analyses, hence kinetics could also be determined from the analytical results. Due to the total reaction time of 10 minutes, it was decided that it was adequate to start measurement with one sample in one minute. Higher sampling frequency is also possible if needed. Due to high concentration of the starting material, and hence of the reaction products, a liquid sample from the reaction vessel was first diluted with methanol by 100–fold prior to the analysis to avoid overloading of the analytical instrument and especially ES ionization. Dilution was made with chilled solvent to prevent the reaction from proceeding further before the analysis.

The mass spectra of the synthesis products supported the postulated synthesis route (Fig. 7.4a). The starting compound was observed at *m/z* 305, intermediates at *m/z* 321 and at *m/z* 515 and the final product at *m/z* 279. The ion at m/z 337 is most probably dioxygenated byproduct of the starting compound A. The ion at *m/z* 321 may represent two compounds, namely the protonated molecule of the oxidation product of A and tropylium carbocation. The ion at *m/z* 515 is most likely a sodium adduct of intermediate D. The ^{37}Cl isotope ion at *m/z* 517 confirmed the presence of one chlorine atom in the molecule. The identity of product D was not previously confirmed with any other method due to its relatively rapid reaction rate. The structures of the products were confirmed by MS/MS spectra (Table 7.1). All the synthesis products showed ion $[M+H-HF]^+$ confirming that the products contained at least one fluorine atom (in $-CF_3$ group) and are derived from the starting material A. Increase and/or decrease of starting material and reaction products as a function of time are shown in Figure 7.4c. The analytical cycle was fast enough for the measurement of a relative abundance of each reaction's products. Interestingly, the µPESI-MS measurement of the pure starting compound (A) also showed mono- and dioxygenated products (ions at *m/z* 321 (B) and 337), even without using any oxidant. This was probably due to oxidation reactions occurring during ES ionization.[28,29] One advantage of the new method is the very low amount of the starting compound needed for the analysis (150 pmol ~ 50 ng), therefore the synthesis could be done in microscale, for example using a microreactor on a chip. The results obtained in this experiment show that the multitip-µPESI-MS can be used for easy, convenient, and rapid monitoring of organic reactions.

Table 7.1. MS/MS data of the starting compound and reaction products measured by multitip µPESI with ion trap MS.

Compound	Precursor ion, *m/z*	Product ions in MS/MS, *m/z*					
A	305	303	289	285	283	269	
E	279	259	251	239	231	211	
B/C	321	319	301	299	291	283	279
Dioxygenation product of A	337	335	315	304	283	262	242
D	515	495	475	359	339	286	

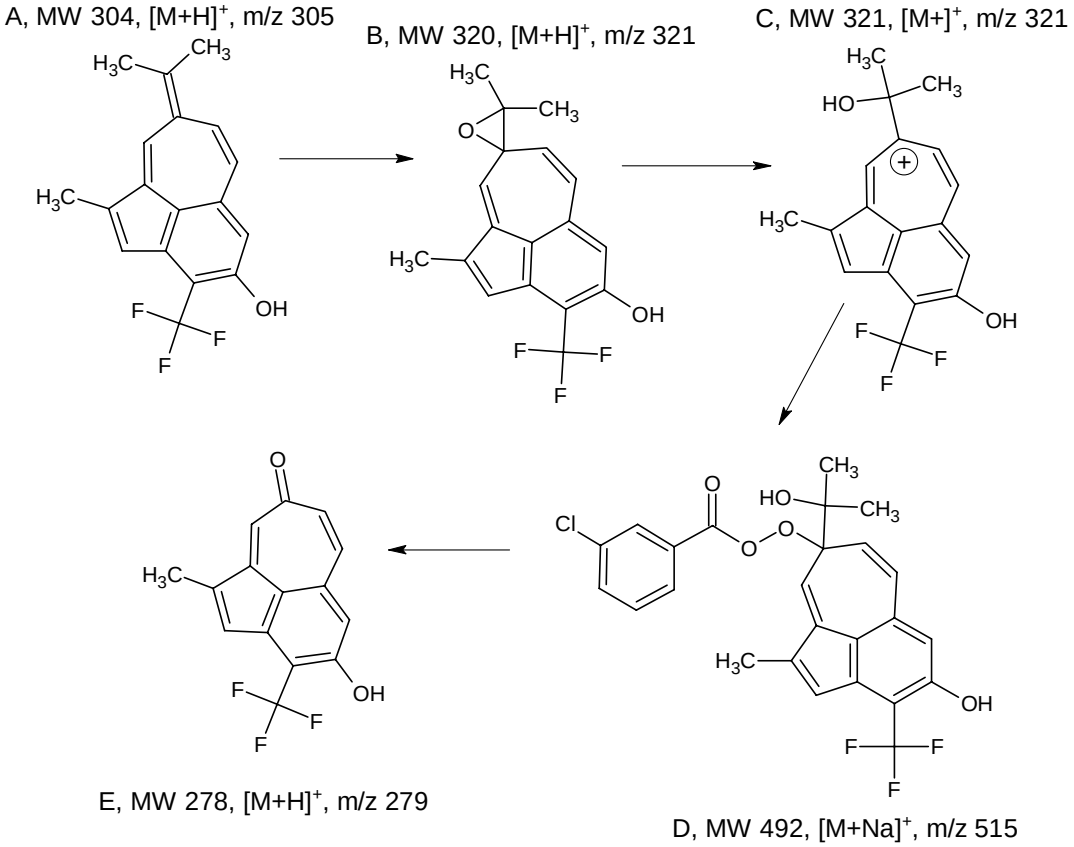

a)

Figure 7.4. **a)** A synthesis reaction pathway and structures of the intermediates[27] and final reaction products, showing their molecular weights and the *m/z* values of ionized molecules. **b)** A mass spectrum of synthesis products measured at 2.5 min after starting the reaction. **c)** Relative intensities of the starting compound and the reaction products by a function of time measured by multitip µPESI with ion trap MS.

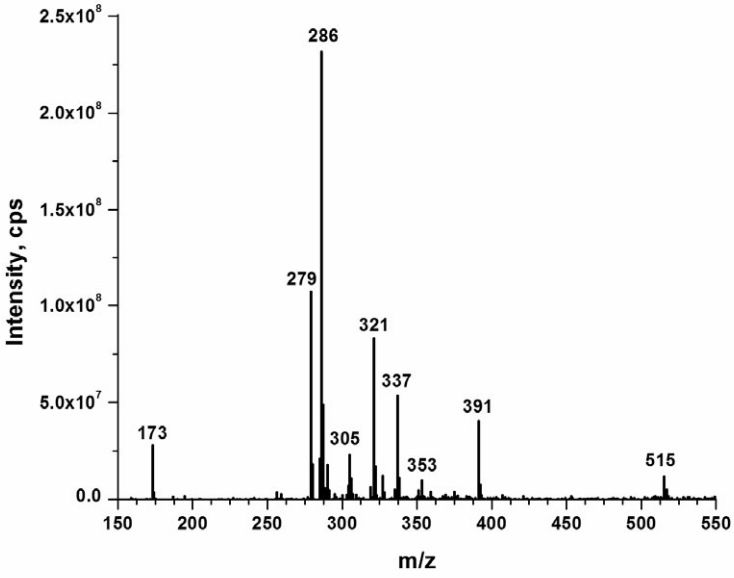

b)

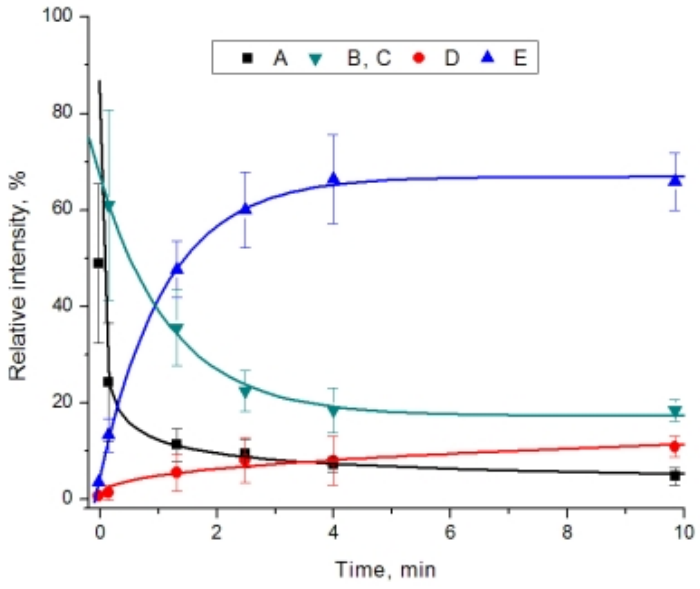

c)

Figure 7.4. Continues.

7.3.3 High throughput screening of drugs

Screening of drugs from urine samples is commonly performed with immunological methods, but the drawback of those methods is that they can give false positive or negative results because of the lack of specificity or sensitivity. Liquid chromatography with mass spectrometry (LC-MS) is a more specific and sensitive method for screening, but it is still relatively slow for high throughput screening analysis. Therefore, the feasibility of the multitip-µPESI-chip combined with TOF/MS instrument was evaluated

in this study for screening of benzodiazepines from urine samples. For sample treatment, a rapid ZipTip based method was chosen to take advantage of the fast analytical method. The purpose was also to minimize the total volume of urine used, and it was noticed that 50 µL of urine sample was enough to achieve the sensitivity level required for detection of drugs at cut-off concentrations used in immunological screening methods. The analytes were eluted with 3 µl of 95% MeOH with 1% of formic acid which was directly deposited on the µPESI sampling spot and subsequently analyzed with MS. Temazepam, oxazepam, nordiazepam, hydroxylated midazolam, and hydroxylated alprazolam are commonly screened benzodiazepines in urine samples and therefore these compounds were selected for the µPESI-MS analysis.[30]

The compatibility of the ZipTip-multitip-µPESI-QTOF/MS for screening of benzodiazepines was demonstrated with an analysis of a spiked urine sample and an authentic positive urine sample. Figure 7.5a shows a mass spectrum of a spiked urine sample measured with µPESI-QTOF/MS. The spiked urine sample contained benzodiazepines, namely nordiazepam, oxazepam, temazepam, α-OH-alprazolam, and α-OH-midazolam with a concentration of 200 ng/mL. All benzodiazepines were detected with adequate signal intensity for positive identification. Figure 7.5b shows a typical mass spectrum measured with the multitip-µPESI-TOF instrument from an authentic urine sample that contained oxazepam (protonated molecule at *m/z* 287) and α-OH-midazolam (protonated molecule at *m/z* 342). The ion at *m/z* 289 was concluded to be protonated oxazepam with ^{37}Cl isotope. The sample was previously analyzed with GC/MS and the same compounds were detected, showing the capability of multitip-µPESI-method for high throughput screening of benzodiazepines from urine samples.

7.4 Conclusions

The design of the microchip with electrospray tips as an array at the edge of a single wafer is unique. Parallelization of the µPESI-tips to a rotating multitip array combined with MS was shown to be a promising method for high throughput screening in qualitative and semi-quantitative analyses. Repeatability of tip to tip was examined to be adequate for qualitative analysis and the method was rapid, as 60 samples can be analyzed in 10 minutes. Repeatability of the technique could be improved more by using an automatic sampler and an internal standard method. The system combined with ZipTip^{TM} solid phase extraction method showed to be a potential choice for specific screening of benzodiazepines from urine, being rapid, sensitive, and specific. The speed and easiness of the rotating multitip µPESI-MS also proved to be adequate for rapid monitoring of reaction products in an organic synthesis. The amount of the starting compound needed for the analysis was at pmol range, which enables utilization of microreactors for the synthesis, still providing high sensitivity in the analysis.

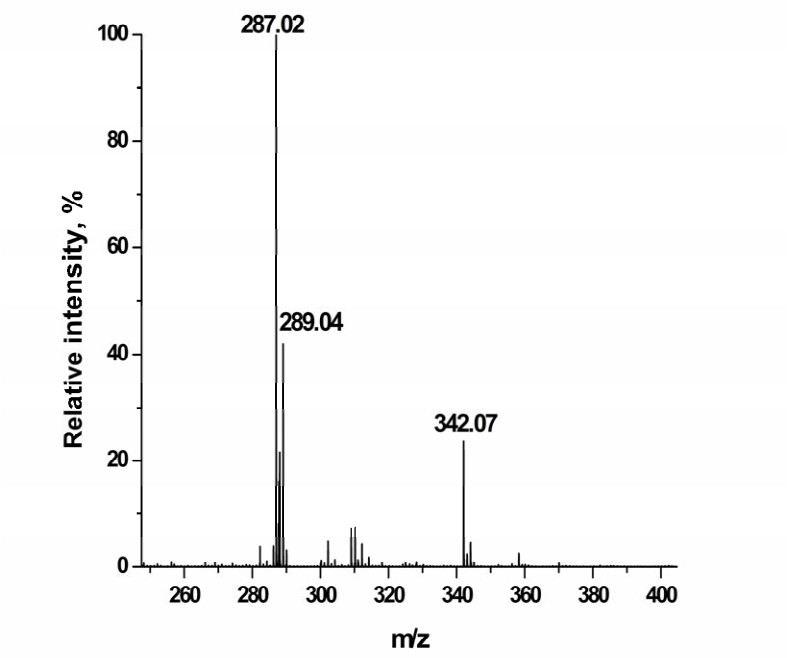

a)

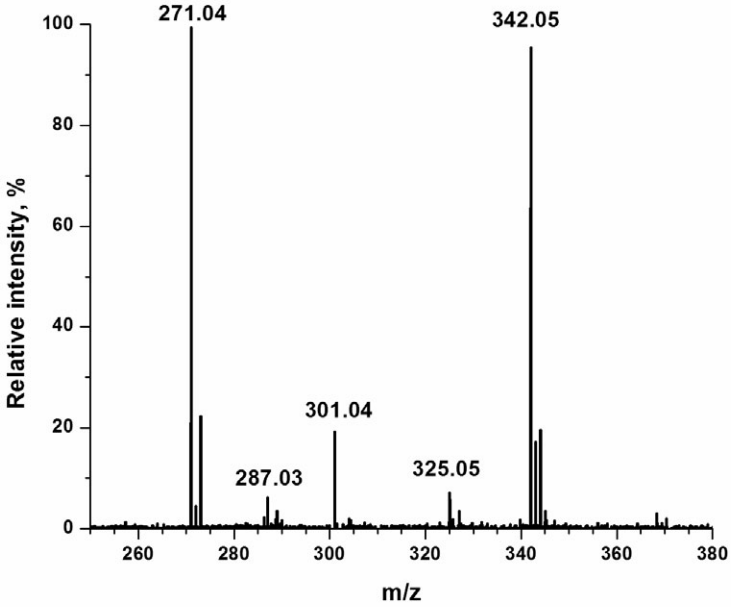

b)

Figure 7.5. a) A mass spectrum of a spiked urine sample containing nordiazepam (*m/z* 271), oxazepam (*m/z* 287), temazepam (*m/z* 301), α-OH-alprazolam (*m/z* 325), and α-OH-midazolam (*m/z* 342) with a concentration of 200 ng/mL analyzed with ZipTip-µPESI-QTOF/MS combination. **b)** An ESI mass spectrum of an authentic positive urine sample that contained oxazepam (*m/z* 287) and α-OH-midazolam (*m/z* 342) measured with multitip-µPESI-TOF/MS.

References

1 T. Sikanen, S. Franssila, T. J. Kauppila, R. Kostiainen, T. Kotiaho, R. A. Ketola, Microchip technology in mass spectrometry, Mass Spectrom. Rev. 2010, 29, 351-391.

2 S. Koster, E.Verpoorte. A decade of microfluidic analysis coupled with electrospray mass spectrometry: An overview. Lab Chip, 7, 1394–1412, 2007.

3 R. Ramsey, J. Ramsey. Generating electrospray from microchip devices using electroosmotic pumping. Anal. Chem. 69, 1174–1178, 1997.

4 Q. Xue, F. Foret, Y. Dunayevskiy, P. Zavracky, N. McGruer, B. Karger. Multichannel microchip electrospray mass spectrometry. Anal. Chem. 69,426–430, 1997.

5 A. Desai, Y. Tai, M. Davis, T. Lee. A MEMS electrospray nozzle for mass spectrometry. Proc Transducers ’97 (Chicago, IL), 927–930, 1997.

6 K. Huikko, P. Östman, K. Grigoras, S. Tuomikoski, V. Tiainen, A. Soininen, K. Puolanne, A. Manz, S. Franssila, R. Kostiainen, T. Kotiaho. Poly(dimethylsiloxane) electrospray devices fabricated with diamond-like carbon-poly(dimethylsiloxane) coated SU-8 masters. Lab Chip, 3, 67–72, 2003.

7 T. Rohner, J. Rossier, H. Girault. Polymer microspray with an integrated thick-film microelectrode. Anal Chem 73, 5353–5357, 2001.

8 M. Haapala, L. Luosujärvi, V. Saarela, T. Kotiaho, R. Ketola, S. Franssila, R. Kostiainen: Microchip for Combining Gas Chromatography or Capillary Liquid Chromatography with Atmospheric Pressure Photoionization-Mass Spectrometry. Anal Chem. 79, 4994-4999, 2007,

9 G. Schultz, T. Corso, S. Prosser, S. Zhang. A fully integrated monolithic microchip electrospray device for mass spectrometry, Anal Chem. 72, 4058-4063, 2000.

10 V. Kertesz and G. Van Berkel, Fully automated liquid extraction-based surface sampling and ionization using a chip-based robotic nanoelectrospray platform, J. Mass. Spectrom. 45, 252–260, 2010.

11 C. Van Pelt, S. Zhang, J. Henion, Characterization of a Fully Automated Nanoelectrospray System with Mass Spectrometric Detection for Proteomic Analyses, J. Biomol. Tech., 13, 72-84, 2002.

12 A. Merrill Jr, M. Sullards, J. Allegood, S. Kelly, E. Wang, Sphingolipidomics: high-throughput, structure-specific, and quantitative analysis of sphingolipids by liquid chromatography tandem mass spectrometry, Methods.36, 207-224, 2005.

13 J. Kapron, E. Pace, C. Van Pelt, J. Henion. Quantitation of midazolam in human plasma by automated chip-based infusion nanoelectrospray tandem mass spectrometry, Rapid Commun Mass Spectrom. 17, 2019-2026, 2003.

14 C. Van Pelt, S. Zhang, E. Fung, I. Chu, T. Liu, C. Li, W. Korfmacher, J. Henion, A fully automatic nanoelectrospray tandem mass spectrometric method for analysis of Caco-2 samples, Rapid Commun. Mass Spectrom. 17, 1573-1578, 2003.

15 V. Kertesz, G. Van Berkel, Fully automated liquid extraction-based surface sampling and ionization using a chip-based robotic nanoelectrospray platform, J Mass Spectrom. 45, 252-260, 2010.

16 L. Hanghui, C. Felten, Q. Xue, B. Zhang, P. Jedrzejewski, B. Karger, and F. Foret, Development of Multichannel Devices with an Array of Electrospray Tips for High-Throughput Mass Spectrometry Anal. Chem. 72, 3303-3310, 2000.

17 R. Kelly, J. Page, K. Tang, and R. Smith. Array of Chemically Etched Fused-Silica Emitters for Improving the Sensitivity and Quantitation of Electrospray Ionization Mass Spectrometry, Anal. Chem. 79, 4192-4198, 2007.

18 S. Tuomikoski, T. Sikanen, R.A. Ketola, R. Kostiainen, T. Kotiaho, S. Franssila, Fabrication of enclosed SU-8 tips for electrospray ionization-mass spectrometry, Electrophoresis, 26, 4691–4702, 2005.
19 S. Aderogba, J. Meacham, F. Degertekin, A. Fedorov, F. Fernandez. Nanoelectrospray ion generation for high-through-put mass spectrometry using a micromachined ultrasonic ejector array. Appl Phys Lett 86, 203110, 2005.
20 V. Kertesz, G. Van Berkel. Improved desorption electrospray ionization mass spectrometry performance using edge sampmling and a rotational sample stage, Rapid Commun. Mass Spectrom. 22, 3846-3850, 2008.
21 T. Nissilä, L. Sainiemi, T. Sikanen, T. Kotiaho, S. Franssila, R. Kostiainen, R.A. Ketola, Silicon micropillar array electrospray chip for drug and biomolecule analysis, Rapid Commun. Mass Spectrom. 21, 3677-3682, 2007.
22 L. Sainiemi, Nissilä, T., Jokinen, V., Sikanen, S., Kotiaho, T., Kostiainen, R., Ketola, R.A., Franssila, S. Fabrication and characterization of silicon micropillar array electrospray ionization chip, Sens. Actuat. B 132, 380-387, 2008.
23 T. Nissilä, L. Sainiemi, S. Franssila, R.A. Ketola. Fully polymeric integrated microreactor/electrospray ionization chip for on-chip digestion and mass spectrometry, Sens. Actuat. B 143, 414-420, 2009.
24 T. Nissilä, L. Sainiemi, M-M. Karikko, M. Kemell, M. Ritala, S. Franssila,R. Kostiainen, R.A. Ketola, Integrated photocatalytic nanoreactor electrospray ionization microchip for mimicking phase I metabolic reactions, Lab Chip, 2011, DOI: 10.1039/C0LC00689K
25 J. Erve, W. DeMaio, R. Talaat, Rapid metabolite identification with sub parts-permillion mass accuracy from biological matrices by direct infusion nanoelectrospray ionization after clean-up on a ZipTip and LTQ/Orbitrap mass spectrometry, Rapid Commun. Mass Spectrom. 22, 3015–3026, 2008.
26 J. Erve, C. Beyer, L. Manzino, R. Talaat, Metabolite identification in rat brain microdialysates by direct infusion nanoelectrospray ionization after desalting on a ZipTip and LTQ/Orbitrap mass spectrometry, Rapid Commun. Mass Spectrom. 23, 4003–4012, 2009.
27 I. Aumüller, J.Yli-Kauhaluoma, The Benzo[cd]azulene Skeleton – Azulene, Heptafulvene, and Tropone Derivatives, Org. Lett. 11, 5363-5365, 2009.
28 G. Van Berkel, R. Cole, In Electrospray ionization mass spectrometry, (Ed), wiley, USA, 65-105, 1997.
29 M. Prudent, H. Girault, Functional electrospray emitters, Analyst 134, 2189-2203, 2009.
30 J. Valentine, R. Middleton, C. Sparks, Identification of urinary benzodiazepines and their metabolites: Comparison of automated HPLC and GC-MS after immunoassay screening of clinical specimens. J. Anal. Toxicol. 20, 416-420, 1996

8 Monolithically integrated micropillar liquid chromatography-electrospray ionization microchip for mass spectrometric detection (VI)

We present the first monolithically integrated silicon/glass liquid chromatography-electrospray ionization microchip for mass spectrometry. The microchip is fabricated by bonding a silicon wafer, which has deep-reactive ion etched micropillar-filled channels, together with a glass lid. Both the silicon channel and the glass lid have a through-wafer etched sharp tip that produces a stable electrospray without a nebulizer gas or a sheath liquid flow at a flow rate range from 100 nL/min to 5 µL/min. The microchip is also compatible with laser induced fluorescence (LIF) detection, due to the glass lid. The micropillar array coated with a C_{18} stationary phase contains approximately 600,000 micropillars in a channel of 1-mm width and 35-mm length, thus having enough capacity to produce reduced plate heights from 0.1 to 0.2 µm for organic compounds. Separation of drugs in less than 10 minutes with good sensitivity was demonstrated with mass spectrometric detection as well as separation of fluorescent compounds with LIF detection.

8.1 Introduction

A current trend in analytical chemistry has been miniaturization and microfabrication of analytical instruments and integration of different kinds of functionalities on the same microchip. There are advantages when instruments are miniaturized: in analytical chemistry microfabricated devices can be used with decreased flow rates, which significantly reduce solvent consumption. Due to shorter distances in a microchip, the diffusion is a more effective process, thus useful in microreactors where diffusion is no longer limiting reaction rates, but rather speeding up the reactions. Analysis times are also decreased due to the reduced time needed to transfer liquids. Furthermore, shorter distances without external junctions also provide smaller dead volumes, and therefore narrower peaks in chromatography, increasing analytical performance. Microfabrication technology, which is commonly known as a technique for fabrication of electronics, is also usable in the fabrication of analytical microdevices, allowing the mass production of microchips to make them more cost effective to produce and use.

Ramsey and Ramsey (1997) reported the first glass microfabricated planar-edge devices for electrospray.[1] Consequently, the first silicon ESI emitter, for which the tip diameter was as small as about 2 µm, was fabricated in 1997.[2] Arscott et al. (2005) developed a self standing polysilicon ESI tip which was proposed to work with 0.7 kV, one of the lowest voltages that have been used in ESI tips.[3] Silicon multinozzle ESI array was developed by Kim et al. (2007) for proteomic total analysis systems.[4] Legrand et al. (2007) reported combination of microelectromechanical systems and microfluidic rules for a nanoESI emitter and, as such observed lysozyme at a concentration of 100 nM.[5] Nissilä et al.

(2007) demonstrated a microchip which was able to ionize and detect a 2.5µL drug sample with 30 pM concentration corresponding to 75 amol with MS. The chip also contained self filling pillar structure that used capillary forces for reliable sample transportation.[6] Quantitative bioanalysis was shown to be possible with automated sampling combined with off-line fabricated silicon ESI-tip.[7]

Various microchips have been microfabricated for liquid chromatography since He, Tait and Regnier (1998) published inspirational articles about nanocolumns for liquid chromatography.[8,9] Ordered pillar arrays have many practical benefits when compared to particle packed or monolithic columns. Monolithic pillar array is very precisely fabricated and therefore the array is very homogenous when compared with particle packing, where the packing process is cumbersome and hard to reproduce. Similar challenges are also evident with monolithically packed polymer and silica columns where patch to patch repeatability proves difficult to achieve. It was shown that perfectly ordered non-porous pillars, such as the LC-column, has the best separation performance, in theory, when plate heights are considered.[10] Malsche et al. (2007) have published micropillar array separation microchips for LC of coumarins combined with laser induced fluorescence detection.[11] The chip was coated with C8 reversed phase material. Separations they made achieved plate heights of H = 2 µm and plate number N = 4000-5000 over the 10 mm long channel when the pH was 3. Within the pillar array separation column, it is possible to control the flow by placing pillars wisely, therefore enabling to reduction of band widening through the column at the both sides of the column.[12] Mery et al. (2008) reported peptide separations with a micropillar array column combined with a polysilicon ESI tip.[13] Both liquid phase C_{18} and vapour phase C_{10}-perfluorated silane were tested as coating methods. They were able to separate five peptides (30 fmol) from cytochrome c trypsin digestion in 50 minutes and detect them with MS. High-aspect-ratio micro pillars (1 µm diameter, 20 µm height, and 2 µm pitch between pillars) covered by a silicon dioxide layer of 2 – 3 µm thickness were used as an HPLC column using fluorescence detection.[14] The chip was covered with glass by using polyethylene glycol- methyl ether methacrylate seal. Surprisingly this normal-phase column indicated a hydrophobic separation mechanism. The reduced plate heights obtained were 1.1 and 1.8 µm for fluorescein and sulforhodamine B, respectively. Microchips have also shown potential properties when combined with mass spectrometry.[15] We have previously shown that a micropillar array in an open channel can induce an electrospray plume at a sharp tip on a micropillar array electrospray ionization (µPESI) microchip.[16,17] The open micropillar array channel made of SU-8 polymer can also be used as a microreactor for protein digestion studies.[18] When a silicon based µPESI chip is covered with titanium dioxide (TiO_2) it can be used for performingphotocatalytic reactions with a UV lamp and a direct analysis of reaction products with MS.[19]

The main aim of this study was to fabricate a monolithically integrated silicon/glass liquid chromatography-ESI microchip for direct mass spectrometric analysis. The glass cover of the microchip makes it suitable for analyses with laser induced fluorescence (LIF) detection and novel design and fabrication of a sharp three-dimensional monolithic glass-

silicon ESI tip makes the chip suitable for mass spectrometric analyses. The microchip contained a micropillar array based liquid chromatographic separation channel, which was coated with a reversed-phase separation stationary phase (C_{18}), and with SiO_2 for normal phase separations. The feasibility of the microchip for normal phase and reversed phase LC-ESI/MS and LC-LIF analyses is demonstrated.

8.2 Experimental

8.2.1 Design

The chip (see Fig 8.1e) consists of a through silicon etched inlet. The inlet channel (256 µm wide) is divided into two channels (with half widths) seven times, thus forming channels with 2 µm widths. This leads to a 1 mm wide pillar array column, which consists of 6 µm wide round pillars with 1-2 µm gaps between the pillars (see Fig. 8.1b). After the end of pillar array there are similar channels as previous to the pillar array column (see Fig 8.1a) culminating in a sharp glass silicon, three dimensional, sharp electrospray tip (Fig 8.1c and 8.1d). There are also two 50 µm wide channels for sheath liquid flow that are placed to both sides of the separation column.

8.2.2 Fabrication

The liquid chromatography microchips are fabricated by bonding silicon and glass wafers together. The silicon wafer carries channels with a micropillar array, the inlets, and the sharp tips, while the glass wafer has only the sharp isotropically through-etched tip (see Fig.8.1).

The microfabrication of a micropillar array in a channel on a silicon wafer has been previously published.[17] The silicon microfabrication of channels started with a 320 µm thick oxidized <100> wafer, with a thermal oxide thickness of 622 nm. The patterns of the flow channels were etched into the oxide layer using lithography and CHF_3/Ar based RIE (Plasmalab System 80, Oxford Instruments), respectively. From the backside of the wafer the oxide was removed using a similar RIE process. The photoresist was removed in acetone and a 200 nm thick layer of aluminum was sputtered (Plasma-lab System 400, Oxford Instruments) on top of the patterned SiO_2 layer. Both patterns that define the inlets and the electrospray ionization tips were defined to the aluminum and underlying silicon dioxide layers with the second lithography, followed by phosphoric acid etching and CHF_3/Ar based RIE, respectively. After photoresist removal, the silicon wafer was thru-etched using cryogenic DRIE (Plasmalab System 100, Oxford In-struments) with SF_6/O_2 plasma.[20] Then, the aluminum mask was removed in phosphoric acid to expose more silicon and the patterned silicon dioxide mask. The following cryogenic DRIE step also

utilized SF_6/O_2 chemistry and it formed the flow channels. The SiO_2 mask was removed in buffered hydrofluoric acid (BHF) and finally the wafer was treated in oxygen plasma to make the channels hydrophilic.

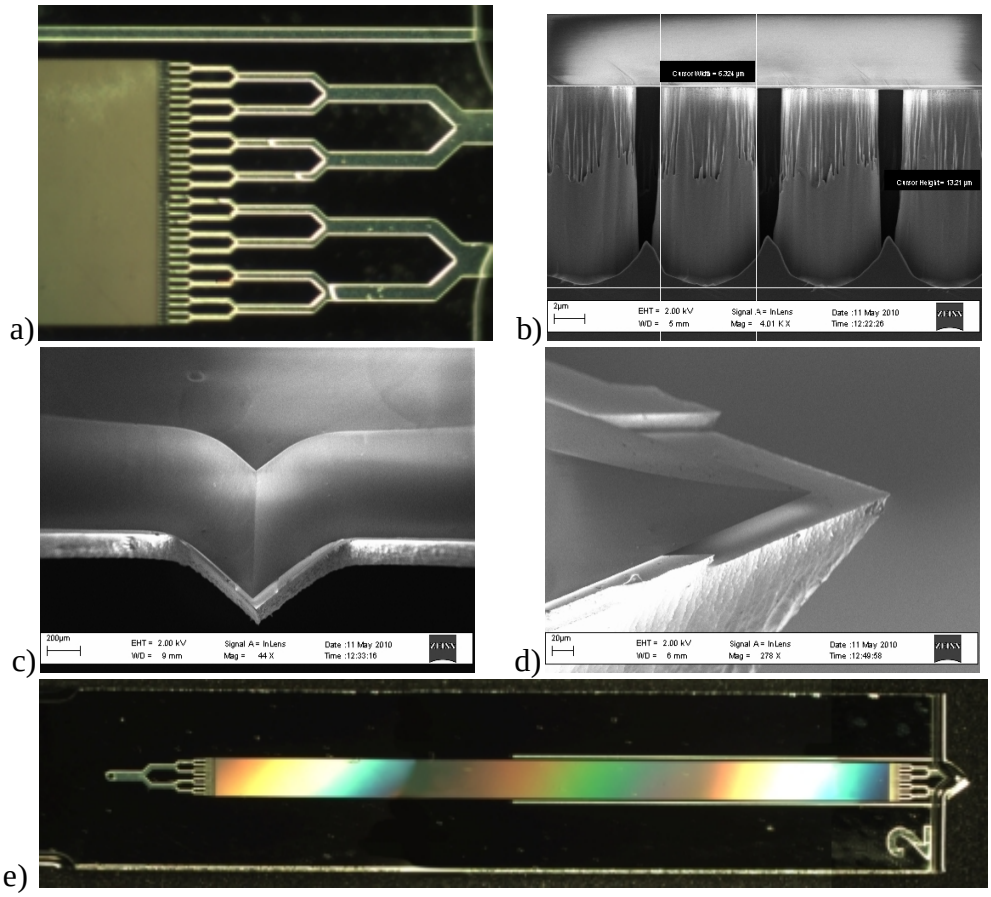

Figure 8.1. a) A micropillar array column with a Regnier style outlet. **b)** Micropillars inside the channel. Heights of the pillars were 13 µm and diameter 6 µm. **c)** A scanning electron micrograph (SEM) from the front of sharp ESI tip. Upper part is isotropic etched glass cover and the silicon part is below. **d)** A SEM from the side of sharp ESI tip. **e)** A photograph of the whole LC-µPESI chip.

Glass microfabrication commenced with low pressure chemical vapor deposition (LPCVD) of a 400 nm thick amorphous silicon layer on a 500 µm thick borosilicate glass (Borofloat 33) wafer. The patterns of electrospray ionization tips were defined to the amorphous silicon layer on the wafer topside by photolithography and SF_6 based RIE process, respectively. The amorphous silicon layers acted as etch masks during the isotropic thru-wafer etching in 10:1 HF-HCl solution. After glass etching, the photoresist was removed in acetone and the amorphous silicon layers in SF_6 based RIE process. After the silicon and glass microfabrication the wafers were anodically bonded together at the temperature of 360 °C (AWB-04, AML). The applied voltage was 600 V. Finally, the bonded wafers were diced using a dicing saw.

8.2.3 Coating

The column in the chip was coated with octadecyltrichlorosilane (C18, 90+%, Sigma-Aldrich) for liquid chromatographic separations. The coating protocol commenced with a toluene (Sigma-Aldrich, HPLC-grade) wash of the channel. Toluene was injected through the channel by the syringe pump, using a 100 µL syringe, for 30 minutes with a flow rate of 100 µL/hr. A custom made chip holder was used to connect the capillary with Upchurch scientific super flangeless fittings tightly on the chip. After that the chip was placed on the plate at 70 ^{0}C. C18 (1%) in toluene was pushed through the channel for 30 minutes and the chip was then cleaned with 100 µL of toluene. The coating of the pillars was endcapped with 30% trimethylchlorosilane (TMCS, 99% GC-grade, Fluka) in toluene. Approximately 50 µL of TMCS was pushed through the channel with a flow rate of 100 µL/hr, and the chip was washed with 500 µL of toluene pushed through by hand. The chip was conditioned overnight with methanol (J.T. Baker, Deventer, Netherlands, HPLC-grade) using a flow rate of 50 µL/hr.

8.2.4 Laser induced fluorescence analyses

Laser induced fluorescence (LIF) studies were performed with a Leica inverted microscope (Leica, Nilomark, Espoo, Finland) equipped with a 488 nm blue laser (Cheos, Espoo, Finland) with 450-490 nm excitation and a 515 nm high bandpass emission filter. A photomultiplier tube, signal amplifier module (Cairn Research) and PicoLog software (Pico Technology, St. Neots, UK) were used for fluorescence signal acquisition, processing and recording respectively.

An Agilent 1100 LC (Santa Clara, CA, USA) was used for gradient pumping. The chip was connected to the LC with 50 µm ID silica capillary. Rhodamine 110 Cl, fluorescein and 6-carboxyfluorescein were used as test compounds atconcentrations of 5 µg/ml. Solvent was 20 mM phosphate buffer (pH 4.5) and B was 100% methanol. A 3 min gradient of 0-95% B was used. Injection volume was 3 µL and the flow rate was set to 130 µL/min. The flow was split 1:200 before reaching the chip, thus was about 650 nL/min inside the chip, the injection amount also decreased to 15 nL being, thus 225 fmol per compound. Back pressure was 190 bar at the start and maximum pressure during the analysis was 300 bar. The chip was tested with UPLC (Waters, Manchester, UK) to function with pressure up to 500 bar.

Normal phase separation was performed using SiO_2 coated micropillar array. Flow rate inside the channel was approximately 500 nL/min. Both 10 nL of 15µM Rhodamine 110 Cl and 15µM Bodipy were injected to the chip corresponding to a total amount of 150 fmol for each compound. The gradient commenced after a 1 minute wait, with 100% isopropanol (IPA), and lasted 5 minutes ranging from 100% IPA to 100% ammonium bicarbonate, pH 7.5. The LIF detection window was set to 400 µm x 200 µm at the center of the channel and end of the pillar array.

8.2.5 Mass spectrometric analyses

Mass spectrometric analyses were performed with Micromass/Waters (Manchester, UK) QTOF Micro and Agilent 6330 ion trap mass spectrometers. Stability and sensitivity measurements were done with a QTOF mass spectrometer in positive ion mode. The chip was placed 5 mm in front of the cone of the mass spectrometer and 5 kV was connected to a silicon part of the microchip. Sample cone voltage was set to 35 V, extraction cone to 2 V, desolvation temperature to 150 ^{0}C and source temperature to 120 °C. Cone gas was 150 L/hr and no other gases were used for ionization. Methanol (50%) was sprayed with 1µM verapamil at flow rates of 100, 250, 500, 1000, 5000 nL/min. The mass spectrometer accumulated ions 1.0 s for each spectrum and 2 minutes of data collected for each flow rate. The average spectrum calculated from whole 2 minute chromatogram. Extracted ion currents for protonated verapamil $[M+H]^+$ at *m/z* 455.3 were obtained and relative standard deviations (RSDs) were calculated at each flow rate.

For liquid chromatography with mass spectrometer, the same LC was used as with LIF studies. Verapamil, propranolol, metoprolol and ranitidine standards (5 µM) in H_2O (Milli-Q, Millipore, Molsheim, France) was used for LC samples. Flow rate was 20 µL/min and it splitted before reaching the chip by rate about 1:30 so the flow rate on the chip was 650 nL/min. The solvent was 2% MeOH with 0.1% FA and B was pure methanol. A gradient was performed in 10 minutes from 5% B to 95% of B.

8.3 Results and discussion

8.3.1 Fabrication of monolithically integrated silicon/glass micropillar LC-ESI microchip

Fabricating complex structures in silicon is fairly straightforward, but fabrication of sharp electrospray ionization tips out of glass has been more problematic due to limited capabilities of DRIE of glass. Instead of DRIE, our approach is based on isotropic wet etching of glass which results in a three-dimensionally sharp electrospray ionization tip as shown in the SEM images in Figure 8.1 c and d. The mask openings for both the silicon and the glass ESI tips were identical, although silicon was etched using anisotropic DRIE, and glass using isotropic wet etching. The etch rate of HF-HCl etching solution at room temperature was measured to be approximately 7.8 µm/min. It is a worth noting that the etch rate of the solution decreases slowly, because the etchant is not buffered. Timing the glass etching process accurately is important, because overetching moves the edges of the thru-hole further at the rate of 7.8 µm/min. Etching through a 500 µm thick wafer takes 64 minutes. Still, we used a total etch time of 66 minutes, because we wanted to ensure that the coverlid would not exceed the edge of the silicon tip. Producing a stable electrospray is very difficult if the coverlid fully covers the microchannel.

Due to the isotropic nature of the HF-HCl glass etching, the ESI tip is three-dimensionally sharp as clearly shown in Figures 8.1 c and d. The sharpness of the tip is crucial for the performance of the chip, as it directs the electrospray to a predetermined location and thus eases the operation of the chip. The sharpness of the tip also reduces the voltage required for the electrospray formation, and reduces the spreading of liquids along the edges of the tip during operation.[21] The amorphous silicon etch mask was removed from the glass wafer after thru-wafer etching using RIE process. In principle, the removal could be done using wet chemistry as well, but most of the wet etchants generate roughness on the surface of the wafer, and therefore it is difficult to achieve good bond strength.

The main strengths of our fabrication process flow are its simplicity and scalability. All of the process steps are standard microfabrication processes and the ESI tip is monolithically integrated to the chip. This circumvents manual and cumbersome insertion of fused capillary tips at the microchip level. An obvious limitation of our microchip design is that the bottom part is made of silicon. Therefore, an electroosmotic flow cannot be used for sample transportation and the use of electrophoresis for sample separation before ESI is impossible.

8.3.2 Analytical performance of the silicon/glass µPESI tip

The properties of the silicon/glass ESI tip were studied with respect to solvent composition and a flow rate. Water, methanol, and acetonitrile, with various compositions were tested at a flow rate range of 100 nL/min to 5 µL/min. It is possible to roughly estimate the sensitivity of the system when the flow rate of liquid, the concentration of the analyte, and the accumulation time are known. The best sensitivity without a nebulizing gas or a sheath liquid flow was obtained at a flow rate of 1 µL/min when 1 µM verapamil solution was sprayed with a solvent composition of 50 % aqueous methanol (Fig. 8.2a). When the injection time was 1.0 s and the average intensity was 1418 counts/s, then 10 amol of the analyte was needed to produce one count with the QTOF Micro instrument. The estimate is very rough and does not consider, for example, adsorption that might occur on the chip. At higher flow rates the droplet size in electrospray grows, decreasing ionization efficiency and therefore lowering the signal of verapamil. At flow rates of 250 nL/min or below, the sensitivity is decreased due to the unstable electrospray under an insufficient amount of solvent. The stability of the electrospray at different flow rates is shown in Figure 8.2b, expressed as the RSD of the intensity of 1µM verapamil signal (protonated molecule at *m/z* 455.3). It shows that in the range of 1 – 5 µL/min, the RSDs are about 10 % or less, whereas at flow rates from 100 nL/min to 1 µL/min the microchip is still usable but not for quantitative analysis due to large RSD values. Mass spectra obtained with 100 nL/min and 1 µL/min flow rates are shown in Fig. 8.3, where it is evident that the intensity of the background ions are very low and the mass spectra are therefore clear for analyses. When the microchip was used with a sheath liquid flow (methanol at a flow rate of 7 µL/min), the ES plume was also stable at a low flow rate of the eluent (100 nL/min) and usable for gradient separations and analyses.

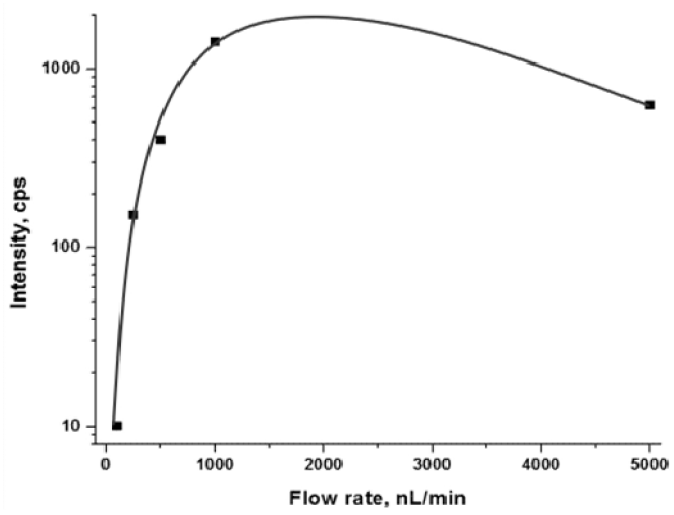

a)

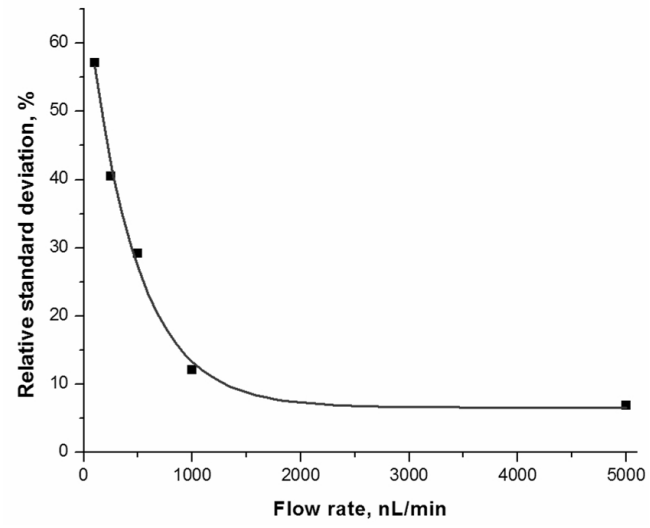

b)

Figure 8.2. a) Intensity of 1µM verapamil with different flow rates of 50% MeOH. **b)** 50% MeOH with 1 µM verapamil spray stability at *m/z* 455.3 with different flow rates without nebulizing gas and sheath flow.

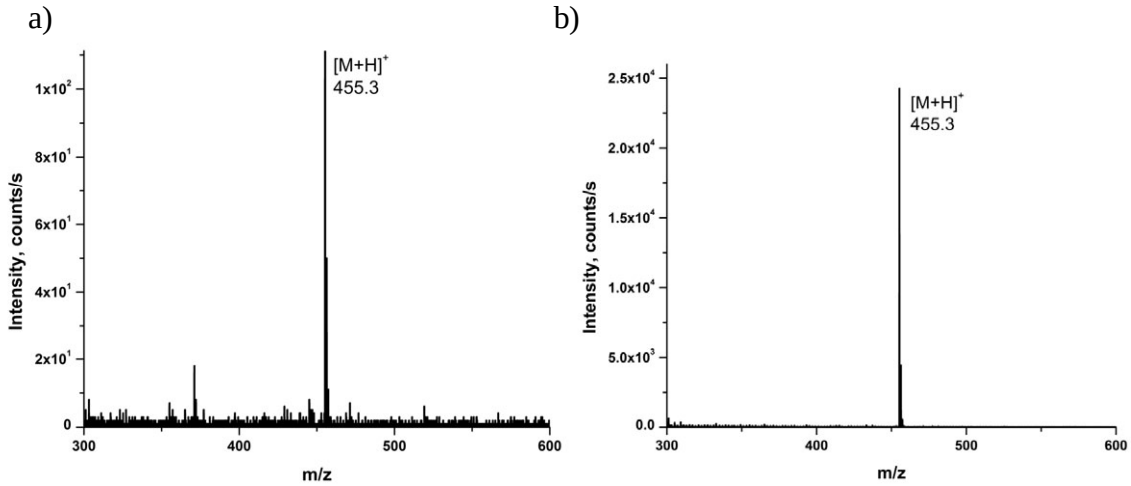

Figure 8.3. a) An average mass spectrum from 100nL/min flow measurement and **b)** from 1000 nL/min measured with a monolithic silicon/glass µPESI tip and ion trap MS.

8.3.3 Separation performance of micropillar LC microchip with LIF detection

The performance of the micropillar LC microchip was first evaluated using LIF detection. The detection window was located to the end of the pillar array and 100 µm away from the edges of the channel. The area of the detection window was approximately 2 mm^2, thus it gave an average signal only from the middle of the channel, not from the whole separation band. The separation of rhodamine 110 Cl, fluorescein and 6-carboxyfluorescein (see Fig. 8.4) showed peak widths at full width at half of maximum height (FWHM) from 7 s to 9 s. Plate numbers, calculated from equation $N = 5.54(t'_r/w_{1/2})^2$, were 3,300 – 5,500 and calculated plate heights (H = L/N) were 5.7 – 9.6 µm. Reduced plate heights, that are calculated from an equation ($h = H/d_p$) and also take into consideration the micropillar diameter d_p, were 0.95 – 1.6. For UPLC, the plate number for the 100 mm column was 80,000, the maximum plate height obtained 4.4 µm and reduced plate height 2.6, with d_p=1.7 µm particle.[22] The micropillar column showed a good performance, but plate numbers are still not at the level of the UPLC or Rapid Resolution columns. Nonetheless, when reduced plate heights are compared, the pillar array appears to be better. Possible reasons for low plate numbers are shorter column and also propably lower peak capacity, as the micropillars are not porous; thus the number of C_{18} groups at the surface of the micropillars is much lower than at the surface of porous 1.7 µm beads used in UPLC columns. However, the benefit of the microchip LC column is a very low injection volume of the sample (15 nL). The limits of detection (LODs) with the LIF system for studied compounds were around 15 µM, thus the absolute LOD was in the fmol range (1 fmol).

The SiO_2 coated pillar array was used for normal phase separations. A typical chromatogram of normal phase separation is shown in Fig. 8.6. Peak widths obtained for bodipy was FWHM 15 s and 14 s for rhodamine 110 Cl, producing plate number N = 1400 for rhodamine 110 Cl. Plate number corresponds to plate height of 2.6 µm and reduced plate height of 0.4.

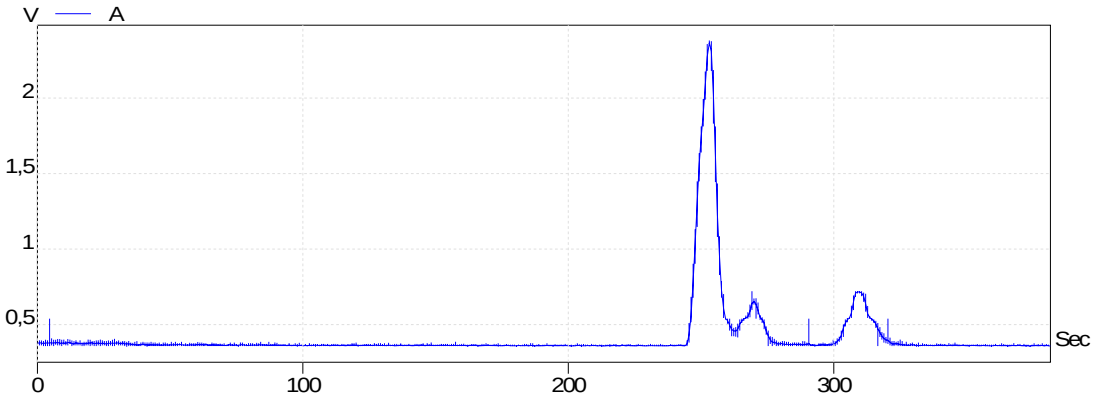

Figure 8.4. Separation of 6-carboxyfluorescein, fluorescein, and rhodamine 110 Cl (respectively from left) with a micropillar array LC microchip and LIF detection.

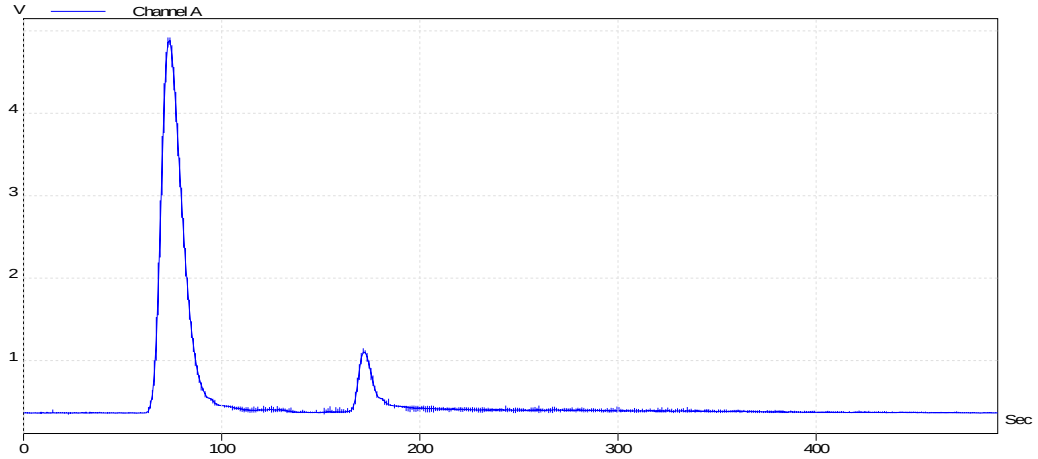

Figure 8.5. Reversed phase separation with C_{18} coated pillar array. A 5 min gradient starting with 98% A = H2O + 0.1% Triethylamine ending to 65% B = acetonitrile. A 5 nL injection of 100 µM 6-carboxyflourescein and 10 µM rhodamine 110 chloride.

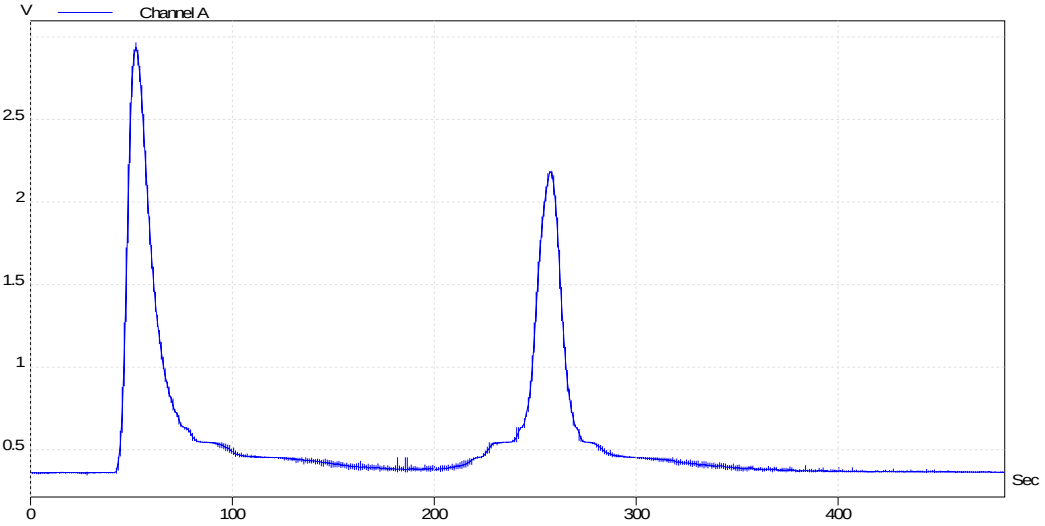

Figure 8.6. Normal phase separation of bodipy and rhodamine 110 Cl with SiO_2 coated pillar array LC column combined to LIF detection.

8.3.4 Separation performance of micropillar LC-ESI microchip with C_{18} coating and MS detection

In order to determine the most suitable flow rate for separations, a Van Deemter plot was done (see Fig. 8.7a). From the Van Deemter plot, it can be seen that the best performance for separations is obtained with a linear flow rate between 1.0 - 2.5 mm/s (reduced plate height h < 2) corresponding to a volume flow rate of 100 – 400 nL/min. A study with the micropillar LC-ESI microchip combined with an ion trap mass spectrometer showed a separation of small drug molecules (propranolol, ranitidine, metoprolol, and verapamil) within 9 minutes using a gradient elution (Fig. 8.7b). As can be seen from the figure, there is some peak tailing, probably due to non-perfect column coating as there can be free hydroxyl groups at the surface, despite performing an end-capping procedure with trimethylchlorosilane after the actual C_{18} coating procedure. Still, the peak widths at the half of maximum intensities were between 8 to 14 seconds and for verapamil the plate number was 12,000 the plate height was 2.6 µm, and the reduced plate height was 0.44, which are similar to those obtained with UPLC™ and Rapid Resolution™ liquid chromatographic columns.[22]

8.4 Conclusions

We have designed, fabricated and tested a micropillar array based C_{18} column for LC separation and fabricated the first ever three-dimensionally sharp glass-silicon tip for electrospray ionization. The microchip produces stable electrospray at a flow rate range from 100 nL/min up to 5 µL/min and is therefore usable for chromatographic separations. The microchip is suitable for low amount analyses with less than 10 minute analysis times. Plate numbers of the column were in range of 3,300 – 5,500, plate heights 5.7 - 9.6 µm, and reduced plate heights 0.95 – 1.6. For one of the best commercially available LC device UPLC, plate number for 100 mm column was 80,000, maximum plate height obtained 4.4 µm, and reduced plate height 2.6 with 1.7 µm particles.[22] From this point of view, our pillar array chip has not such elevated plate numbers, due to a shorter column, but it is better with regard to plate heights and especially with reduced plate heights having therefore better capacity to separate compounds. The chip can be used with LIF detection as well as with mass spectrometry.

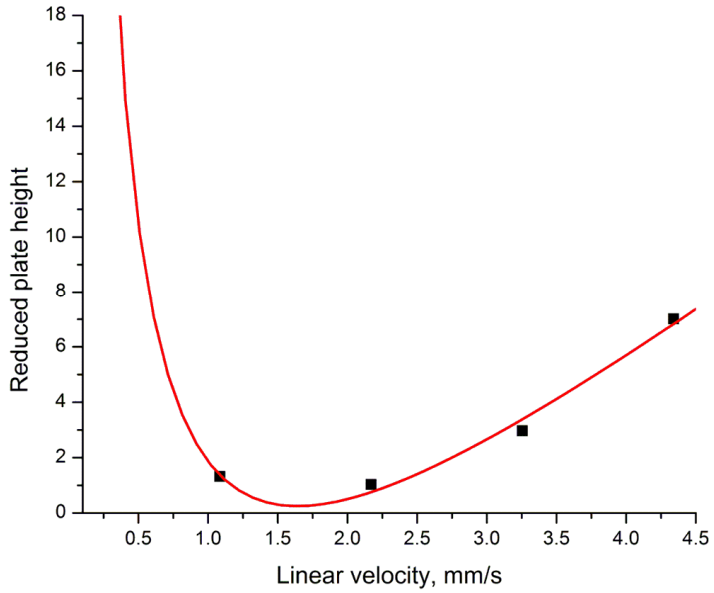

a)

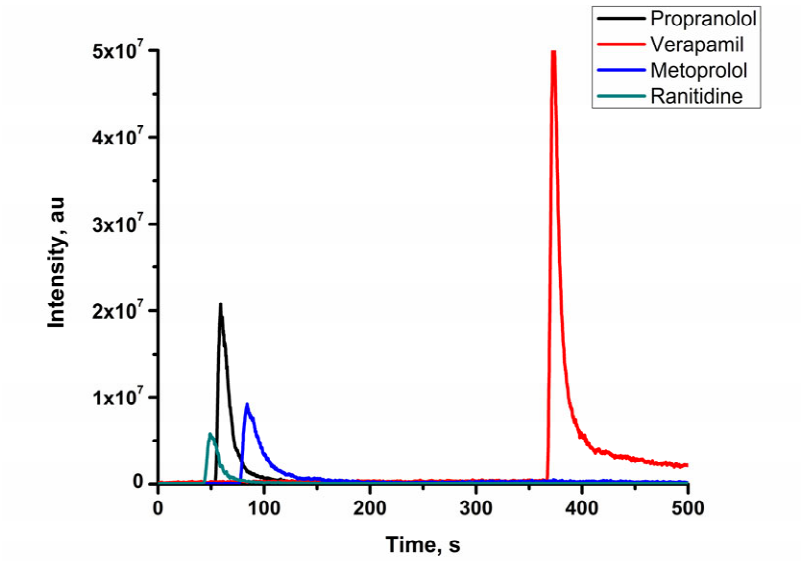

b)

Figure 8.7. a) Van Deemter plot. b) Chromatogram obtained with micropillar LC microchip – ion trap MS.

References

1 R: Ramsey, J. Ramsey. Generating electrospray from microchip devices using electroosmotic pumping. Anal Chem, 69, 1174–1178, 1997.

2 A. Desai, Y. Tai, M. Davis, T. Lee, A MEMS electrospray nozzle for mass spectrometry. Proc Transducers ’97 (Chicago, IL), pp. 927–930, 1997.

3 S. Arscott, S. Le Gac, C. Rolando. A polysilicon nanoelectrospray-mass spectrometry source based on a microfluidic capillary slot. Sens Actuators B 106, 741–749, 2005.

4 W. Kim, M. Guo, P. Yang, D. Wang. Microfabricated monolithic multinozzle emitters for nanoelectrospray mass spectrometry. Anal Chem 79:3703–3707, 2007.
5 B. Legrand, A. Ashcroft, L. Buchaillot, S. Arscott. SOI-based nanoelectrospray emitter tips for mass spectrometry: A coupledMEMS and microfluidic design. J Micromech Microeng 17:509–514, 2007.
6 T. Nissilä, L. Sainiemi, T. Sikanen, T. Kotiaho, S. Franssila, R. Kostiainen, R.A. Ketola. Silicon micropillar array electrospray chip for drug and biomolecule analysis. Rapid Commun Mass Spectrom 21:3677–3682, 2007.
7 J. Dethy, B. Ackermann, C. Delatour, J. Henion, G. Schultz. Demonstration of direct bioanalysis of drugs in plasma using nanoelectrospray infusion from a silicon chip coupled with tandem mass spectrometry. Anal Chem 75:805–811, 2003.
8 B. He, N. Tait, and F. Regnier, Fabrication of Nanocolumns for Liquid Chromatography, Anal. Chem., 70, 3790–3797, 1998.
9 B. Slentz, N. Penner, F. Regnier, Geometric effects of collocated monolithic support structures on separation performance in microfabricated systems, J. Sep. Sci. 25, 1011–1018, 2002.
10 J. Eijkel, Chip-based HPLC: the quest for the perfect column, Lab Chip, 7, 815–817, 2007.
11 W. De Malsche, H. Eghbali, D. Clicq, J. Vangelooven, H. Gardeniers, G. Desmet, Pressure-Driven Reverse-Phase Liquid Chromatography Separations in Ordered Nonporous Pillar Array Columns, Anal. Chem. 79: 5915, 2007.
12 N. Vervoort, J. Billen, P. Gzil, G. V. Baron, G. Desmet, Importance and Reduction of the Sidewall-Induced Band-Broadening Effect in Pressure-Driven Microfabricated Columns, Anal. Chem. 76, 4501-4507, 2004.
13 E. Mery, F. Ricoul, N. Sarrut, O. Constantin, G. Delapierre, J. Garin, F. Vinet. A silicon microfluidic chip integrating an ordered micropillar array separation column and a nano-electrospray emitter for LC/MS analysis of peptides. Sens Actuators B 134, 438–446, 2008.
14 L. Taylor, N. Lavrik, M. Sepaniak, High-aspect-ratio, silicon oxide-enclosed pillar structures in microfluidic liquid chromatography, Anal. Chem. 82, 9549-9556, 2010.
15 T. Sikanen, S. Franssila, T.J. Kauppila, R. Kostiainen, T. Kotiaho, R.A. Ketola, Microchip technology in mass spectrometry, Mass Spectrom. Rev. 29, 351-391, 2010.
16 T. Nissilä, L. Sainiemi, T. Sikanen, T. Kotiaho, S. Franssila, R. Kostiainen, R.A. Ketola, Silicon micropillar array electrospray chip for drug and biomolecule analysis, Rapid Commun. Mass Spectrom. 21, 3677-3682, 2007.
17 L. Sainiemi, T. Nissilä, V. Jokinen, T. Sikanen, T. Kotiaho, R. Kostiainen, R.A. Ketola, S. Franssila, Fabrication and characterization of silicon micropillar array electrospray ionization chip, Sens. Actuat. B 132, 380-387, 2008.
18 T. Nissilä, L. Sainiemi, S. Franssila, R.A. Ketola, Fully polymeric integrated microreactor/electrospray ionization chip for on-chip digestion and mass spectrometry, Sens. Actuat. B 143, 414-420, 2009.

19 T. Nissilä, L. Sainiemi, M-M. Karikko, M. Kemell, M. Ritala, S. Franssila, R. Kostiainen, R.A. Ketola, Integrated photocatalytic nanoreactor electrospray ionization microchip for mimicking phase I metabolic reactions, Lab Chip, 11, 1470-1476, 2011.
20 L. Sainiemi, S. Franssila, Mask material effects in cryogenic deep reactive ion etching, J. Vac. Sci. Technol. B 25, 801-807, 2007.
21 S. Koster and E. Verpoorte, A decade of microfluidic analysis coupled with electrospray mass spectrometry: An overview. Lab Chip, 7, 1394–1412, 2007.
22 A. de Villiers, F. Lestremau, R. Szucs, S. Gélébart, F. David and P. Sandra, Evaluation of ultra performance liquid chromatography: Part I. Possibilities and limitations, J. Chrom. A, 1127, 15, 60-69, 2006.

9 Conclusions and future perspectives

In this thesis I have presented silicon and SU-8 based ESI chips with an array of micropillars and a sharpened ESI tip for the analysis of organic molecules. The µPESI chips provide reliable liquid filling and are stable during the ESI process. The sample transport from the sample introduction spot to the ESI tip of the chip is spontaneous because of the capillary forces facilitated by the micropillar array. The open, lidless, micropillar system makes sample application to µPESI chips very easy, and the microchip is not prone to clogging, due to multiple pathways for the liquid to move forward to the tip. This filling method circumvents the use of pumps and cumbersome fluidic connectors. The micropillar array inside the channel is shown to have an essential role in the sample transport. Without the pillar array wide lidless channels cannot be filled without external pumping. The capillary action was further increased by oxygen plasma treatment in order to get hydrophilic and more extensive silicon dioxide layer on the chip. Titanium dioxide layer is very hydrophilic and it can be used for higher capillary action for polar solutions. The microchip provides high surface-to-volume ratio for capillary action and also it is therefore usable as an on-chip microreactor.

Properties of the micropillar array electrospray ionization chip are characterized when it is combined with mass spectrometry. This has demonstrated that µPESI provides reliable and quantitative long-term analysis with no clogging problems, and the sensitivity with organic molecules is high, similar to or better than that achieved with nanospray or other microfluidic chips. The microchips are simple, relatively cheap to fabricate and also suitable for disposable use. The chip can be easily connected to various mass spectrometers having an atmospheric pressure ion source, such as QTOF, triple-quadrupole, and ion trap instruments. For high throughput analysis and more convenient handling of the chip, multitip µPESI chip was designed. The design of a microchip having electrospray tips as an array at the edge of a single wafer is unique. Parallelization of the µPESI-tips to a rotating multitip array combined with MS was shown to be a potential method for high throughput screening. Tip-to-tip repeatability was shown to be adequate for qualitative and semi-quantitative analyses, and the method was rapid, as 60 samples can be analyzed in 10 minutes. Repeatability of the technique could be further improved more by using an automatic sampler and an internal standard method. Cross contamination between the tips can be further avoided by using a hydrophobic nanolayer such as PTFE or C_{18} between the tips. The system combined with the ZipTip^{TM} solid phase extraction method was shown to be a potential choice for specific screening of benzodiazepines as well as other drugs from urine, being rapid, sensitive, and specific. The last washing step in ZipTip^{TM} solid phase extraction protocol can be further optimized for benzodiazepines. Other miniaturized solid phase extraction techniques, such as microextraction of packed sorbent (MEPS^{TM}) in syringe could be utilized with µPESI chips for extraction of biological samples. The speed and easiness of the rotating multitip µPESI-MS also proved to be adequate for rapid monitoring of reaction products in an organic synthesis. The amount of the starting compound needed for the analysis was in the pmol range, which enables utilization of microreactors for the synthesis, still providing high sensitivity in the

analysis. Furthermore, the µPESI chip could be used for other reaction applications and for the monitoring of reaction kinetics.

The microfabrication of the chips is straightforward, providing very accurate and reproducible chip production. Silicon as a fabrication material is well suited for precise fabrication of two and three dimensional structures. Therefore, a truly three dimensional in-plane ESI tip and a flow channel filled with an array of perfectly ordered high aspect ratio micropillars can be fabricated. Because there is no need to seal the channel, no bonding is required in the fabrication process. On the other hand, the benefits of the polymeric chips are their straightforward, simple fabrication process and low price.

With an SU-8 fabricated µPESI-chip I have demonstrated a protocol to perform on-chip reactions. In trypsin digestion of bovine serum albumin and cytochrome c experiments there was no need for an external device for sample transfer or sample treatment before the direct ESI/MS measurement. The on-chip digestion and measurement can be conducted in ten minutes, making the system ideal for rapid screening of proteins. The simplicity of the digestion process and the high digestion efficiency show that the current method could be applicable to the automated high-throughput protein analysis, using a platform of multiple microreactor-ESI chips, as was done with rotating multitip chips. Due to the lack of immobilization of trypsin, the same microreactor chip could be used, after cleaning, for digestion experiments using a variety of different enzymes, thus making it cost-effective. For that reason the microreactor could also be used for performing other chemical or biochemical reactions. Therefore the usability of µPESI chips as micro- and nanoreactors was further increased by coating micropillars with a 100 nm TiO_2 layer. The TiO_2-µPESI chip was used for production, detection, and identification of the photocatalytic reaction products of selected drugs. The integration of nanoreactor and ESI source on the same microchip enabled rapid on-line analyses with MS. The correlation between the reaction products observed on the TiO_2-µPESI chip and the metabolites detected with *in vitro* and *in vivo* methods was remarkable. The TiO_2 nanoreactor/ESI microchip can therefore be used for a rapid prediction of phase I metabolites in the early preclinical stage of drug research and it has potential to speed up the discovery of new potential drug candidates. If a TiO_2-nanolayer is introduced to a rotating multitip chip it will make analyses considerably faster and the method much more attractive to commercial users. Furthermore, the TiO_2 multitip µPESI chip would be ideal for screening of large chemical libraries.

A micropillar array based separation column was designed and fabricated for direct laser induced fluorescence detection. The micropillar liquid chromatographic column was also integrated to the same microchip with the first ever fabricated three-dimensionally sharp glass-silicon tip for electrospray ionization. Therefore the chip can be used for laser induced fluorescence detection as well as for mass spectrometry. The flow rate through the column was optimized to be suitable for both ESI and separation. Injection volume used with microchip LC was at a µL level, but the actual sample volume injected into the microchip was at the nL level. Therefore, with optimization of the injection system, the

sample volume needed could be decreased to the nL level. The micropillar array LC chip has not as high plate numbers as can be obtained with UPLC, but peak widths at half maximum were similar with both systems. The performance of the LC microchip can be further optimized by using sheath flow channels that are connected to a main LC channel prior to the electrospray tip for a more stable electrospray. Furthermore, if precision of glass etching and bonding can be improved, the width of the outlet channel at the tip can be decreased for more sensitive and stable electrospray and also solvents with higher water concentrations are then enabled to be sprayed without a sheath flow. Backside etching of the tip would make the tip even sharper and it may decrease the high voltage needed for ionization. An integrated injection channel would increase separation efficiency by decreasing band broadening during injection. The pillar array structure can be further optimized at both side walls of the column to reduce side wall effect of the flow and reduce band broadening using “the magic gap” between pillars and the column side wall. External and internal porosity of the pillars could be further optimized in order to lower back pressure and increase column capacity. Therefore, the column length could be increased. The flow distributor could be changed from a bifurcated distributor to a radially integrated distributor to get a flatter flow profile in a separation channel. A coating protocol for the pillar array column could be further optimized and better separation efficiency can be obtained. It is worth noting that, due to homogeneity of the pillar array column, it is an excellent platform to test new kinds of coating materials. Therefore, when multidimensional separation platforms are designed, pillar array columns could be a very useful choice for that purpose.